EFFECT OF HIGH HYDROSTATIC PRESSURE ON LIPID CRYSTALLINE STRUCTURES IN PALM STEARIN EMULSIONS

A THESIS SUBMITTED TO
THE GRADUATE SCHOOL OF NATURAL AND APPLIED SCIENCES
OF
MIDDLE EAST TECHNICAL UNIVERSITY

BY

SEZEN SEVDİN

IN PARTIAL FULFILLMENT OF THE REQUIREMENTS
FOR
THE DEGREE OF DOCTOR OF PHILOSOPHY
IN
FOOD ENGINEERING

JUNE 2017

Approval of the thesis:

EFFECT OF HIGH HYDROSTATIC PRESSURE ON LIPID CRYSTALLINE STRUCTURES IN PALM STEARIN EMULSIONS

submitted by **SEZEN SEVDİN** in partial fulfillment of the requirements for the degree of **Doctor of Philosophy in Food Engineering Department, Middle East Technical University** by,

Prof. Dr. Gülbin Dural Ünver
Dean, Graduate School of **Natural and Applied Sciences** ________________

Prof. Dr. Serpil Şahin
Head of Department, **Food Engineering** ________________

Prof. Dr. Hami Alpas
Supervisor, **Food Engineering Dept., METU** ________________

Examining Committee Members:

Prof. Dr. Alev Bayındırlı
Food Engineering Dept., METU ________________

Prof. Dr. Hami Alpas
Food Engineering Dept., METU ________________

Prof. Dr. Semra İde
Physics Engineering Dept., Hacettepe University ________________

Prof. Dr. Vural Gökmen
Food Engineering Dept., Hacettepe University ________________

Assist. Prof. Dr. Mecit Halil Öztop
Food Engineering Dept., METU ________________

Date: 16.06.2017

I hereby declare that all information in this document has been obtained and presented in accordance with academic rules and ethical conduct. I also declare that, as required by these rules and conduct, I have fully cited and referenced all material and results that are not original to this work.

Name, Last name : Sezen Sevdin

Signature :

ABSTRACT

EFFECT OF HIGH HYDROSTATIC PRESSURE ON LIPID CRYSTALLINE STRUCTURES IN PALM STEARIN EMULSIONS

Sevdin, Sezen
Ph.D., Food Engineering Department, METU
Supervisor: Prof. Dr. Hami Alpas

June 2017, 191 pages

Lipid crystal structures (polymorphs) are the determinant factors for sensorial, textural properties and the stability of the emulsions. Therefore, controlled crystallization gains importance during the production of foods such as margarine, confectionery, chocolate, etc. In literature, studies on the effect of high hydrostatic pressure (HHP) on lipid crystallization have contradictory results. To inspect the crystallization characteristics and response to the HHP treatment, palm stearin-water emulsions were prepared with two different emulsifiers (sodium caseinate and hydrogenated soy lecithin-xanthan gum mixture) and pressurized at 100 and 500 MPa, at 10, 20 and 40°C for 15 minutes. Particle size analysis, differential scanning calorimetry (DSC), transverse relaxation time (T_2) and self-diffusion coefficient (SDC) determinations and small angle x-ray scattering (SAXS) were conducted to investigate the changes induced by HHP treatment. According to the results, HHP did not affect droplet size of sodium caseinate (SC) emulsions so it was observed that mean particle size was affected only by the types of emulsifiers and storage time. In addition, sodium caseinate has the capability to produce smaller particles than 80H_XG emulsion. HHP has no significant effect on the melting temperature of polymorphs; but pressure and storage time have significant effect on crystal polymorphs' content in emulsions. HHP induced formation of more stable β crystals in both sodium caseinate and soy lecithin-xanthan gum mixture emulsions. In addition to this, HHP also induced solid wall formation in soy lecithin-xanthan gum mixture emulsions. Changes in α and β contents with respect to pressure and storage time were detected by T_2 and SDC measurements. These findings suggested that the beginning of emulsions' destabilization can be detected by NMR measurements. The pressure effect may easily be seen in the *ab-initio* structural model with SAXS measurements. The pressure application caused a structural change from spherical form to cylindrical form in sodium caseinate (SC) solution and SC emulsion droplets reached more compact spherical like aggregations.

Keywords: Lipid Crystallization, Polymorphs, High Hydrostatic Pressure, Transverse Relaxation Time, Self-Diffusion Coefficient

ÖZ

YÜKSEK HİDROSTATİK BASINCIN PALM STEARİN EMÜLSİYONLARININDAKİ YAĞLARIN KRİSTALİN YAPILARI ÜZERİNE ETKİSİ

Sevdin, Sezen
Doktora, Gıda Mühendisliği Bölümü, ODTÜ
Tez Yöneticisi: Prof. Dr. Hami Alpas

Haziran 2017, 191 sayfa

Yağların kristalin yapıları (polimorflar), emülsiyonların duyusal, yapısal özelliklerini ve stabilitelerini belirleyen önemli faktörlerdendir. Bu sebeple, kontrollü kristalizasyon, margarin, şekerleme ve çikolata gibi ürünlerin üretiminde önem kazanmıştır. Literatürde, yüksek hidrostatik basıncın (YHB) yağ kristalizasyonu üzerindeki etkileri ile ilgili çelişkili bilgiler bulunmaktadır. Kristalizasyon özelliklerini ve YHB uygulamasından kaynaklanan etkileri incelemek amacıyla, palm stearin-su emülsiyonları iki farklı emülgatör (sodyum kazeinat ve soya lesitini-ksantan gam karışımı) kullanılarak üretilmiş; 100 ve 500 MPa basınçta, 10, 20 ve 40°C sıcaklıkta 15 dakika basınçlanmıştır. YHB uygulamasından kaynaklanan değişimleri belirlemek için, parçacık boyutu analizi, diferansiyel taramalı kalorimetre, transvers relaksasyon zamanı ve öz-yayılma katsayısı ölçümleri ve küçük açılı x-ışını saçılma analizleri yapılmıştır. Sonuçlara göre, YHB, sodyum kazeinat emülsiyonlarının parçacık boyutunda değişikliğe sebep olmamış, parçacık boyutunun emülgatör çeşidi ve depolama süresine göre değiştiği gözlemlenmiştir. Buna ek olarak, sodyum kazeinatın soya lesitini-ksantan gam karışımından daha küçük parçacıklar oluşturabildiği görülmüştür. YHB'ın polimorfların erime sıcaklığına önemli bir etkisi olmamasına rağmen, basınç ve depolama süresinin emülsiyon içerisindeki kristal polimorfların içeriğine belirgin etkileri vardır. YHB uygulaması sodyum kazeinat ve soya lesitini-ksantan gam karışımı emülsiyonlarında β kristal yapı oluşumunu arttırmıştır. Bunlara ek olarak, YHB soya lesitini-ksantan gam karışımı emülsiyonlarında katı duvar oluşumunu arttırmıştır. α ve β kristal miktarındaki basınca ve depolama süresine göre oluşan artışlar ise transvers relaksasyon zamanı ve öz-yayılma katsayısı ölçümleri ile belirlenebilmektedir. Bu bulgular ise emülsiyonların içerisinde oluşması muhtemel destabilizasyonun tespit edilmesinde nükleer manyetik rezonasyonun (NMR) kullanılabileceğini öngörmektedir. Basınç uygulamasının etkileri is küçük açılı x-ışını saçılma (SAXS) analizi sonuçlarıyla oluşturulan *ab-initio* yapısal modelinde kolaylıkla görülebilmektedir. SAXS analizi sonuçları, emülsiyon içindeki yapıların küresel yapıdan silindirik yapıya doğru kaydığını göstermektedir.

Anahtar Kelimeler: Yağ Kristalleşmesi, Polimorflar, Yüksek Hidrostatik Basınç, Transvers Relaksasyon Zamanı ve Öz-Yayılma Katsayısı, Küçük Açılı X-Işını Saçılma Analizleri

To my family

ACKNOWLEDGEMENTS

Many people have contributed either directly or indirectly to my thesis, I would like to mention them and show my gratitude.

I would like to thank my supervisor Prof. Dr. Hami Alpas for all his support and advices not only for academic works but also for my private life. My special thanks go to Assist. Prof. Dr. Mecit Halil Öztop for his valuable suggestions and guidance through my research and his patience and help during any problems that I faced.

I want to express my thanks to my thesis advisory committee member Prof. Dr. Vural Gökmen for his guidance. In addition, I also would like to thank to COST Organisation and Anne-Laure Rollet for giving me the chance to work in Phenix Laboratory, France.

I also want to thank my friends, Armağan Cabadağ for his everlasting presence, Ceren Perk, Nilgün Efe, Sermet Can Beylikçi, Sinem Akkaya and my colleagues, Önay Burak Doğan, Sertan Cengiz, Derya Ucbaş, Ayça Aydoğdu, Emrah Kırtıl, Sevil Çıkrıkcı, Hazal Turasan, Bade Tonyalı, Barış Özel, Selen Güner and Elif Yıldız Bulut.

Lastly, I want to express my deepest gratitude to the members of my big family; Nilgün and Ali Sinan Sevdin, Ayşe Nihan and Ali Güleç, my lovely parents Bilge and Süleyman Dinçel for their support, confidence, patience and love; my sister Selvi Dinçel and my love Emrecan Sevdin for their endless love, help and patience while lucubrating in the laboratory. This study could not be completed without them.

TABLE OF CONTENTS

ABSTRACT v

ÖZ vii

ACKNOWLEDGEMENTS x

TABLE OF CONTENTS xi

LIST OF TABLES xv

LIST OF FIGURES xvi

ABBREVIATIONS xviii

CHAPTERS

1. INTRODUCTION 1

1.1. Emulsion 1

1.1.1. Emulsion Production 2

1.1.2. Emulsion Stability 6

1.1.3. Emulsions in Food Industry 9

1.2. Lipid Crystallization 9

1.3. High Hydrostatic Pressure (HHP) 12

1.3.1. Working Principles 13
1.3.2. Effect of HHP on Lipid Crystallization 15
1.4. Palm Stearin 16
1.5. Characterization of Emulsions 17
1.5.1. Particle Size 17
1.5.2. Differential Scanning Calorimetry (DSC) 20
1.5.3. Low Resolution Nuclear Magnetic Resonance (NMR) Relaxometry 21
1.5.4. Small and Wide Angle X-Ray Scattering 23
1.6. Objectives of The Study 25
2. MATERIALS AND METHODS 26
2.1. Chemicals 26
2.2. Experimental Design 26
2.3. Emulsion Production 27
2.4. High Hydrostatic Pressure (HHP) Treatment 28
2.5. Thermal Characteristic Analysis 30
2.6. Spin-Spin Relaxation Time and Self-Diffusion Coefficient Analyses 31
2.7. Particle Size Analysis 31
2.8. Small and Wide Angle X-Ray Scattering Analysis 31
2.9. Statistical Analysis 32
3. RESULTS AND DISCUSSION 33

3.1. Particle Size Analysis 33

3.2. Melting and Crystallization Characteristics of Emulsions 36

3.3. NMR Relaxometry and Self Diffusion Coefficient Determination ... 46

3.4. Small Angle X-Ray Scattering (SAXS) Analysis 53

4. CONCLUSION 59

APPENDICES

APPENDIX A. ANOVA Results of General Full Factorial Regressions 77

APPENDIX B. Comparison of 80H_XG Emulsion Samples at 1st Day of Storage and Grouping Information 87

APPENDIX C. Comparison of 80H_XG Emulsion Samples at 8th Day of Storage and Grouping Information 101

APPENDIX D. Comparison of 80H_XG Emulsion Samples at 14th Day of Storage and Grouping Information 115

APPENDIX E. Comparison of 80H_XG Emulsion Samples at 28th Day of Storage and Grouping Information 131

APPENDIX F. Comparison of SC Emulsion Samples at 1st Day of Storage and Grouping Information 145

APPENDIX G. Comparison of SC Emulsion Samples at 8th Day of Storage and Grouping Information 155

APPENDIX H. Comparison of SC Emulsion Samples at 14th Day of Storage and Grouping Information 165

APPENDIX I. Comparison of SC Emulsion Samples at 28th Day of Storage and Grouping Information 177

VITA 189

LIST OF TABLES

Table 1. Independent variables of the study..27

Table 2. Sauter mean diameter (D[3,2]) results of emulsions during storage 35

Table 3. Volume weighted mean diameter (D[4,3]) results of emulsions during storage..36

Table 4. α crystal melting temperature and content with respect to storage.........42

Table 5. β crystal melting temperature and content with respect to storage.........43

Table 6. 3rd structure melting temperature and content with respect to storage ...45

Table 7. Radius of gyration of SC and 80H emulsions..55

LIST OF FIGURES

Figure 1. Colloidal mill (McClements, 2005) 3

Figure 2. Schematic design of high speed stirrer (McClements, 2005) 4

Figure 3. Schematic view of microfluidizer (McClements, 2005) 5

Figure 4. Schematic view of microfluidizer (McClements, 2005) 7

Figure 5. Schematic view of HHP processing 14

Figure 6. A symmetrical particle size distribution 19

Figure 7. An example thermogram 21

Figure 8. A representative T_2 curve 22

Figure 9. SAXS profile and specific regions related with the information can be obtained (Boldon et al., 2015) 24

Figure 10. HHP equipment (SITEC-Sieber Engineering AG, Zurich, Switzerland) 29

Figure 11. Pressurization chamber 29

Figure 12. DSC heating and cooling thermograms of unpressurized palm stearin-sodium caseinate sample at first day (heat flow was normalized to sample weight) 37

Figure 13. First day heating thermograms of selected palm stearin emulsions (heat flow was normalized to sample weight) 38

Figure 14. Polymorph fraction of SC emulsions. 40

Figure 15. Polymorph fraction of 80H_XG emulsion. 41

Figure 16. T_2 results of SC sample during storage...47

Figure 17. T_2 results of 80H_XG sample during storage 48

Figure 18. Self diffusion coefficient results of SC emulsions during storage 51

Figure 19. Self diffusion coefficient results of 80H_XG emulsions during storage 52

Figure 20. SAXS profile of SC emulsions..53

Figure 21. SAXS profile of 80H emulsions...54

Figure 22. 3D morphologies, sizes and pair distance distributions of the nanoglobules in samples 56

ABBREVIATIONS

80H: Hydrogenated Soy Lecithin (Phospholipon 80H®, Lipoid GmbH, Ludwigshafen, Germany)

DSC: Differential Scanning Calorimetry

D[3,2]: Sauter Mean Diameter

D[4,3]: Volume Weighted Mean Diameter

E_a: Activation Energy

HHP: High Hydrostatic Pressure

HPvH: High Pressure Valve Homogenizer

I: Intensity

NMR: Nuclear Magnetic Resonance

PS: Palm Stearin

Q: Porod's invariant

SAXS: Small Angle X-ray Scattering

SC: Sodium Caseinate

SDC: Self-Diffusion Coefficient

T_2: Transverse Relaxation Time

XG: Xanthan Gum

CHAPTER 1

INTRODUCTION

1.1. Emulsion

Emulsion is a system that consists of two immiscible fluids. It is formed by two phases; continuous and dispersed phase. Continuous phase is used for surrounding liquid whereas the dispersed phase forms the droplets. In food systems, emulsions are generally formed by water and oil mixtures and they are classified according to the type of the continuous and dispersed phases. If dispersed phase is oil and continuous phase is water, this type of emulsion is called as oil-in-water. Major oil-in-water emulsion products are mayonnaise, milk, dressings and soup. In some cases, food emulsions contain either dispersed or continuous phase in semi-solid or solid form, like as butter or dairy desserts. Crystallization or gelation can be used to produce emulsions containing solid particles (Darling & Birkett, 1987).

Emulsions are produced by systems called as homogenizers which apply high shear stress to the mixtures and this force causes the production of small droplets. However, emulsions are thermodynamically unstable systems by their nature since oil droplets tend to merge due to density difference and this causes phase separation in an emulsion. This phase separation may cause some quality defects (like appearance and texture) on food products. Therefore, some natural or synthetic materials are used during production to provide stability to the emulsions and in food science and industry these substances are named as emulsifiers (McClements, 2005).

1.1.1. Emulsion Production

The process of mixing two immiscible fluids and producing an emulsion is a homogenization process. Equipment used for this purpose is called as homogenizer. Colloidal mills, high speed stirrers and high pressure homogenizers are some examples of homogenizers.

Colloidal mill is a continuous system as shown in Figure 1, schematically. It contains a rotor and stator part to process the emulsions. Stator is a stationary disk but rotor is a rotating disk with high speed (McClements, 2005). There is a gap between stator and rotor and the oil-water mixture is fed into this gap. Due to the shear stress applied by the rotating rotor, coarse emulsion droplets are broken down into smaller ones. Rotation speed of rotor can be adjusted according to the desired droplet size and if rotation speed is increased, then the droplet size decreases. In addition, process time (or residence time) also affects droplet size. However, colloidal mill is more suitable for intermediate or high viscosity liquids and much more effective in decreasing the droplet size when feed is a pre-emulsion not the oil-water mixture. In addition, a cooling system is required to control the system temperature because rotation creates an increase in temperature which may decrease the emulsion stability (Hasenhuettl & Hartel, 2008).

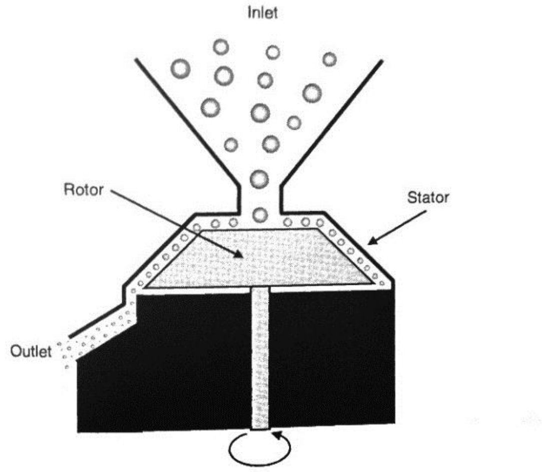

Figure 1. Colloidal mill (McClements, 2005)

High speed stirrer is a batch emulsification equipment as shown in Figure 2. It has a vessel and agitator part. Oil-water mixture is placed into a vessel and stirrer rotates at a high speed (100 to 1000 rpm). This velocity field creates turbulence, disrupt the oil-water interface and three-dimensional shear stress is exerted upon droplets. As a result, smaller droplets and heat are generated. To control the temperature, especially during long processes a cooling system should be integrated to the system (Hasenhuettl & Hartel, 2008). This system is generally appropriate for low viscosity fluids. Droplet size can be adjustable by using baffles, different rotation speeds and different mixing head (McClements, 2005).

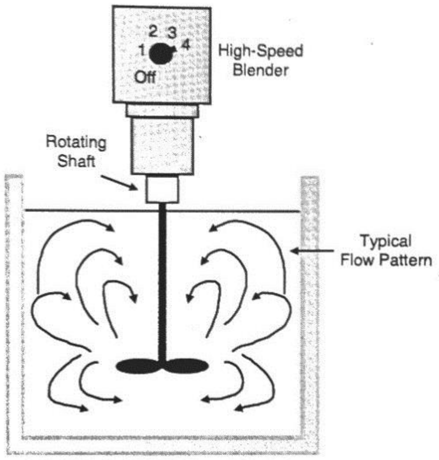

Figure 2. Schematic design of high speed stirrer (McClements, 2005)

High pressure homogenizer (microfluidizer) is one of the continuous processing equipments used for emulsion production and shown schematically in Figure 3. Microfluidizer includes fluid inlet, outlet, chamber and pump (McClements, 2005). This system can be used not only for emulsion production but also to achieve smaller droplet size from a coarser pre-emulsion. In this system, mixtures or emulsions are pumped through the chamber with a high velocity and forced to pass from micro-gaps. High shear stresses and cavitation forces are generated and these forces cause breaking droplets into smaller ones (Hasenhuettl & Hartel, 2008). Microfluidizer can produce pressure between 10 and 275 MPa. Droplet sizes can be changed by varying pressures and number of pass (McClements, 2005).

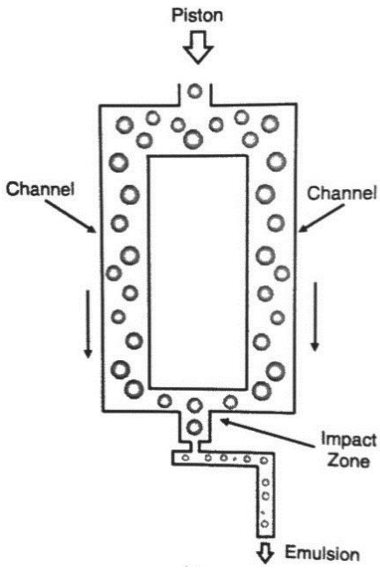

Figure 3. Schematic view of microfluidizer (McClements, 2005)

There are still numerous of emulsification methods in use (Tan et al., 2016). Ultrasonic and high pressure valve homogenizer (HPvH) are some of the most common equipments for this purpose (Trujillo-Cayado, Santos, Alfaro, Calero, & Muñoz, 2016). Ultrasonic and HPvH can be classified as the methods in high-energy approach. High energy approach refers the high energy input to produce the dispersion (Tan et al., 2016). Ultrasonic homogenizer uses sound waves to produce vibrations due to alternating high to low-pressure cycles in the system. During low pressure applications, vacuum bubbles are formed and when these are reached a maximum size, they burst and create the cavitation force. Droplets are broken down into smaller particles due to this cavitation force ("Ultrasonic Homogenizing And Blending," n.d.). HPvH has a very similar mechanism to microfluidizer and the only difference between these two equipments is the geometry of nozzle where homogenization occurs. Homogenization occur in micro-channels in microfluidizer as stated before, however, in HPvH, the nozzle is a valve. When a high pressure applied to the system, inlet materials moves through the valve to the low-pressure and due to mechanical shear stress produced in valve, a decrease in particle size can be achieved (Tan et al., 2016; Trujillo-Cayado et al., 2016).

1.1.2. Emulsion Stability

Emulsion stability refers to the ability of an emulsion to resist changes in its properties for a period of time. Therefore, more stable emulsions maintain its properties unchanged for a longer period. In general, stability may refer two concepts; thermodynamic and kinetic stability.

Oil and water have different densities and this creates an interfacial tension between these two liquids. Emulsion formation increases the interfacial area between oil and water due to smaller droplet size, so interface free energy increases accordingly. Then, increasing free energy causes a thermodynamically unstable system (McClements, 2005). All food emulsions are thermodynamically unstable. This means that emulsion form is not a favorable state and this system will tend to demulsify after a certain period of time. Thermodynamically unstable emulsions should overcome an activation energy to reach a thermodynamically favorable form. This activation energy determines the kinetic stability of the emulsions. If an emulsion is kinetically stable, activation energy is higher. This means that even if an emulsion is thermodynamically unstable, it may remain kinetically stable for a long period which is called as a metastable form. Therefore, kinetic stability, which gives sensorial and textural properties to emulsions, have higher importance in food emulsions (McClements, 2005).

Emulsion destabilization may occur through five mechanisms, namely, gravitational separation, flocculation, coalescence, Oswald ripening and phase inversion. All mechanisms are shown in Figure 4, schematically.

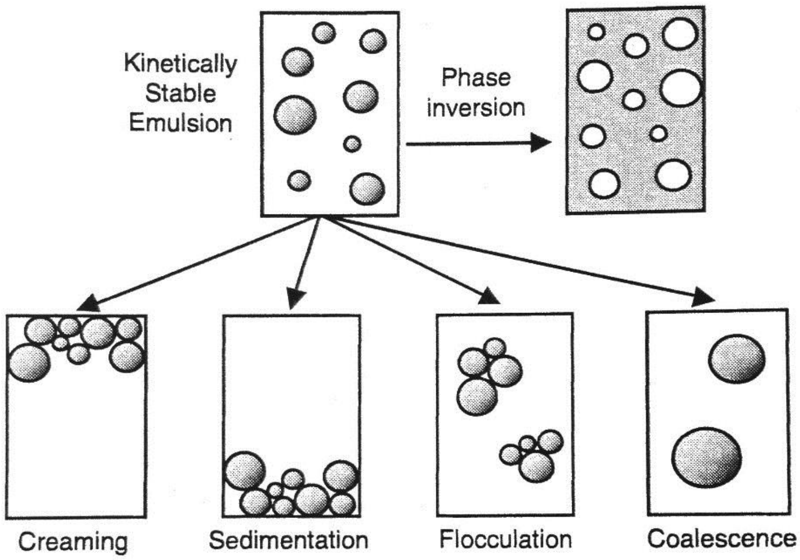

Figure 4. Schematic view of microfluidizer (McClements, 2005)

Gravitational separation (creaming or sedimentation) is caused by density differences between continuous and the dispersed phases. If dispersed phase's density is lower than the continuous phase, gravitational movement of droplets occurs towards upward. Denser droplet layer is formed at the top of an emulsion and this is called creaming. Also, if dispersed phase's density is higher than the continuous phase, gravitational movement of droplets occurs towards downward so denser droplet layer is formed at the bottom of the emulsion and this is called sedimentation. However, gravitational sedimentation does not cause the emulsion instability by itself but it may increase the rate of other destability mechanisms (Tadros, 2009).

Flocculation is a process in that droplets come together and form a three-dimensional structure but in this structure droplets maintain their integrity. Van der

Waals attraction between droplets causes this destability and also, this may accelerate gravitational separation. Flocculation cause significant changes in emulsion's physicochemical and sensorial properties, like texture, viscosity, shelf life and appearance. However, this may be a desirable mechanism in some food product with a certain texture but it should be with a controllable rate (McClements, 2005).

Coalescence is similar with flocculation in a manner of droplet gathering but it is different because in this case droplets merge with each other, not maintain their integrity. The structure formed with coalescence is a more thermodynamically stable system than an emulsion due to decrease in contact area between continuous and dispersed phase. Coalescence causes an increase in rate of gravitational separation due to larger size of droplets (McClements, 2005; Ritzoulis, 2013).

In Oswald ripening, smaller droplets' content is transported into larger droplets through the continuous phase so that large droplets expand while smaller ones are shrinking. Driving force for this process is solubility difference between the small and large droplets (Tadros, 2009). Generally, this mechanism gains importance in oil-in-water emulsions which contain water-soluble lipid such as flavor, or alcohol containing continuous phase, like cream liqueur (McClements, 2005).

An oil-in-water emulsion can be transformed into a water-in-oil emulsion through phase inversion. This is a complex mechanism that involves gravitational separation, flocculation and coalescence. Phase inversion is a desired mechanism in margarine and butter production but in other food systems, it has deleterious effects on stability, texture and other sensorial properties (McClements, 2005).

1.1.3. Emulsions in Food Industry

Numerous naturally and processed foods are partially or fully in emulsion form. Milk is the best example for a naturally-found, oil-in-water emulsion. In addition, there are also plenty of processed food emulsions such as mayonnaise, ice cream, salad dressings, soups and sauces as oil-in-water, butter and margarine as water-in-oil type. High product diversity brings the different requirements for physicochemical, textural and sensorial characteristics (McClements, 2005). These different requirements necessitate different ingredients. Ingredients of a model emulsion system are water, oil and an emulsifier. However, especially oil and emulsifier types have very unique characteristics. Oils used in food industry can have various characteristics such as chemical composition, melting and crystallization temperature, hydrophobicity, etc. Also, emulsifiers present several emulsifying properties such as, emulsifying power, emulsification mechanism, and stability; consequently these are used accordingly to the desired characteristics of the final product. By adjusting the emulsifier and oil type and percent, foods can have numerous characteristics and for the very reason, emulsions are widely used in the food industry.

1.2. Lipid Crystallization

The process of solid to liquid phase transition of lipid is called as crystallization and it is an exothermic process. Crystallization has mainly formed by three steps; supercooling, nucleation and crystal growth. Lipids in liquid state can maintain their liquid form at a certain temperature which is below their melting point for a period of time prior to crystal formation. Temperature difference between melting and freezing can be defined as the supercooling degree and this difference depends on the chemical composition of lipid, purity of the lipids and the processing conditions (rate of cooling, tempering, mechanical friction, pressure, etc.).

In nucleation steps, small triglycerides aggregates are formed. These aggregates are called as embryos. Embryos continue to expand up to a critical point. When the heat of crystallization for this cluster exceed the energy required for surface area increment, this is called as critical point and a stable nucleus is formed at that point. During crystal growth, triglyceride molecules diffuse through the boundary layer and attached to the crystal lattice (Wright & Marangoni, 2006). Nucleation can occur via two different mechanism; heterogeneous and homogeneous nucleation. In heterogeneous nucleation, impurities can act as nuclei and crystal structure grows around it. The energy requirement for the inception of this mechanism is low so heterogeneous nucleation is more common, easier and faster way of nucleation. Also, walls of a container can act as impurity and could trigger the heterogeneous nucleation. However, homogeneous nucleation depends on random nuclei formation. Reaching the required critical energy point, i.e. activation energy, E_a, is slower and less common so homogeneous nucleation is not the dominant way of nucleation. However, in emulsions the story is different and homogeneous nucleation become the common mechanism. In the production of emulsion, dispersed phase is spread into the continuous phase and small droplets (nano or macro-size particles) are formed. Impurities in the system can entrapped into these droplets which lowers the chance of heterogeneous nucleation.

According to Kaneko et al. (1999), emulsifier type is effective on lipid crystallization properties such as crystallization rate. Heterogeneous nucleation can occur from two different pathways. Volume heterogeneous nucleation develops through the catalytic action of impurities in which impurities set ground for nucleation so crystallization may start easily and occur rapidly. However, this type of crystallization is rare. The other pathway is surface heterogeneous nucleation which can be altered by emulsifier type. Emulsifiers can accelerate the nucleation in emulsion by lowering the surface tension at the oil-water interfaces, by increasing van der Waals interaction (between hydrophobic parts of emulsifier and oil) and by crystallizing prior to oil phase (Kaneko et al., 1999)

Each crystal can expand in different type. Crystal growth type may vary according to internal (triglyceride content, structure, molecular interactions, etc.) and external (temperature-time application and mechanical mixing, etc.) factors. These different structures are called as polymorph (McClements, 2005). The most abundant three polymorphic structure are α, β' and β. Lipids generally crystallize in α, β' forms and then turns into β form which is the most stable form (Han et al., 2014). Each polymorphic structure has unique crystallization and melting temperatures. These characteristics may play an important role on the structure, taste and quality of foods (Pérez, Li, & Guo, 2008). For example, in cocoa oil, fat can crystallize as 6 different polymorphic structures and each have own melting temperatures. In chocolate industry, polymorphism is very important to maintain the mouth-feel desired by consumers (Roth, 2010). Although, there are several types of polymorphs in cocoa oil, only crystal form V can be acceptable because when chocolate contains only crystal form V have "noble surface sheen, crisp hardness and pleasant melting sensation in the mouth" (Roth, 2010).

There are several factors which effect the polymorphism. For instance, rate of cooling is very important for the characteristics of crystal nuclei. Rapid cooling increase the energy input to the system and this high input cause high nucleation rate which prevent the ordering of molecules as a well-arranged structures so loose molecular organization is observed. Furthermore, crystallization generally occurs between the molecules with similar structures chain length, saturation degree, double bond content, etc. Therefore, lipids contain mixed triglycerides crystallize slowly and tends to produce less stable structures (Pérez et al., 2008). Therefore, controlling crystallization is very important for food industry.

1.3. High Hydrostatic Pressure (HHP)

Today, thermal treatments are applied to many of the foods in order to inactivate microorganisms and enzymes as conventional processes. However, heat may destroy thermolabile nutritional components of foods and affects physical characteristics such as texture, color, and flavor. In addition, several undesirable compounds can be produced in food materials as byproducts of the reactions take place during thermal processing.

In recent years, consumers' demands for convenient, fresh-like, safe, high quality food products have grown. These demands have encouraged the researchers to use minimal thermal methods. Non-thermal technologies represent a more promising alternative to traditional thermal processing. Methods such as high hydrostatic pressure, super critical carbon dioxide, ultrasound, pulsed electric fields destroy microorganisms and enzymes with no substantial increases in product temperature. Therefore, the sensory characteristics and nutritional value of foods are not degraded to a significant extent. The resulting products have higher quality (Fellows, 2000).

One "new" or emerging technology receiving a great deal of attention is high hydrostatic pressure (HHP). This technology was originally used in the production of ceramics, steels and super-alloys. In the past two decades, high pressure technology was expanded to include the food industry (Rahman, 2007). The first persuasive experiments with microorganisms were reported at the end of the 19th century by Hite (1899). Protein structure in egg-white could be altered by high pressures by Bridgman (1914). Much later, Macfarlane (1973) reported the potential of high pressure technology in pressure-tenderization of meat (Gould, 2012). The first high-pressure product, a high-acid jam, was introduced to the Japanese retail market in April 1990. In 1991, yogurts, fruit jellies, salad dressings, and fruit sauces were also introduced, and two Japanese fruit juice processers installed semi-continuous high-pressure equipment for citrus juice bulk processing (Rahman, 2007). In 2015, there were 350 HHP equipments in use to produce food products and the market capacity of HHP equipment and technical service market was 330 million dollars. In addition, Food produced by HHP has a market value of 9.8 billion dollars and it is expected to reach to 12 billion dollars in 2018 (Salgarkar, 2015).

HHP processing at refrigeration, ambient and moderate temperature which results in less denaturation of thermo-labile compounds, can be used inactivation of pathogenic and spoilage bacteria (Barba, Esteve, & Frígola, 2012). Pressure is an important thermodynamic parameter which has a significant impact on living organisms and biomolecules. Although energy produced by HHP treatment during pressurization is enough to influence microorganisms, it is relatively lower than the energy required for breaking down the strong chemical bonds. Therefore, only weak chemical bonds can be affected by HHP application and sensitive structure such as vitamins, antioxidants and flavor compounds can remain unmodified (Aertsen, Meersman, Hendrickx, Vogel, & Michiels, 2009; Balci & Wilbey, 1999).

According to the working principles of HHP which is given the next part in detail, HHP can cause a decrease in volume and these volume changes may lead to different structures in food compounds (Misra et al., 2017).

1.3.1. Working Principles

A high-pressure system consists of a high-pressure vessel and its closure, pressure-generation system, temperature-control device, and material-handling system. Once loaded and closed, the vessel is filled with a pressure-transmitting medium. Air is removed from the vessel by means of a low-pressure fast-fill-and-drain pump, in combination with an automatic deaeration valve, and high hydrostatic pressure is then generated (Rahman, 2007).

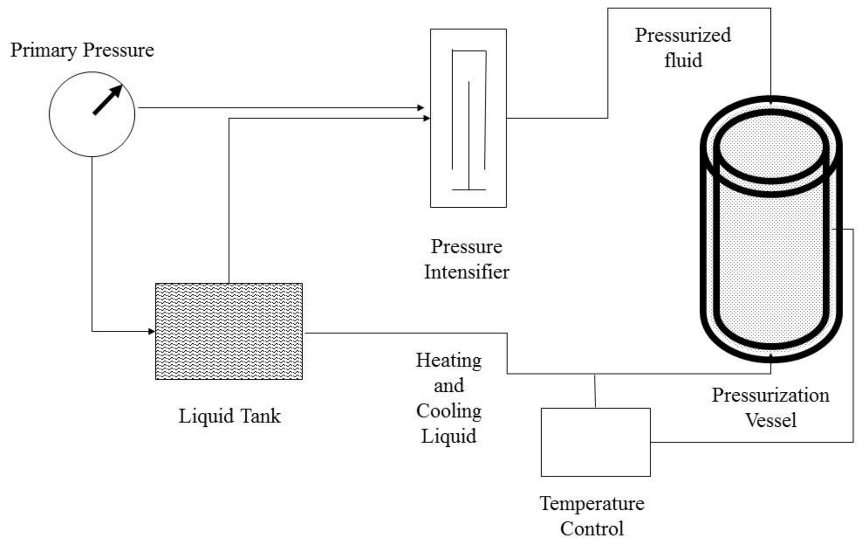

Figure 5. Schematic view of HHP processing

High pressure processing is an isostatic pressure treatment batch wise in the pressure range 200-1000 MPa (Figure 5). Effect of high pressure can be explained by two principles. First, and according to the Le Chatelier's principle, any reaction, conformational change or phase transition is accompanied by a decrease in volume will be favored at high pressures, while reactions involving an increase in volume will be inhibited. Second, pressure is instantaneously and uniformly transmitted independent of the size and the geometry of the food. This is known as isostatic pressure. The food product is compressed by uniform pressure from every direction and then returns to its original shape when the pressure is released (Rahman, 2007).

1.3.2. Effect of HHP on Lipid Crystallization

In recent years, studies on lipids are focused on emulsion production and use of emulsions in food and drug industries. These emulsions have different uses in food and drug industries but the common point is that emulsions should maintain their structures after production (Jores et al., 2004; Jores, Mehnert, & Mäder, 2003; Saupe & Rades, 2006). Emulsions are used to increase some textural and sensorial properties of food materials or to maintain existing properties. Also, emulsion properties change according to production techniques so scientific studies focus on these techniques. Although high hydrostatic pressure application started to be used by food producers, studies about hydrostatic pressure use for emulsion production are not sufficient in literature. In some earlier studies, it was stated that HHP cannot provide a significant decrease in particle size. Therefore, studies about effect of hydrostatic pressure on emulsions were interrupted. However, limited number of studies showed that hydrostatic pressure, applied after emulsion preparation step, can play an active role on production of more stable emulsions (Bigikocin, Mert, & Alpas, 2011; Khan, Mu, Zhang, & Arogundade, 2014)

In literature, it is stated that pressure could have a significant effect on lipid crystallization behavior (Blümer & Mäder, 2005; Ferstl, Eder, Ruß, & Wierschem, 2011; Rostocki et al., 2011; Han et al., 2014). Generally, pressure treatment reduce induction time and increases the rate of crystal growth (Sato, Bayés-García, Calvet, Cuevas-Diarte, & Ueno, 2013). However, pressure treatment is addressed to two different applications; micro-fluidization and high hydrostatic pressure. Han et al. (2014) indicated that micro-fluidization and hydrostatic pressure are two different applications because micro-fluidization uses relatively low pressure and combines pressure with the cavitation forces while hydrostatic pressure uses very high static pressures.

Oh and Swanson (2006) found that HHP treatments up to 600 MPa have no significant effect ($p > 0.05$) on crystallization rate but have little effect on the polymorphic transition of cocoa oil emulsions. However, studies about HHP effect on droplet crystallization are limited in number and conflicting observations were reported in literature to the best of our knowledge. Two other studies dealt with HHP and droplet crystallization stated that (at 200-750 MPa and 4 to 48 °C for 5-30 min.) can induce, accelerate, control crystallization process and may produce more stable crystal structure (Blümer & Mäder, 2005; Ferstl et al., 2011). High pressure was applied (at 10-150 MPa and -30 to 15 °C for 1-60 min) in a continuous production line on emulsion system to solve some problems related with food products (such as, detrimental effects of post-crystallization and long production time, etc.) and this study was presented as innovative technology in patent no.US6495189 (Nosho, Ueshima, Ikehara, Hashimoto, & Kato, 1999). Lipids are pressure sensitive materials since the weak Van der Waals interactions between lipid molecules are easily overcome by pressure treatments (Zulkurnain, Maleky, & Balasubramaniam, 2016). High pressure values (300-600 MPa) cause a substantial reduction in lipid volume (17-30%) (Rostocki et al., 2013). HHP is more effective on saturated fatty acids than unsaturated ones, consequently leading to faster crystallization of saturated fatty acids. Application of HHP decreases the specific surface energy needed for crystallization thus, induces crystal nucleation in an energy efficient way and affects the polymorphism of such crystals (Zulkurnain et al., 2016).

1.4. Palm Stearin

Palm oil is a vegetable oil which is produced from three species of palm trees (*Elaeis* species). The most widely cultivated species is *Elaeis guineensis* and produced palm oil from this species known as African palm oil. Palm is the most produced edible oil in worldwide with 62.6 million tons in 2015 production (“Palm oil production" 2016). In West Africa, it is domestically used as cooking oil but it is used as an ingredient in production of margarine, salad dressing, confectionery and vegetable-based ice cream production in all over of the world.

Palm oil can be fractioned to different edible oil types by using different processing conditions. Dry fractionation of palm oil provides the production of two fractions which are mainly, palm stearin and palm olein (Kellens, Gibon, Hendrix, & De Greyt, 2007). Palm stearin is solid part of palm oil. It is solid at room temperature and its melting temperature may vary between 45°C to 60°C according to fractionation conditions. Common uses of palm stearin are confectionary and margarine production. Due to high melting point, palm stearin eases the margarine production and does not require hydrogenation process. Palm olein is closer to liquid at room temperature and it is generally used as cooking oil after processed for market. Unsaturated fatty acid content relatively higher than the palm oil, but carotenoid content may decrease during processing. However, it is a very stable oil at high temperature. Also, palm olein is used in margarine and shortening production (Mandal & Jayanthi, 2011).

1.5. Characterization of Emulsions

1.5.1. Particle Size

Particle size analysis in emulsions can be conducted with the help of the laser diffraction technique. It is an optical system and generally used to determine the particle size between 0.01-2000 μm. The theory behind the instrument is when a laser beam collides with a particle, it is diffracted with a specific angle which is inversely proportional to the size of the particle.

There are some important concepts to interpret the results; mean, mode, median and distribution width. Mean is a concept which is very similar to average. However, mean can be determined based on number, surface and volume distributions. Related equations are given below.

$$D[p,q] = \frac{\sum_1^n D_i^p v_i}{\sum_1^n D_i^q v_i} \qquad \text{General Equation}$$

D_i: Diameter of i^{th} particle
Σ: summation of D_i^p or D_i^q

$$D[4,3] = \frac{\sum_1^n D_i^4 v_i}{\sum_1^n D_i^3 v_i} \quad \text{and} \quad D[3,2] = \frac{\sum_1^n D_i^3 v_i}{\sum_1^n D_i^2 v_i}$$

D[4,3]: Volume weighted mean diameter
D[3,2]: Surface mean or Sauter mean diameter.

D[4,3] is volume weighted mean diameter and it is very sensitive to volume changes. Therefore, D[4,3] is a good way to monitor the aggregation formation (Horiba Scientific, n.d.). Mode is the peak frequency of the distribution. Median is the point that the number of particles smaller and larger than the median point is equal each other, i.e., median is the central point of distribution graph. For a symmetric particle size distribution mean, mode and median are equal to each other as shown in the Figure 6.

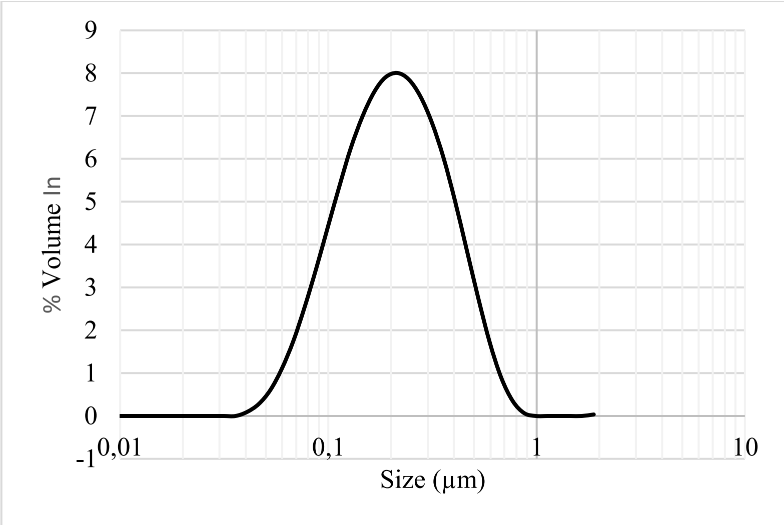

Figure 6. A symmetrical particle size distribution

Distribution width shows the size range of particle and generally span value is used for the explanation of the sample. The determining equation of span is given below.

$$Span = \frac{D_{v0.9} - D_{v0.1}}{D_{v0.5}}$$

$D_{v0.9}$: 90% of particle in the sample smaller at this size
$D_{v0.5}$: 50% of particle in the sample smaller at this size
$D_{v0.1}$: 10% of particle in the sample smaller at this size

1.5.2. Differential Scanning Calorimetry (DSC)

Differential scanning calorimetry (DSC) is a technique for thermal analysis based on heat capacity (C_p) (PerkinElmer Inc., n.d.). There are two types of DSC, namely, power-compensated and heat flux DSC. Both equipments contain two heaters which provide required energy. However, power-compensated DSC systems stabilize the heat flux given to the system and determine the temperature of sample with respect to a reference (Tanaka, 1992). Heat flux DSC lays out the determination of heat requirement to increase the sample temperature with respect to reference material. Heat requirement of the system can change due to endothermic or exothermic reactions. Sample is placed in generally, aluminum DSC pan and hermetically sealed before analysis. Also, an empty DSC pan is used as reference pan (Peyronel & Marangoni, 2014). DSC can be used for determination of glass transition (T_g), melting (T_m) and crystallization (T_c) temperature, heat capacity and enthalpy of transitions. Collected data are expressed in temperature versus heat flow graph which is called as thermogram (Figure 7).

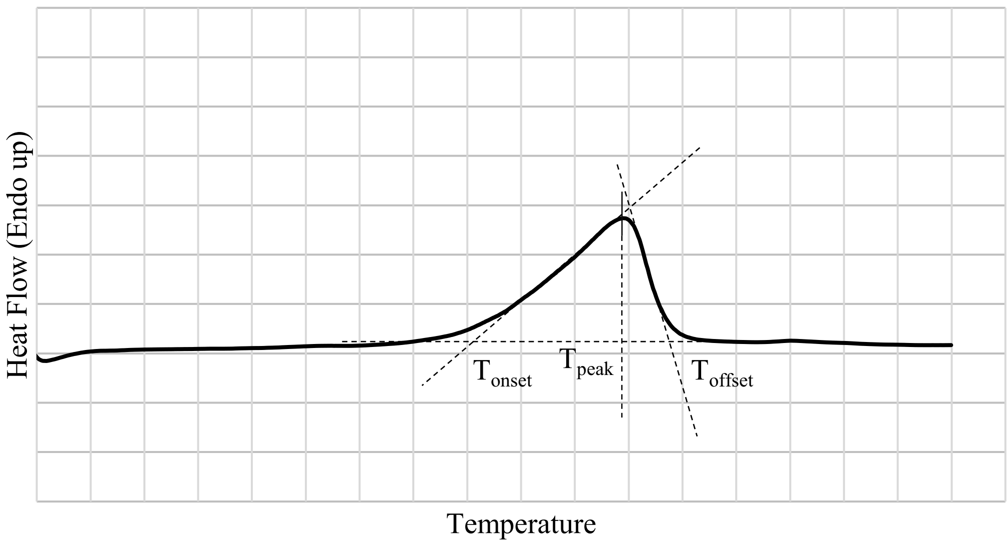

Figure 7. An example thermogram

Peak temperature (T_{peak}) is the maximum or minimum point where the thermal event occur. Onset temperature (T_{onset}) is the point that the tangent and baseline are intercept. Onset temperature and slope of tangents give information about the sample purity. Since T_{onset} should remain unchanged due to different conditions of thermal cycle, it is used to compare different thermal analysis of a sample. Enthalpy requirement for a thermal event can be determined by the area under the curve (Schawe, Riese, Widmann, Schubnell, & Jörimann, 2000).

1.5.3. Low Resolution Nuclear Magnetic Resonance (NMR) Relaxometry

Nuclear Magnetic Resonance (NMR) relaxometry is a non-destructive method to analyze the interior composition of complex food systems (Greiff et al., 2014). NMR may provide characterization of such systems via proton relaxation experiments. The basis of the system is as follows; a sample is placed between magnets, which create external magnetic field (B_0). The protons of the sample align themselves according to the external magnetic field as parallel. When protons are parallel to the B_0, net magnetization is zero and no signal can be detected by the instrument. Then, a radio frequency (RF) pulse is introduced to disturb the system temporarily and signal is produced. After RF pulse removed, protons start to recover their previous states and the relaxation signal is recorded and interpreted (Kirtil & Oztop, 2016). Transverse relaxation time (T_2) which is also known as spin-spin relaxation time, is the time constant for the magnetization decays and reach the equilibrium level. A representative graph of T_2 signal is given in Figure 8. This relaxation data gives information about the interaction between protons.

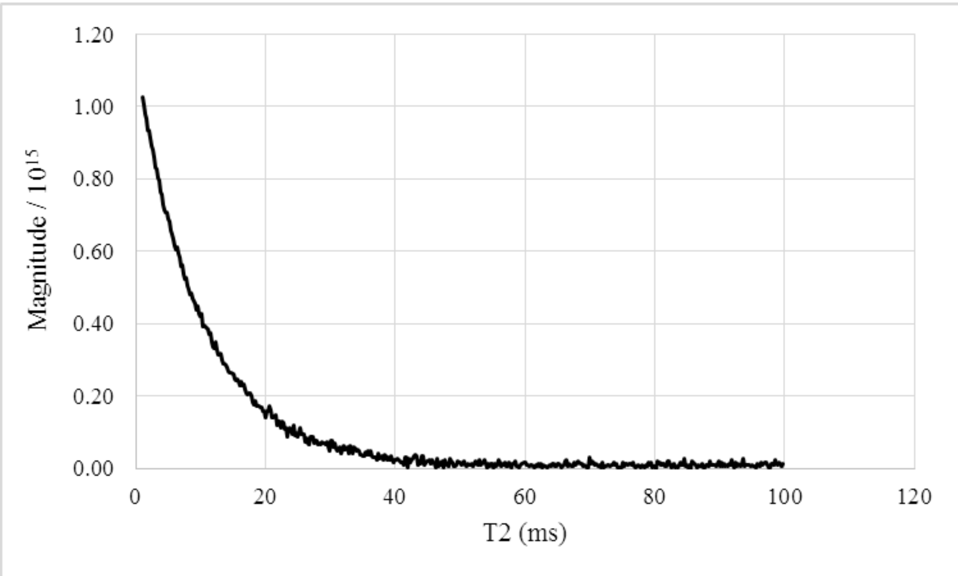

Figure 8. A representative T_2 curve

Since each organic material possesses a distinct relaxation time characteristic, T_2 measurement is a good way to reveal the internal compositions of foods, in this case emulsions (Barrabino, Keleşoğlu, Sørland, Simon, & Sjöblom, 2014; Zhang et al., 2016). In literature, there are some studies investigating the effects of HHP on crystal polymorphism by NMR measurements but they mainly focused on NMR spectroscopy experiments, free induction decay (FID) of sole crystals and again transverse relaxation of sole crystal components (Bouteille et al., 2013; Mazzanti, Mudge, & Anom, 2008; Nadakatti, 1999; Van Duynhoven, Dubourg, Goudappel, & Roijers, 2002). However, NMR relaxometry can also provide transverse relaxation profile for the whole emulsion system and supply information on the overall crystallization process and mechanisms taking place within the emulsion system. Degree of water-surrounding network interactions within a system can be characterized by T_2 measurements. In addition to relaxation profile analysis, self-diffusion coefficients (SDC) can be used for characterizing the mobility of water molecules within food materials (Salami, Rondeau-Mouro, van Duynhoven, & Mariette, 2013).

1.5.4. Small and Wide Angle X-Ray Scattering

Small angle X-ray scattering (SAXS) is an important method to monitor and analyze the structural information of molecules with a size ranging from few kDa to hundreds of kDa (Grishaev, 2012; A. G. Kikhney & Svergun, 2015). In this technique, X-ray beams are scattered by sample's particles and according to the intensity and pattern of scattered radiation, one can come up with the information about the size, shape and distribution of particles in sample (Boldon, Laliberte, & Liu, 2015).

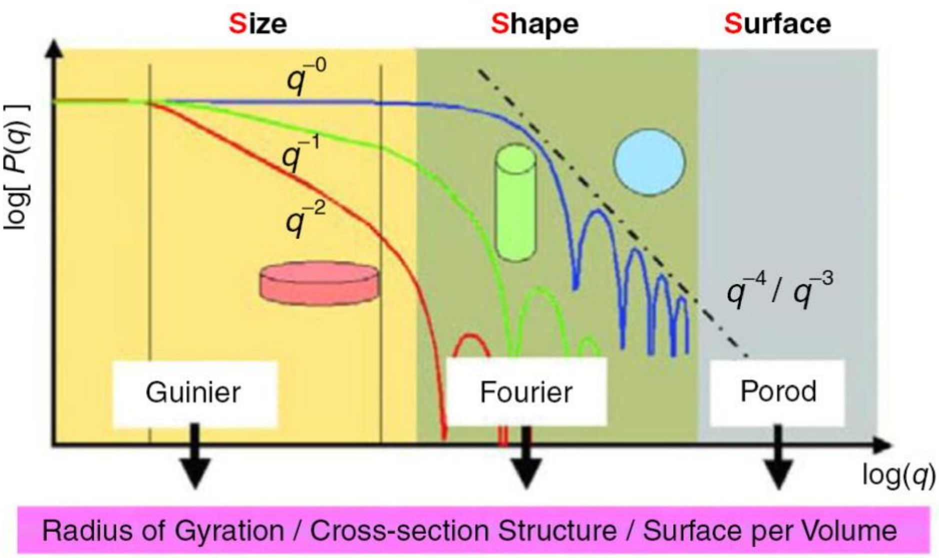

Figure 9. SAXS profile and specific regions related with the information can be obtained (Boldon et al., 2015)

There are three different regions in SAXS profile. In Guinier region, natural logarithm of intensity vector, ln(I(q), is correlated with square of scattering angle, q^2, and information about radius of gyration, R_g, and intensity at zero scattering angle, I(0), can be extracted (Kikhney, 2012). Radius of gyration is the overall size of a particle, i.e., mass weighted overall radius. Intensity at zero scattering angle is inversely proportional to the number of scattering particle per unit volume, N, and square of the particle volume ($\Delta\rho V^2$) as given below. I(0) can be used for the estimation of molecular mass of a sample (Mylonas & Svergun, 2007).

$$I(0) = N(\Delta\rho V^2)$$

In Fourier region, indirect Fourier transformation is applied to determine the pair distribution function and obtain form factor, P(q), which is related with the particle shape (Jacques & Trewhella, 2010; Boldon et al., 2015).

In Porod region, the Porod invariant, Q, are determined to obtain the information about the particle surface such as, surface to volume ratio, complex particle structure, etc. (Boldon et al., 2015).

1.6. Objectives of The Study

In this study, it is aimed;

- to observe the changes in crystallization properties of polymorphic materials after HHP,
- to observe the stability of emulsions during storage,
- to correlate self-diffusion coefficient and T_2 relaxation time of samples,
- to observe changes in crystal structure due to HHP with SAXS analysis.

CHAPTER 2

MATERIALS AND METHODS

2.1. Chemicals

Palm stearin (fully hydrogenated palm stearin with a min 55°C melting point) was donated by Cargill Turkey (Bursa, Turkey). Casein sodium salt (C8654) was purchased from Sigma-Aldrich (St. Louis, Missouri, USA). High boiling point soy lecithin Phospholipon 80H were donated by Lipoid GmbH (Ludwigshafen, Germany)

2.2. Experimental Design

Three different emulsion samples were prepared with two different emulsifiers, sodium caseinate, and high melting point soy lecithin-xanthan gum mixture. HHP treatment conditions were selected according to the results of preliminary works. As a sample, SC emulsion were prepared and DSC analysis was conducted to determine roughly the melting and crystallization temperature (Sevdin, Yücel, & Alpas, 2017). 40°C was selected as the point there is no crystal formation depending on the temperature, 20°C was selected as the point that crystal formation depending on the temperature was completed and 10°C was selected as a lower temperature point for comparison with the other temperature levels. Pressure levels were selected to be one low and one high level as 100 and 500 MPa. Pressure application time was constant and relatively longer than general HHP applications to remove the effect of time on the crystal formation. Emulsion samples were pressurized at two pressure level (100 and 500 MPa), three temperature (10, 20 and 40°C) for 15 minutes. Applied independent variables are given at Table 1.

Table 1. Independent variables of the study

Independent Variables			
Emulsifier Type	Pressure (MPa)	Temperature (°C)	Storage (day)
Sodium Caseinate Soy Lecithin & Xanthan Gum	100 500	10 20 40	1 8 14 28

After production of emulsion samples, 1st day analysis were conducted and samples stored for 28 days at refrigeration temperature. At the 8th, 14th and 28th days of storage all experiments were repeated. DSC, particle size and NMR measurements were conducted for all samples. SAXS analysis were conducted at Hacettepe University, Physics Engineering Department (Ankara, Turkey) within the 1st week of storage.

2.3. Emulsion Production

Emulsions were prepared by using a hot homogenization technique (Yucel, Elias, & Coupland, 2013). Phospholipon 80H and xanthan gum mixture solution (3 g/ml

80H and 0.1 g/ml XG) were prepared separately in double distilled water by stirring at 80 ºC for 1 hour to hydrate and disperse in water. Sodium caseinate emulsifier solution (2 g/ml) was prepared in double distilled water by overnight stirring at room temperature and heating up to 80ºC to ensure dissolution and crystal formation prior to mixing with palm stearin. Palm stearin was incubated at 70ºC for 30 minutes to ensure no crystal structure is present and then mixed with emulsifier solutions with a ratio of 1:9 (w/w) by using T18 digital ULTRA TURRAX® (IKA, Staufen, Germany) with a speed of 1000 rpm for 30 seconds. Coarse emulsion was passed 3 times throughout M-110Y Microfluidizer® (Microfluidics Corporation, MA, USA) at 1000 bar at 60-65ºC. The hot samples were stored at 45ºC (i.e., above crystallization temperature of palm stearin droplets) for less than 1 h in water bath until HHP treatment. Unpressurized samples were used as control.

2.4. High Hydrostatic Pressure (HHP) Treatment

HHP was performed with 760.0118 type pressure equipment supplied by SITEC-Sieber Engineering AG, Zurich, Switzerland Figure 10. The vessel had a volume of 100 ml with internal diameter (ID) 24 mm and length 153 mm Figure 11. A built-in heating-cooling system (Huber Circulation Thermostat, Offenburg, Germany) was used to maintain and control required temperature, which is measured by a thermocouple type K in the vessel. The vessel was filled with a pressure transmitting medium consisting of distilled water. Pressurization rate was 75 MPa/min for 100 MPa and 300 MPa/min for 500 MPa. Pressure release times were less than 20 s. Pressurization time reported in this study did not include the pressure increase and release times. Control group samples were prepared with hot homogenization technique and not pressurized.

Figure 10. HHP equipment (SITEC-Sieber Engineering AG, Zurich, Switzerland)

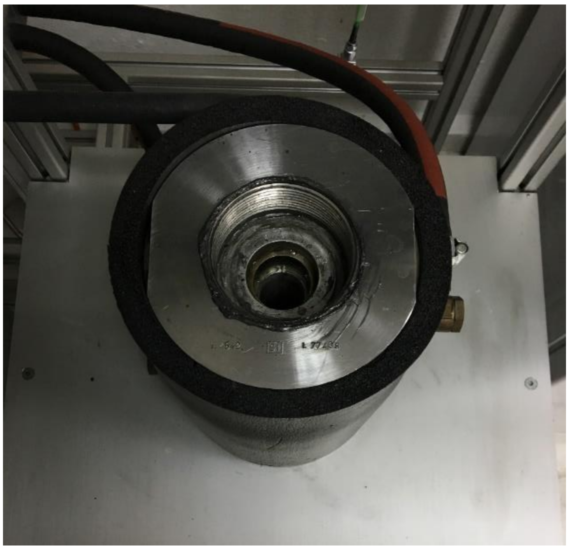

Figure 11. Pressurization chamber

Prepared emulsions were pressurized in 2.5 mL sterile polyethylene cryotubes (Biosigma Srl, CLEARLINE®, CryoGen®Tubes) at two different pressure (100 and 500 MPa) and three different temperature (10, 20 and 40 ºC) values for 15 minutes. SC abbreviation was used for samples prepared with palm stearin as dispersed phase and sodium caseinate as emulsifier; 80H_XG abbreviation was used for samples prepared with palm stearin as dispersed phase and Phospholipon 80H and xanthan gum mixture as emulsifier. For instance, an 80H_XG sample pressurized at 500 MPa at 40^0 C for 15 minutes, was named as 80H_XG_500_40_15. For unpressurized control samples, the name 80H_XG_unpressurized was used. After HHP treatment, samples were held at room temperature until the analyses were completed and then stored at refrigeration temperature (4 ºC) for 28 days. This notation was used throughout this thesis and in the tables and figures.

2.5. Thermal Characteristic Analysis

Crystallization and melting behavior of palm stearin in bulk and emulsified forms were determined by using differential scanning calorimetry (DSC) (Perkin Elmer, DSC 4000, MA, USA). Approximately 10 mg of samples were placed into DSC pan and an empty DSC pan was used as a reference. Bulk palm stearin samples were heated from -10 to 70 ºC with a rate of 2.5 ºC/min, held for 5 min at 70 ºC and cooled from 70 to -10 ºC with a rate of 2.5 ºC/min and heating cycle was repeated once again. Emulsified samples were heated from 35 to 70 ºC with a rate of 2.5 ºC/min, held for 5 min at 70ºC and cooled from 70 to -10 ºC with a rate of 2.5 ºC/min. All samples were subjected to DSC analysis at the 1^{st}, 8^{th}, 14^{th} and 28^{th} days of storage.

2.6. Spin-Spin Relaxation Time and Self-Diffusion Coefficient Analyses

NMR experiments were conducted on a 0.5 T NMR spectrometer operating at a Larmor frequency of 23.2 MHz, equipped with a 10-mm diameter radio frequency coil (SpinCore Inc., Gainsville, FL, USA). Carr-Purcell-Meiboom-Gill (CPMG) pulse sequence was used to record relaxation data with 1 ms echo time, 2000 echoes, 16 scans and 3s repetition time. For self-diffusion coefficient (SDC) measurements, stimulated spin echo pulse sequence containing three 22 us, 90° pulses were used in a 0.32 T NMR system (Spin Track SB4, Mary El, Russia). The time intervals between the first and the second pulses and between the second and the third pulses were 2ms and 60 ms, respectively. Acquisition time was 500 us. The duration of the pulsed gradient field was 1ms and the gradient strength was $1.66*10^{-2}$ T/m.

2.7. Particle Size Analysis

Particle size distribution of emulsions were analyzed by using Malvern Mastersizer 2000 particle size analyzer (Worchester, United Kingdom) at discrete time intervals (1, 8, 14 and 28th days) during storage. Refractive index, density and absorption index were used as 1.52, 0.9 g/ml and 0.01; respectively.

2.8. Small and Wide Angle X-Ray Scattering Analysis

An HECUS System3 was used to measure the scattered intensities (I) as a function of the magnitude of scattering vectors [I(q)-q] in q range of 0.003-0.1 $Å^{-1}$. The used camera has a Kratky collimator system (Hecus M. Braun-Graz X-ray Systems) on a conventional X-ray source (Seifert generator ID3003, CuKα=1.54 Å, Ni filter, and 40 kV- 50 mA: 2kW). The measured 1024 data (in 900 sec.) for each samples were evaluated by using EasySWAXS (HECUS software), IGORpro, GNOM and

DAMMIN programs (Franke & Svergun, 2009; Kline, 2006; Semenyuk & Svergun, 1991).

2.9. Statistical Analysis

Experiments were conducted in duplicate. Data were analyzed by using Minitab 16 (Minitab Inc., Penn State, USA). ANOVA was conducted at 95% confidence interval. Tukey multiple comparison test was used if significant differences were found between the samples. All statistical analysis results are given in Appendix A-I.

CHAPTER 3

RESULTS AND DISCUSSION

3.1. Particle Size Analysis

Particle size of emulsions were given as Sauter mean diameter (D[3,2]) and volume weighted mean diameter (D[4,3]). D[3,2] values of the SC emulsions were in the range of 0.182 and 0.188 µm at the 1st day measurements, and no significant changes was determined in SC samples due to HHP processing. This may be caused that SC was already produced smaller particle and the volume decrease due to increase pressure, was not sufficient for the significant droplet size change. However, SC_unpressurized, SC_100_10_15, SC_100_20_15 and SC_500_40_15 results have significantly affected by storage time as shown in Table 2. The changes in D[3,2] values of SC samples became significant at 14th day of storage, Sauter mean diameter were the largest at that day in unpressurized sample but the smallest in the pressurized samples. Also, it can be seen that it is a reversible change for the pressurized sample. D[3,2] values of the 80H_XG droplets were in the range of 3.200 and 6.489 µm at the 1st day measurements. HHP application and storage were both effective on particle size ($p<0.05$). HHP caused a significant change in Sauter mean particle size and general trend is that pressurization may produce smaller particle sizes in 80H_XG emulsions. This may be caused by the pressure application which forces the system for volume reduction and solid particle can be ordered towards more complex structures. In addition, particle size change during storage has a similar trend for each 80H_XG sample and particle size generally at the largest values at 14th day of storage (Table 2).

Volume weighted mean diameter (D[4,3]) results gave similar results and trends with Sauter mean diameter with respect to storage time (Table 3). In addition, the particle size increase at 14th day of storage became very remarkable. However, in 80H_XG samples, significant droplet size difference cannot be observed between pressurized and unpressurized samples.

D[4,3] is sensitive to larger particles, the increase in D[4,3] values is an indication of aggregation or flocculation in the emulsions (Salminen et al., 2014). The results were higher at the 14th day of storage in both SC and 80H_XG emulsions may be the indication of partial coalescence mechanism where droplets adhere with each other but each of them maintain its integrity (Sevdin, Özel, Yücel, Öztop, & Alpas, 2017). The structure inside the droplets is one of the factors affecting the partial coalescence rate. According to Sugimoto et al. (2001), β-crystal may increase the partial coalescence rate due to their needle-like structure. This needle-like structure may prick the droplet wall of its own and also the other droplets, finally increasing the partial coalescence rate. This droplet wall rupture may further cause the leakage of the inside material to the continuous phase. Therefore, increase in D[4,3]values of the samples specified above can be explained with the beginning of the partial coalesce process and the decrease can be explained with the leakage theory.

When the emulsifier effect on particle size was analyzed, it can be easily seen that SC led to formation of smaller particles ($p<0.05$) during emulsification than the 80H_XG. SC has very strong amphiphilic characteristics so it can be associated with the interface very rapidly during emulsification process (Sevdin, Özel, et al., 2017). Therefore, newly formed oil droplets can be stabilized by SC and emulsions with small droplet size can be produced (Eric Dickinson, 1999; Eric Dickinson & Golding, 1997).

Table 2. Sauter mean diameter (D[3,2]) results of emulsions during storage

Sample Name	Sauter Mean Diameter ± SD* (µm)			
	1st day	8th day	14th day	28th day
SC_unpressurized	0.182±0.005^{BC}	0.182±0.002^{C}	0.179±0.004^{A}	0.185±0.000^{AB}
SC_100_10_15	0.185±0.002	0.182±0.001	0.192±0.002	0.188±0.000
SC_100_20_15	0.183±0.001^{AB}	0.182±0.000^{AB}	0.176±0.004^{B}	0.187±0.003^{A}
SC_100_40_15	0.188±0.001^{A}	0.181±0.001^{B}	0.182±0.003^{B}	0.189±0.001^{A}
SC_500_10_15	0.185±0.003	0.181±0.002	0.183±0.005	0.184±0.002
SC_500_20_15	0.186±0.002	0.182±0.001	0.187±0.013	0.187±0.002
SC_500_40_15	0.188±0.004^{A}	0.182±0.000^{AB}	0.176±0.001^{B}	0.187±0.004^{A}
80H_XG_unpressurized	5.177±0.374^{D,b}	10.763±0.545^{C,a}	17.843±0.468^{A,a}	13.633±0.899^{B,a}
80H_XG_100_10_15	6.489±0.144^{B,a}	6.033±0.277^{B,cd}	9.647±0.756^{A,cd}	10.167±0.741^{A,b}
80H_XG_100_20_15	3.358±0.293^{D,d}	6.320±0.603^{C,bcd}	12.107±0.642^{A,b}	8.833±0.538^{B,bc}
80H_XG_100_40_15	3.533±0.209^{B,cd}	7.230±0.474^{A,bc}	7.017±0.503^{A,e}	4.143±0.188^{B,e}
80H_XG_500_10_15	4.445±0.423^{D,bc}	7.040±0.184^{C,bc}	12.653±0.760^{A,b}	9.923±0.625^{B,b}
80H_XG_500_20_15	4.753±0.293^{C,b}	7.610±0.663^{B,b}	10.667±0.685^{A,bc}	6.573±0.658^{BC,d}
80H_XG_500_40_15	3.200±0.283^{D,d}	4.987±0.161^{C,d}	8.173±0.071^{A,de}	6.967±0.666^{B,cd}

*SD: Standard Deviation
**All data are expressed as mean ± standard deviation (n=3). Only significantly different results were lettered. The results that do not share a letter are significantly different according to Tukey with 95% confidence interval. The capital letters show a sample's significant difference between Sauter mean diameters with respect to storage time. The small letters show samples' Sauter mean diameter at a specific day. Comparisons were conducted for each emulsifier separately.

Table 3. Volume weighted mean diameter (D[4,3]) results of emulsions during storage

Sample Name	Volume Weigthed Mean Diameter ± SD* (µm)			
	1st day	8th day	14th day	28th day
SC_unpressurized	0.266±0.004^{B**}	0.259±0.007^{B}	0.539±0.026^{A,b}	0.276±0.001^{B,b}
SC_100_10_15	0.278±0.007^{B}	0.256±0.005^{B}	0.732±0.027^{A,a}	0.283±0.004^{B,b}
SC_100_20_15	0.279±0.008^{BC}	0.264±0.002^{C}	0.387±0.027^{A,c}	0.326±0.025^{B,a}
SC_100_40_15	0.280±0.007^{B}	0.249±0.000^{C}	0.465±0.001^{A,bc}	0.287±0.004^{B,b}
SC_500_10_15	0.270±0.002^{B}	0.254±0.003^{B}	0.500±0.018^{A,b}	0.274±0.004^{B,b}
SC_500_20_15	0.274±0.004^{B}	0.250±0.000^{B}	0.515±0.037^{A,b}	0.282±0.009^{B,b}
SC_500_40_15	0.280±0.007^{B}	0.258±0.007^{B}	0.466±0.043^{A,bc}	0.284±0.007^{B,b}
80H_XG_unpressurized	22.500±1.061^{B}	25.000±1.445^{B}	37.267±2.779^{A,bc}	33.367±3.163^{A,ab}
80H_XG_100_10_15	23.900±2.351^{C}	27.533±2.604^{BC}	45.367±1.775^{A,b}	33.800±2.177^{B,a}
80H_XG_100_20_15	18.427±1.593^{C}	27.400±2.099^{BC}	70.647±7.053^{A,a}	33.433±1.517^{B,ab}
80H_XG_100_40_15	22.000±1.364^{B}	29.17±0.850^{A}	2.867±0.519^{A,c}	22.867±2.027^{B,c}
80H_XG_500_10_15	21.900±1.818^{B}	30.167±1.700^{B}	84.933±7.583^{A,a}	34.100±0.712^{B,a}
80H_XG_500_20_15	22.567±2.254^{B}	31.033±2.968^{B}	44.233±3.738^{A,bc}	27.000±1.393^{B,bc}
80H_XG_500_40_15	20.233±0.754^{C}	27.533±1.922^{B}	43.467±1.008^{A,bc}	31.600±1.283^{B,ab}

*SD: Standard Deviation
**All data are expressed as mean ± standard deviation (n=3). Only significantly different results were lettered. The results that do not share a letter are significantly different according to Tukey with 95% confidence interval. The capital letters show a sample's significant difference between volume weighted mean diameters with respect to storage time. The small letters show samples' volume weighted mean diameter at a specific day. Comparisons were conducted for each emulsifier separately.

3.2. Melting and Crystallization Characteristics of Emulsions

DSC heating and cooling thermograms were used to study the crystallization behavior and the nature of crystalline structure as a function of emulsifier type, HHP treatment (P-T-t) and storage, respectively. Temperature limits for preparation conditions and DSC analysis were selected according the result of full scanned (-10 to 70 °C and 70 to -10 °C) DSC thermograms of unpressurized emulsion produced with sodium caseinate in which melting was observed between 40 to 57 °C and crystallization was observed between 35 to 23 °C (Figure 12). Therefore, the heating thermogram from 35 to 70 °C was used to characterize the crystalline structure and polymorphic form. The cooling thermogram from 70 to -10 °C was used to characterize the onset point of crystallization and differentiate surface crystallization properties as discussed below.

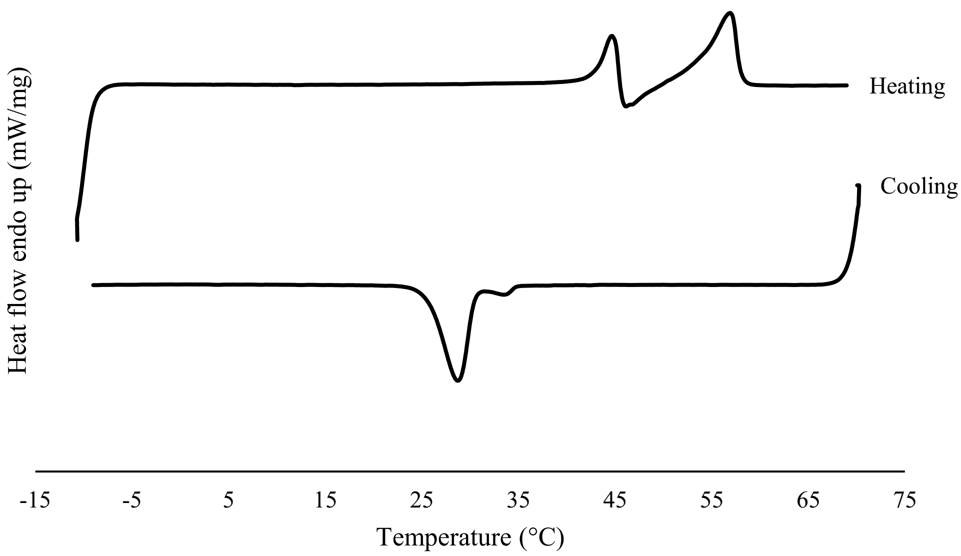

Figure 12. DSC heating and cooling thermograms of unpressurized palm stearin-sodium caseinate sample at first day (heat flow was normalized to sample weight)

DSC heating thermograms indicated that there were two crystal structures in SC samples and three crystal structure can be observed in 80H_XG samples. Thermograms of unpressurized and pressurized at 500 MPa and 40 °C SC and 80H_XG samples, were given in Figure 13
as an example. The first peak corresponded to less dense α-crystal structure with a melting temperature at 45°C and the second one corresponded to β-crystal structures with a melting temperature at 56°C. Similar results were also reported by

Sonoda et al. (2004). The melting characteristics of α and β crystals in SC emulsions and α, β and the 3rd structure in 80H_XG were shown in Table 4 - *6*, respectively.

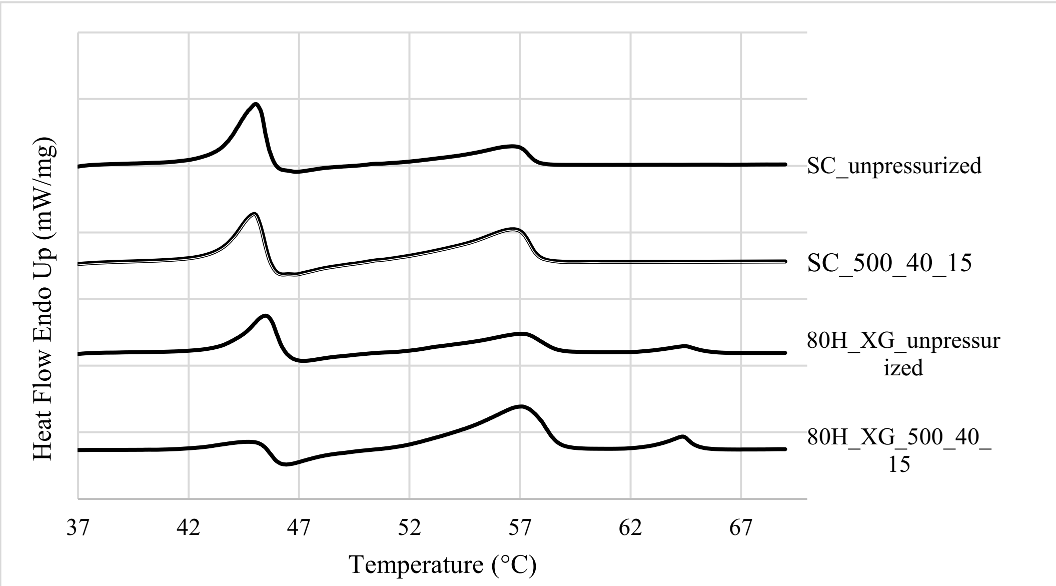

Figure 13. First day heating thermograms of selected palm stearin emulsions (heat flow was normalized to sample weight)

According to the results, melting temperature of α crystals decreased significantly during storage period in samples of 80H_XG_100_20_15 80H_XG_500_40_15, SC_unpressurized and SC_500_40_15. Also, at the first day, a decrease in α crystal melting temperature in comparison with the unpressurized sample was observed in the SC_100_10_15, SC_500_10_15, SC_500_20_15 samples. The decrease in melting temperature may be caused by the increase in number of lattice defects in the lipid crystal network (Freitas & Müller, 1999).

After the analysis of crystal structures' melting temperature, melting enthalpies of each crystal structure were used to calculate crystal content in emulsions as percent ratio showed. The crystal content ratio in the samples of SC and 80H_XG are shown in Figure 14 and Figure 15, respectively. The numeric results and lettering according statistical results were given in Table 4 - **6**.

According to the analysis, it was found that emulsifier type is significantly effective on crystal composition of emulsions and 80H_XG emulsions had higher β-crystal content than SC emulsions ($p<0.05$). Also, it was observed that all pressurized samples contained lower α crystal content than the unpressurized ones at the first day ($p<0.05$). This result proved that pressure by itself has a significant effect on the crystal content where pressure favoring volume reduction that further triggers the formation of β crystals which is a denser form (Coupland, 2002; Sonoda et al., 2004). Pressurization temperature had no significant effect on crystal content of emulsion at 500 MPa, but at 100 MPa ($p<0.05$). It was observed that the sample which was pressurized at 100 MPa and 10 °C had more α crystal content compared to other temperatures studied at the same pressure level. Based on the results it may be proposed that pressurization temperature is effective on the crystal structure at/around 100 MPa but the same effect of temperature may not be differentiated at higher pressurization levels at/around 500 MPa. A similar changing trend in crystal content can be observed when the effect of emulsifier-pressure and emulsifier-storage time interactions were examined ($p<0.05$). SC samples had higher α crystal content than 80H samples of unpressurized and pressurized samples at 100 MPa. However, when the pressurization level reached up to 500 MPa, the difference that was coming from the emulsifier difference has disappeared.

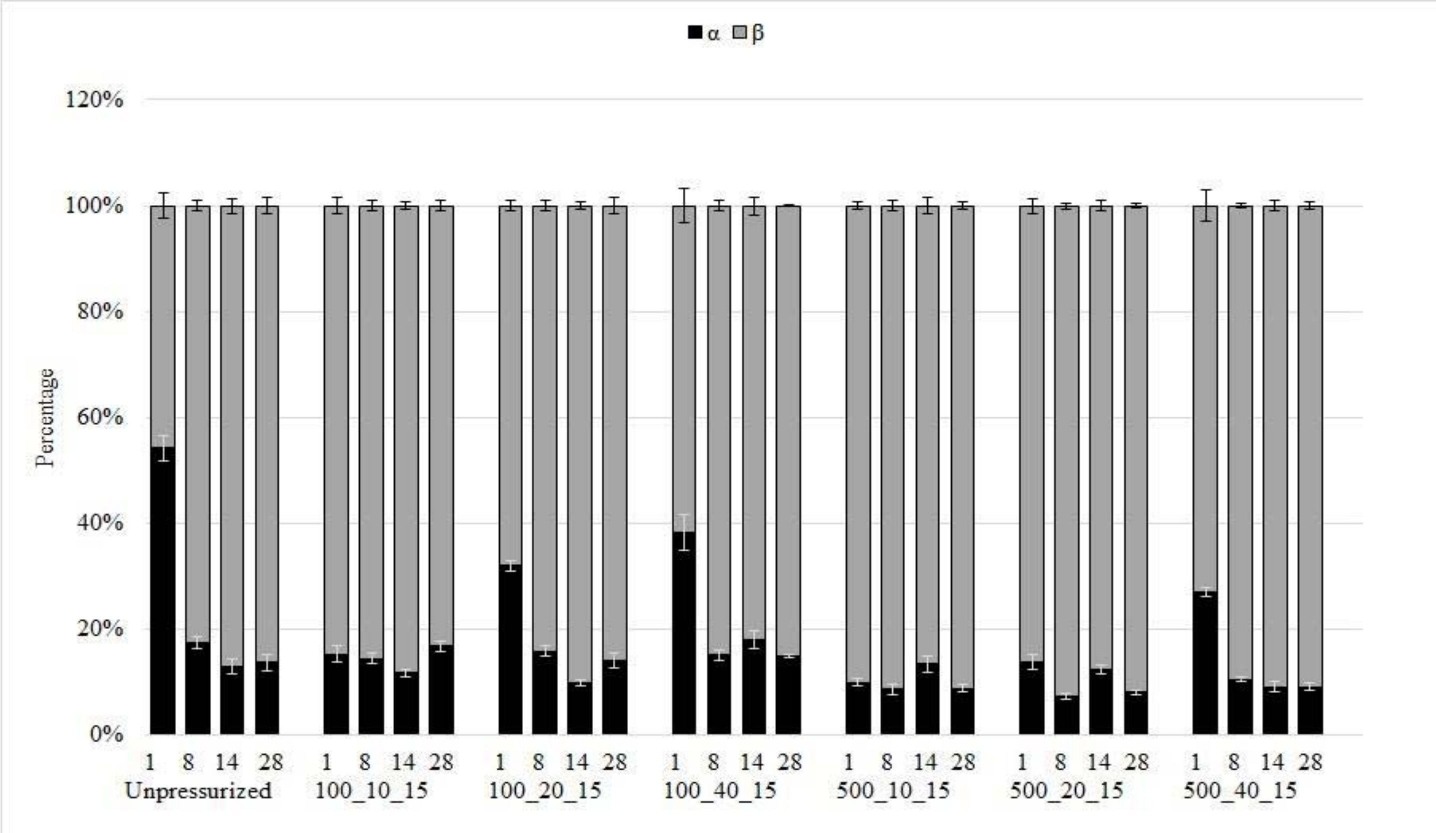

Results maintained during storage for each sample are showed in a single cluster and the name of the sample is written beneath the clusters. In each cluster, from left to right, the bars are representing 1st, 8th, 14th and 28th day of storage respectively.

Figure 14. Polymorph fraction of SC emulsions.

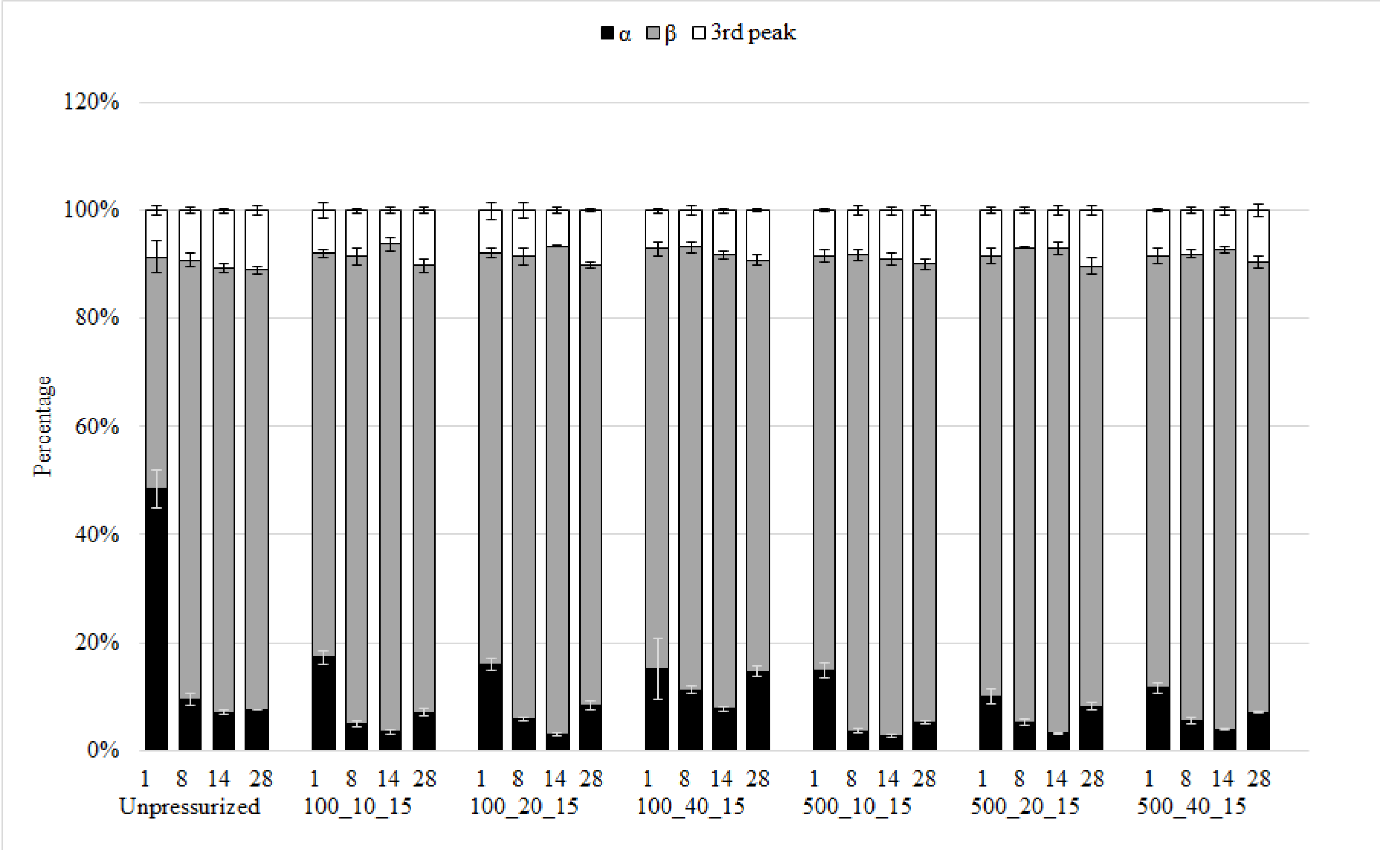

Results maintained during storage for each sample are showed in a single cluster and the name of the sample is written beneath the clusters. In each cluster, from left to right, the bars are representing 1st, 8th, 14th and 28th day of storage respectively.

Figure 15. Polymorph fraction of 80H_XG emulsion.

Table 4. α crystal melting temperature and content with respect to storage

Sample Name	1st day		8th day		14th day		28th day	
	Melting T (°C)	Content (%)	Melting T (°C)	Content (%)	Melting T (°C)	Content (%)	Melting T (°C)	Content (%)
SC_unpressurized	45.10±0.04^{A,a}	54.21±2.34^{A,a}	44.55±0.17^{B}	17.44±1.09^{B,a}	44.31±0.08^{B}	13.12±1.41^{B,bc}	44.56±0.18^{B}	13.71±1.52^{B,a}
SC_100_10_15	44.49±0.24^{b}	15.37±1.50^{AB,d}	44.51±0.16	14.52±1.07^{AB,a}	44.25±0.17	11.80±0.76^{B,bc}	44.57±0.15	16.88±1.01^{A,a}
SC_100_20_15	44.79±0.20^{ab}	32.03±1.06^{A,c}	44.52±0.16	15.88±0.96^{B,a}	44.29±0.09	9.94±0.62^{C,bc}	44.55±0.11	14.06± 1.46^{B,a}
SC_100_40_15	44.87±0.21^{ab}	38.38±3.34^{A,b}	44.91±0.38	15.17±1.02^{B,a}	44.45±0.03	18.04±1.67^{b,A}	44.59±0.11	15.02±0.25^{B,a}
SC_500_10_15	44.34±0.16^{b}	9.95±0.75^{B,d}	44.35±0.10	8.71±1.03^{B,b}	44.32±0.27	13.42±1.54^{A,b}	44.28±0.06	8.84±0.682^{B,b}
SC_500_20_15	44.42±0.09^{b}	13.86±1.42^{A,d}	44.30±0.05	7.48±0.56^{B,b}	44.28±0.16	12.44±0.87^{A,bc}	44.30±0.05	8.17±0.47^{B,b}
SC_500_40_15	44.74±0.16^{A,ab}	26.43±0.81^{A,c}	44.44±0.10^{AB}	10.56±0.47^{B,b}	44.25±0.12^{B}	9.16±0.92^{B,c}	44.46±0.04^{AB}	9.16±0.68^{B,b}
80H_XG_unpressurized	45.27±0.30	48.45±3.46^{A,a}	44.88±0.34^{a}	9.44±1.06^{B,a}	44.82±0.26^{a}	7.03±0.48^{B,a}	44.80±0.22^{B}	7.55±0.11^{B,b}
80H_XG_100_10_15	44.79±0.48	17.25±1.37^{A,b}	44.14±0.21^{ab}	5.05±0.53^{BC,bc}	43.90±0.17^{bc}	3.47±0.39^{C,bc}	44.45±0.43	7.06±0.67^{B,bc}
80H_XG_100_20_15	44.80±0.46^{A}	15.92±1.17^{A,b}	44.31±0.10^{AB,ab}	5.90±0.26^{C,b}	43.73±0.13^{B,c}	3.03±0.16^{D,bc}	44.43±0.35^{AB}	8.36±0.91^{B,b}
80H_XG_100_40_15	44.98±0.19	15.07±5.61^{A,b}	44.57±0.43^{ab}	11.29±0.68^{a}	44.57±0.32^{ab}	7.67±0.51A	44.80±0.29	14.67±0.92^{a}
80H_XG_500_10_15	44.61±0.56	14.86±1.33^{A,b}	43.79±0.09^{b}	3.66±0.49^{BC,c}	43.59±0.27^{c}	2.67±0.26^{C,c}	44.12±0.24	5.26±0.23^{B,c}
80H_XG_500_20_15	44.58±0.42	10.03±1.30^{A,b}	43.99±0.20^{b}	5.30±0.50^{B,bc}	43.76±0.18^{c}	3.18±0.19^{B,bc}	44.34±0.16	8.13±0.68^{A,b}
80H_XG_500_40_15	44.71±0.34^{A}	11.63±1.09^{A,b}	44.16±0.12^{AB,ab}	5.48±0.53^{BC,bc}	43.80±0.05^{B,c}	3.98±0.22^{C,b}	44.09±0.25^{AB}	6.98±0.12^{B,bc}

All data are expressed as mean ± standard deviation (n=3). Only significantly different results were lettered.
(A-C) The capital letters show a sample's significant difference between its α crystal melting temperatures and contents with respect to storage time. The results that do not share a letter are significantly different according to Tukey test with 95% confidence interval.
(a-c) The small letters show samples' α crystal melting temperature and content at a specific day.
The results that do not share a letter are significantly different according to Tukey test with 95% confidence interval. Comparisons were conducted for melting temperature, content and each emulsifier separately.

Table 5. β crystal melting temperature and content with respect to storage

Sample Name	1st day		8th day		14th day		28th day	
	Melting T (°C)	Content (%)	Melting T (°C)	Content (%)	Melting T (°C)	Content (%)	Melting T (°C)	Content (%)
SC_unpressurized	56.58±0.07	$45.79±2.34^{B,d}$	56.76±0.00	$82.56±1.09^{A,b}$	56.47±0.06	$86.88±1.41^{A,ab}$	56.70±0.06	$86.29±1.52^{A,b}$
SC_100_10_15	56.75±0.03	$84.63±1.50^{AB,a}$	56.85±0.11	$85.48±1.07^{AB,b}$	56.70±0.07	$88.20±0.76^{A,ab}$	56.66±0.05	$83.12±1.01^{B,b}$
SC_100_20_15	56.78±0.05	$67.97±1.06^{C,bc}$	56.75±0.06	$84.12±0.96^{B,b}$	56.74±0.04	$90.06±0.62^{A,ab}$	56.70±0.05	$85.94±1.46^{B,b}$
SC_100_40_15	56.70±0.06	$61.62±3.34^{B,c}$	56.70±0.07	$84.83±1.02^{A,b}$	56.69±0.01	$81.96±1.67^{A,c}$	56.68±0.04	$84.98±0.25^{A,b}$
SC_500_10_15	56.72±0.03	$90.05±0.75^{A,a}$	56.67±0.07	$91.29±1.03^{A,a}$	56.66±0.12	$86.58±1.54^{B,b}$	56.63±0.04	$91.16±0.68^{A,a}$
SC_500_20_15	$56.68±0.02^{AB}$	$86.14±1.42^{B,a}$	$56.71±0.06^{A}$	$92.52±0.56^{A,a}$	$56.66±0.03^{AB}$	$87.56±0.87^{B,ab}$	$56.57±0.03^{B}$	$91.83±0.47^{A,a}$
SC_500_40_15	56.72±0.06	$71.57±0.81^{B,b}$	56.62±0.08	$89.44±0.47^{A,a}$	56.70±0.04	$90.84±0.92^{A,a}$	56.66±0.08	$90.84±0.68^{A,a}$
80H_XG_unpressurized	57.55±0.04	$42.93±3.46^{B,c}$	57.34±0.10	$81.36±1.06^{A,c}$	57.46±0.18	$82.38±0.48^{A,b}$	57.31±0.41	$81.40±0.11^{A,a}$
80H_XG_100_10_15	57.44±0.23	$74.86±1.37^{C,b}$	57.08±0.36	$87.07±0.53^{A,a}$	56.74±0.49	$90.30±0.39^{A,a}$	57.30±0.22	$82.72±0.67^{B,a}$
80H_XG_100_20_15	56.98±0.15	$76.28±1.17^{D,b}$	57.07±0.30	$85.62±0.26^{B,ab}$	56.80±0.58	$90.29±0.16^{A,a}$	57.11±0.25	$81.52±0.91^{C,a}$
80H_XG_100_40_15	56.94±0.08	$77.85±5.61^{B,ab}$	56.83±0.31	$81.89±0.68^{A,bc}$	56.93±0.27	$84.09±0.51^{A,b}$	56.91±0.07	$76.19±0.92^{B,b}$
80H_XG_500_10_15	57.03±0.21	$76.65±1.33^{C,ab}$	56.97±0.41	$88.13±0.49^{AB,a}$	56.93±0.56	$88.27±0.26^{A,a}$	57.23±0.25	$84.83±0.23^{B,a}$
80H_XG_500_20_15	56.95±0.17	$81.58±1.30^{B,a}$	56.85±0.55	$87.81±0.50^{A,a}$	56.82±0.54	$89.84±0.19^{A,a}$	56.90±0.13	$81.60±0.68^{B,a}$
80H_XG_500_40_15	56.90±0.12	$79.86±1.09^{C,ab}$	56.85±0.30	$86.42±0.53^{AB,a}$	56.72±0.20	$88.78±0.22^{A,a}$	57.02±0.29	$83.46±0.12^{B,a}$

All data are expressed as mean ± standard deviation (n=3). Only significantly different results were lettered.
(A-D) The capital letters show a sample's significant difference between its β crystal melting temperatures and contents with respect to storage time. The results that do not share a letter are significantly different according to Tukey test with 95% confidence interval.
(a-d) The small letters show samples' β crystal melting temperature and content at a specific day.
The results that do not share a letter are significantly different according to Tukey test with 95% confidence interval. Comparisons were conducted for melting temperature, content and each emulsifier separately.

A 3rd structure in 80H_XG emulsions was observed and proposed as a solid wall structure around the emulsion droplets, since soy lecithin with high-melting point has an effect mechanism during production of emulsion. When soy lecithin absorbed the interface, it crystallizes prior to oil and act as a crystal nuclei for the oil inside the droplets. This preformed crystal layer around the droplets can be called as a solid wall structure. Melting temperature of solid wall was not affected from HHP process and storage time ($p<0.05$) (Table 6). However, solid wall content affected by storage time especially in some samples (80H_XG_unpressurized, 80H_XG_100_10_15, 80H_XG_100_20_15 and 80H_XG_500_20_15). At the end of the storage period solid wall content reached at maximum point for all mentioned samples. In addition, according to results obtained at the 14th day, solid wall content is relatively high in unpressurized 80H_XG sample rather than pressurized one. This may be concluded as β crystal and solid wall structure become competitive structures towards the end of the storage period.

Table 6. 3rd structure melting temperature and content with respect to storage

Sample Name	1st day		8th day		14th day		28th day	
	Melting T (°C)	Content (%)	Melting T (°C)	Content (%)	Melting T (°C)	Content (%)	Melting T (°C)	Content (%)
80H_XG_unpressurized	64.39±0.05	8.62±0.91^{B}	64.40±0.12	9.20±0.60^{AB}	64.51±0.13	10.60±0.40^{AB,a}	64.38±0.05	11.06±0.92^{A}
80H_XG_100_10_15	64.33±0.04	7.89±1.44^{AB}	64.37±0.07	8.55±0.44^{AB}	64.32±0.05	6.23±0.66^{B,c}	64.35±0.05	10.22±0.64^{A}
80H_XG_100_20_15	64.25±0.21	7.79±1.55b	64.41±0.04	8.49±1.30^{B}	64.32±0.03	6.69±0.64^{AB,c}	64.37±0.03	10.11±0.35^{A}
80H_XG_100_40_15	64.36±0.01	7.09±0.42	64.36±0.05	6.82±0.82	64.35±0.03	8.23±0.44^{bc}	64.35±0.10	9.14±0.34
80H_XG_500_10_15	64.27±0.09	8.49±0.31	64.37±0.09	8.21±0.78	64.36±0.02	9.05±0.72^{ab}	64.37±0.12	9.91±0.83
80H_XG_500_20_15	64.37±0.03	8.39±0.61^{AB}	64.29±0.16	6.89±0.54^{B}	64.37±0.03	6.98±0.85^{B,bc}	64.37±0.02	10.27±0.92^{A}
80H_XG_500_40_15	64.38±0.02	8.51±0.28	64.37±0.09	8.10±0.61	64.12±0.40	7.24±0.70^{bc}	64.39±0.04	9.56±1.18

All data are expressed as mean ± standard deviation (n=3). Only significantly different results were lettered.
(A-B) The capital letters show a sample's significant difference between its 3rd crystal structure melting temperatures and contents with respect to storage time. The results that do not share a letter are significantly different according to Tukey test with 95% confidence interval.
(a-c) The small letters show samples' 3rd crystal structure melting temperature and content at a specific day.
The results that do not share a letter are significantly different according to Tukey test with 95% confidence interval. Comparisons were conducted for melting temperature, content and each emulsifier separately.

3.3. NMR Relaxometry and Self Diffusion Coefficient Determination

In addition to the direct effects of applied pressure on polymorph contents; T_2 and SDC, storage time after HHP also had significant impacts. Firstly, longer storage times induced higher content of more ordered crystal contents (Table 4- **6**).
The steep decrease in α content and respective increase in β and solid lipid wall content was observed between the 1st and the 8th day of storage ($p<0.05$). The crystal ratios were more or less the same from the 8th day up to 28th day, however, as a general trend both SC and 80H_XG samples showed the highest β contents at the 14th day of storage. HHP and storage time has no significant effect on T_2 relaxation time of SC samples (Figure 16). However, T_2 and SDC trends in 80H_XG samples were comparable to changes in morphology of samples since they showed a traceable pattern with respect to changes in α, β and solid wall contents. The lowest T_2 at 14th day, lower T_2 on the 8th and 28th day with respect to 1st day of storage were observed in 80H_XG samples and this was inversely proportional with the pressure results since higher pressures increase β contents which led to lower T_2 values (Figure 17). In this way, the higher β crystal formation during storage was observed by T_2 results. Formation of β crystals content were associated with a close and compact alignment of crystallized lipid molecules and these intense relations between ordered crystals can decrease the relaxation time of the system.

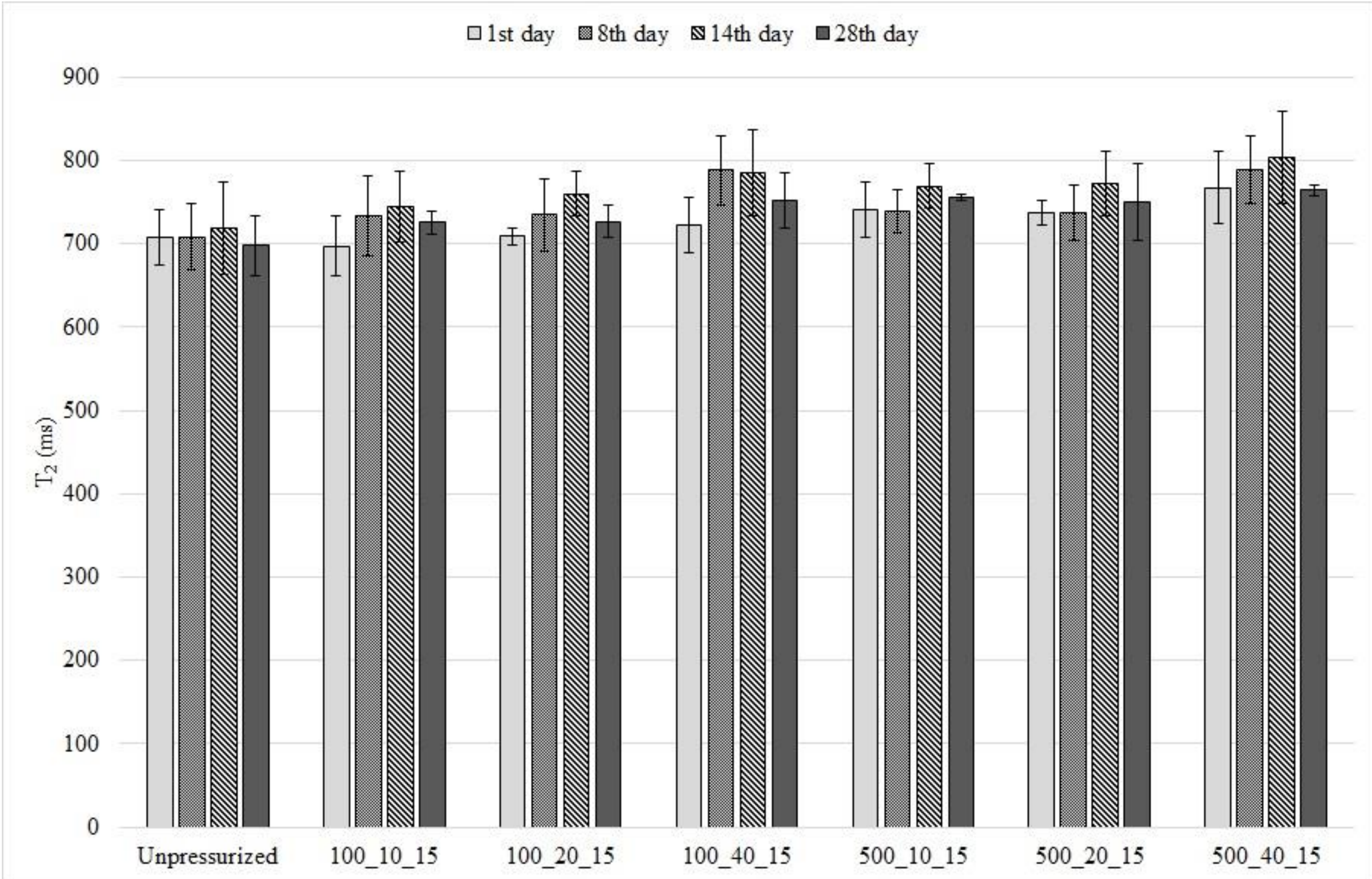

Figure 16. T_2 results of SC sample during storage

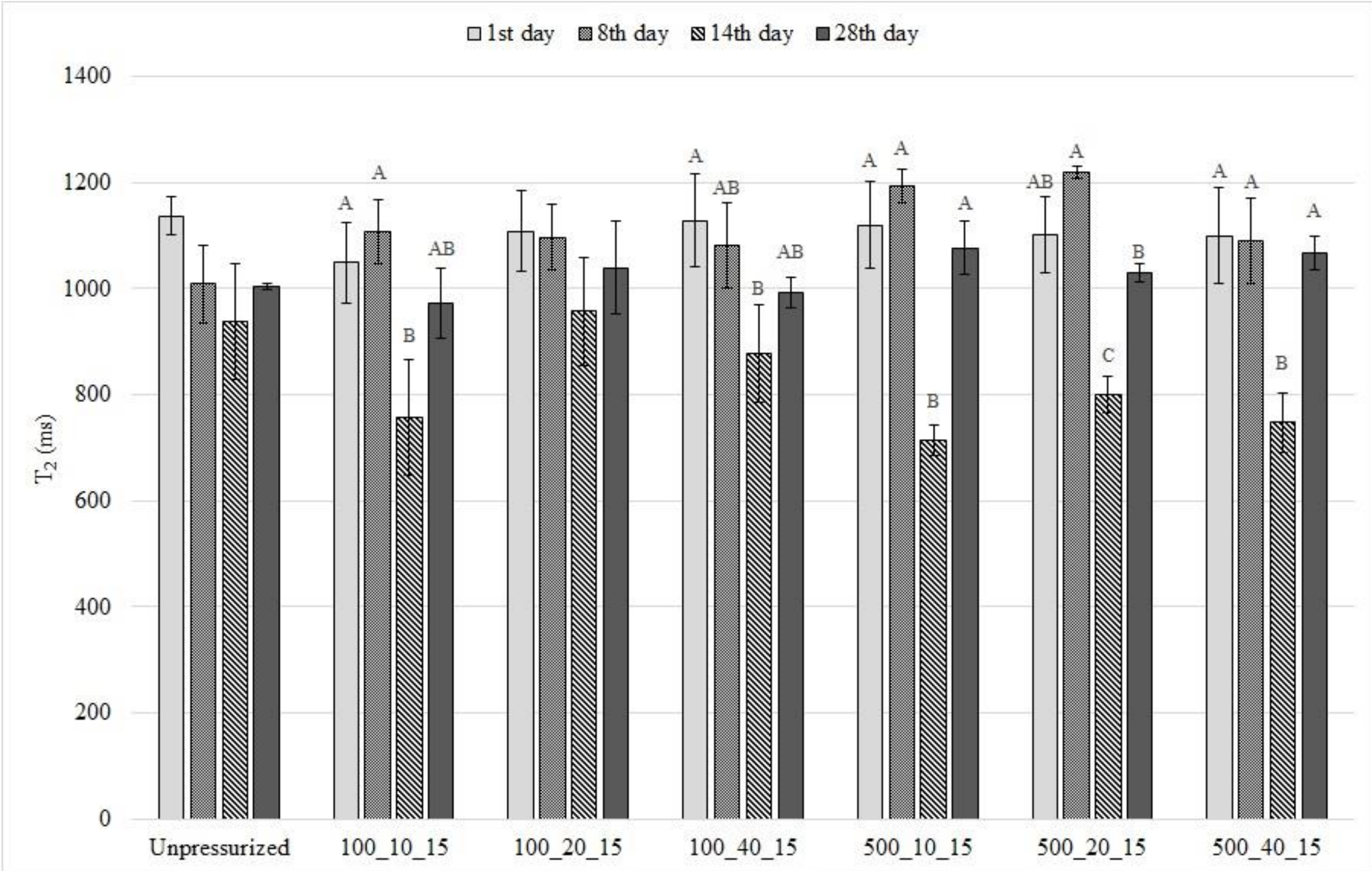

All data are expressed as mean ± standard deviation (n=3). Only significantly different results were lettered.
(A-C) The capital letters show a sample's significant difference between its T_2 results with respect to storage time. The results that do not share a letter are significantly different according to Tukey test with 95% confidence interval.

Figure 17. T_2 results of 80H_XG sample during storage

SDC results of SC samples were not affected by HHP application or storage time except SC_100_10_15 (Figure 18). This sample showed an increase in 8^{th} and 14^{th} day and reached to the maximum SDC value and then start to decrease during last week of storage. The increase in SDC suggested that up to 14^{th} day, water phase present in the emulsion system became more continuous. The statistically similar particle sizes of droplets at that time interval proved that claim since a change in the particle size promoted discontinuity in such systems (Eric Dickinson & Golding, 1997). Therefore, since diffusing water molecules did not experience a heterogeneous distribution of droplets in the emulsion, their SDC increased. However, SDC and T_2 experiments of 80H_XG samples exerted a straight correlation in storage experiments (Figure 17 and Figure 19). Both T_2 and SDC decreased with storage time up to 14^{th} day than they both experienced an increase on the 28^{th} day ($p<0.05$). Nevertheless, both the T_2 and SDC decreased between the 14^{th} and 28^{th} days. This phenomenon was also seen in overall α and β contents, with a slight increase in α crystals and slight decrease in β crystals on the 28^{th} day with respect to 14^{th} day. The observed changes could have been attributed to the beginning of destabilization on the 14^{th} day of the storage since a tendency for an increase in the presence of bigger droplets throughout the emulsion was also detected by particle size measurements (Table 2 and Table ***3***). On the 28^{th} day, the bigger particles formed on the 14^{th} day disappeared since significant decrease in bigger particle sizes (d_{43}) were observed at that day. There are some destabilization mechanisms proposed in the literature such as flocculation, coalescence and partial coalescence of droplets (Vanapalli, Palanuwech, & Coupland, 2002) as explained before. In this study, the beginning of slight destabilization on 14^{th} day was mainly attributed to the partial coalescence due to the dispersed oil phase fraction, emulsifier type and ratio characteristics of the prepared emulsions. As the storage time increased, previously formed β crystals began to penetrate through the droplet surface and overcome the surface resistance. These needle like crystals then took part in the partial coalescence leading to an increase in droplet size since these surface migrated crystals changed the surfactant conformation on the droplet surface (Sugimoto et al., 2001). The decline in the bigger droplet size on 28^{th} day with respect to 14^{th} day, originated from the diffusion of crystals from one droplet to another. The disruption of oil droplet surfaces by crystal migration from the interiors of the droplet to the surface occurred and this phenomenon altered the droplet shape. Consequently, bigger droplets were disrupted on the 28^{th} day and formation of more disordered α crystals proved this claim. The oil droplet aggregation is reported to have a viscosity increasing effect in emulsions which is also consistent with the decreasing trend of T_2 at the 14^{th} day of the storage (Sugimoto et al., 2001). The increased surfactant concentration and merging of droplets probably created new interaction sites for water and droplet surfaces resulting in lower T_2 on the 14^{th} day. The lower SDC similar to T_2 through at 14^{th} day of the storage, proved the more heterogeneous order of droplet size and distribution within the emulsion system. At that point water molecules encountered more impairment and hurdles during diffusing.

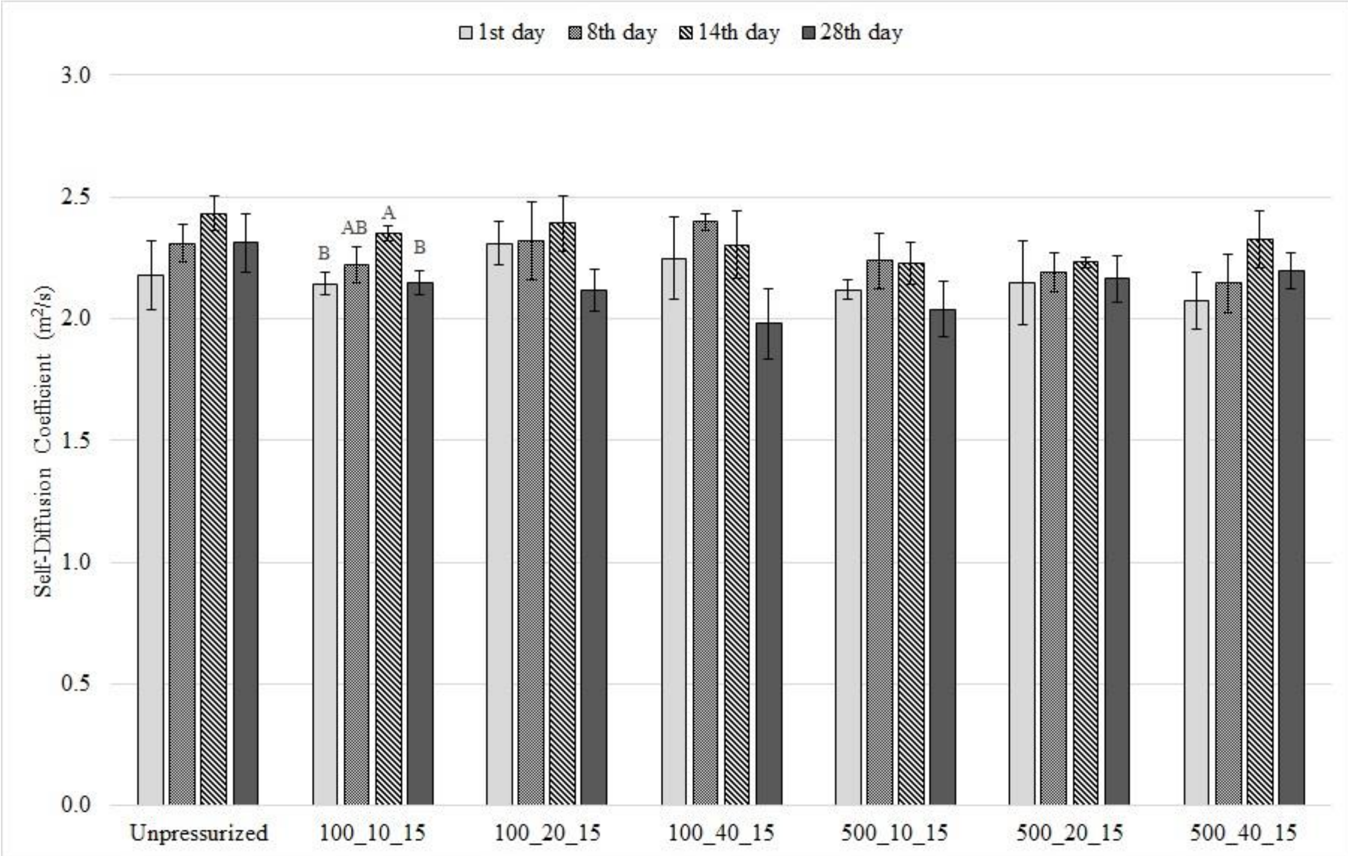

All data are expressed as mean ± standard deviation (n=3). Only significantly different results were lettered.
(A-B) The capital letters show a sample's significant difference between its self diffusion coefficient with respect to storage time. The results that do not share a letter are significantly different according to Tukey test with 95% confidence interval.

Figure 18. Self diffusion coefficient results of SC emulsions during storage

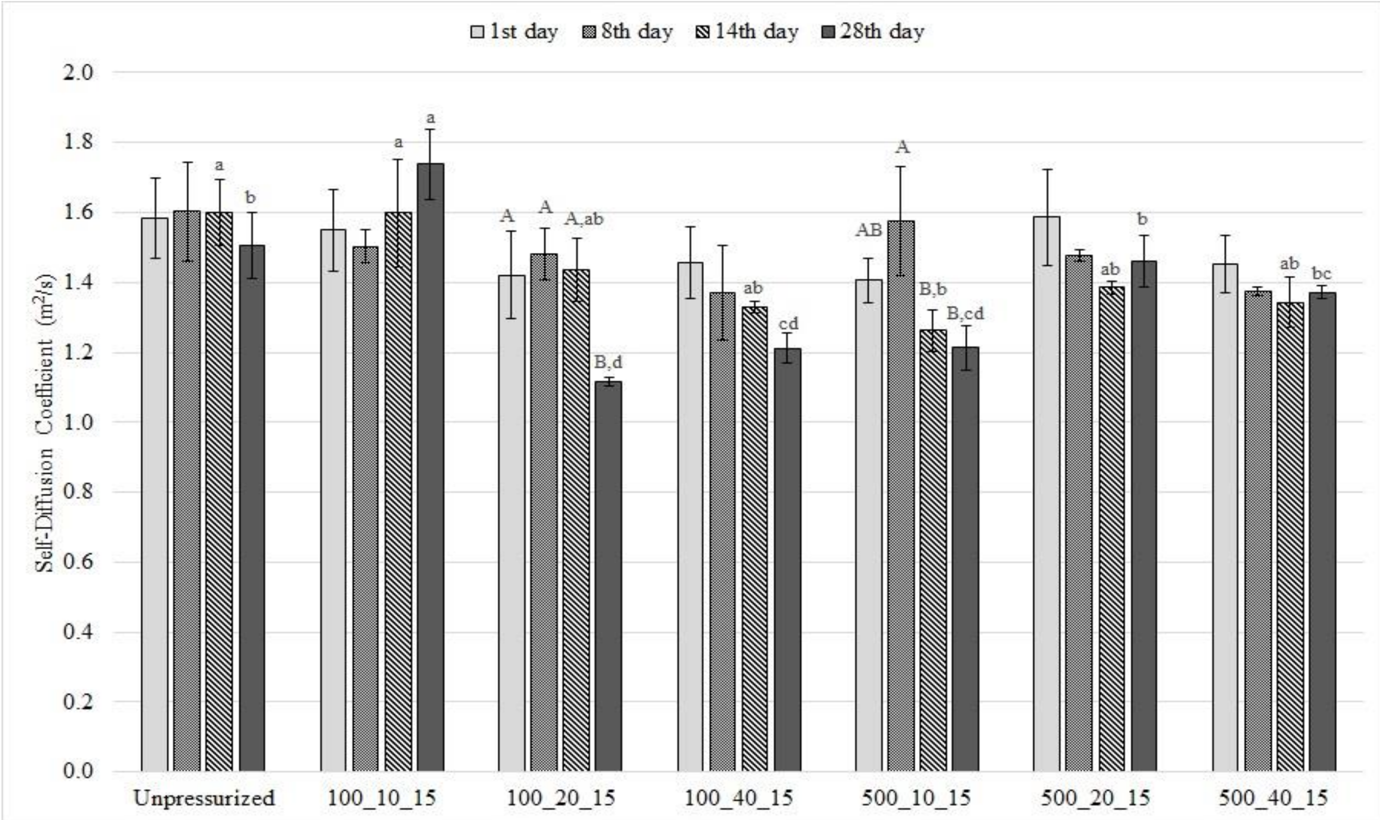

All data are expressed as mean ± standard deviation (n=3). Only significantly different results were lettered.
(A-B) The capital letters show a sample's significant difference between its self diffusion coefficient with respect to storage time. The results that do not share a letter are significantly different according to Tukey test with 95% confidence interval.
(a-d) The small letters show samples' self diffusion coefficients at a specific day.
The results that do not share a letter are significantly different according to Tukey test with 95% confidence interval.

Figure 19. Self diffusion coefficient results of 80H_XG emulsions during storage

3.4. Small Angle X-Ray Scattering (SAXS) Analysis

To monitor the structural changes in HHP treated emulsions, a set of SAXS experiments was designed. Main aim is to observe the effect of pressure not the temperature so the highest temperature (40 °C) in previous parts of the study was used as the pressurization temperature and pressure was applied at 5 different levels (100, 200, 300, 400 and 500 MPa). Lecithin samples were prepared without addition of xanthan gum to work on the similar particle sizes for both emulsion samples (SC emulsions and 80H emulsions) (Sevdin, Çınar Bam, Alpas, Öztop, & İde, 2017).

SAXS results of SC and 80H_XG emulsions were given in Figure 20 and Figure 21, respectively.

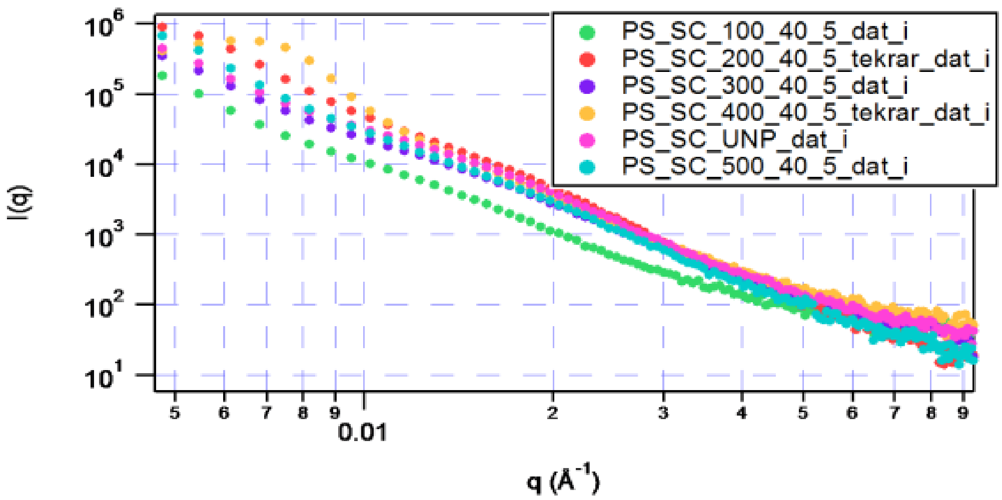

Figure 20. SAXS profile of SC emulsions

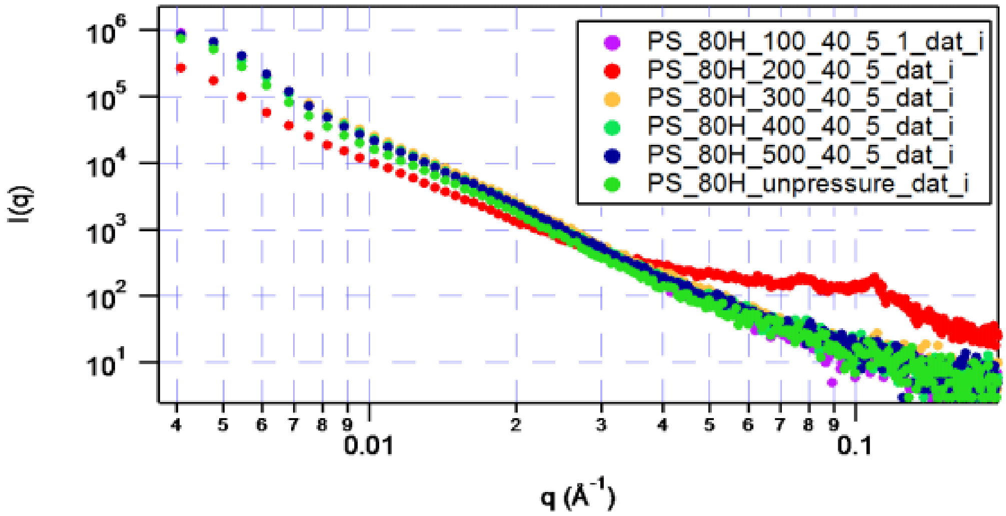

Figure 21. SAXS profile of 80H emulsions

SAXS profile of SC and 80H_XG emulsions had homogenously distributed nano-globular aggregations and revealed generally similar trends except two dramatically different samples; SC_400_40_5 and 80H_200_40_5. Radius of gyration (R_g) of samples were determined from Guinier region of the scattering graph and given in Table 7. SC_400_40_5 sample scattering results showed that larger aggregates or nanoparticles can be found in the samples however, gyration radius of this sample found as relatively smaller than the other SC samples, especially in globular and rod forms. 80H_200_40_5 sample results showed that surface to volume ratio is higher for that sample and gyration radius of rod and flat forms were determined as very smaller than the other 80H samples.

Table 7. Radius of gyration of SC and 80H emulsions

Samples	Gyration Radius (nm)		
	Globular	Rod	Flat
SC_unpressurized	42.2	27.9	17.0
SC_100_40_5	45.4	29.7	17.5
SC_200_40_5	37.5	29.2	17.3
SC_300_40_5	40.7	28.1	16.2
SC_400_40_5	34.8	25.8	16.7
SC_500_40_5	41.0	30.8	17.2
80H_unpressurized	46.8	34.6	21.2
80H_100_40_5	44.1	29.7	18.0
80H_200_40_5	44.4	19.2	14.7
80H_300_40_5	41.9	30.2	17.5
80H_400_40_5	42.9	31.2	19.4
80H_500_40_5	43.3	33.4	21.0

Due to these dramatic changes for given samples, further investigations were conducted and different sample types were prepared to observe the effect of ingredients on structure. Prepared samples were emulsifier-water mixtures without lipid addition (SC solution or 80H solution), SC and 80H emulsions. SC solution and SC emulsion were pressurized at 400 MPa and 40°C for 5 minutes and 80H solution and 80H emulsion were pressurized at 200 MPa and 40°C for 5 minutes.

The most possible 3D morphologies and their sizes were determined as seen in the Figure 22, after the data evaluation, fitting processing and *ab-initio* shape determination was conducted by using GNOM and DAMMIN programs.

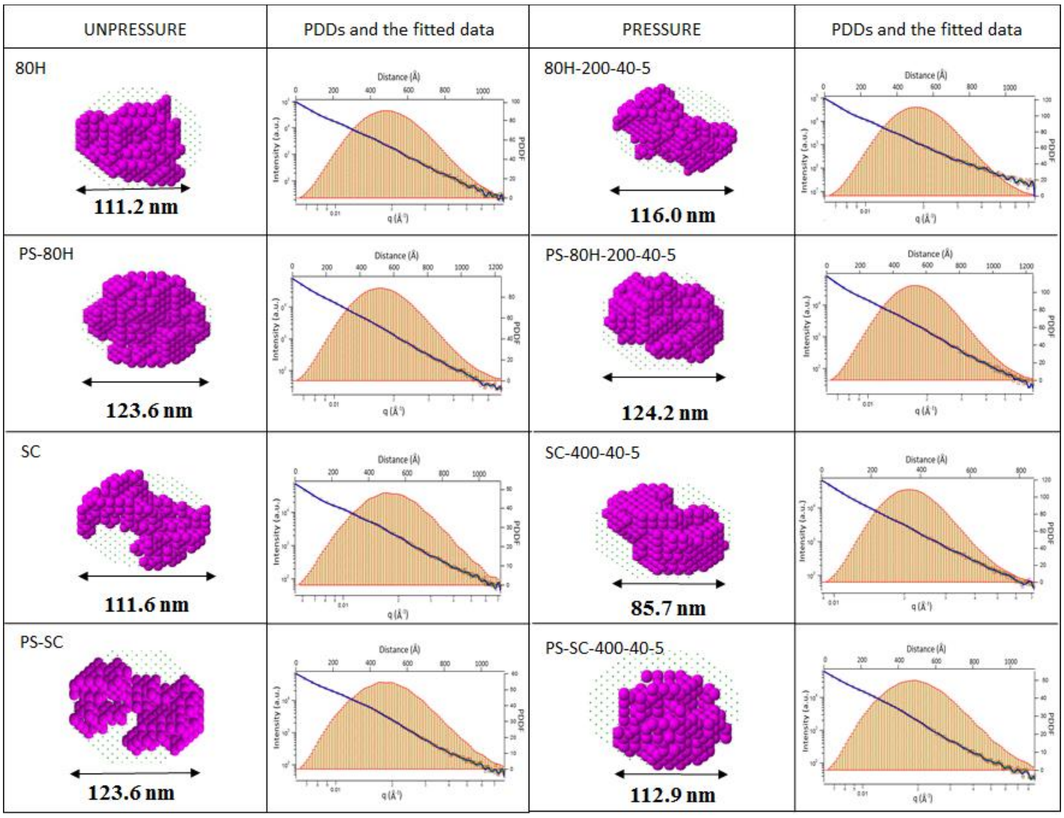

* Pink shapes show 3D morphologies and sizes of particles, graphs show pair distance distributions (PDDs) combined with the fitted data. 80H: unpressurized 80H solution, PS-80H: unpressurized 80H emulsion, 80H-200-40-5: 80H solution pressurized at 200 MPa and 40°C for 5 min., PS-80H-200-40-5: 80H emulsion pressurized at 200 MPa and 40°C for 5 min., SC: unpressurized SC solution, PS-SC: unpressurized SC emulsion, SC-400-40-5: SC solution pressurized at 400 MPa and 40°C for 5 min., PS-SC-400-40-5: SC emulsion pressurized at 400 MPa and 40°C for 5 min.

Figure 22. 3D morphologies, sizes and pair distance distributions of the nanoglobules in samples

Macromolecular structure of sodium caseinate (in single crystal form) is known and the previously carried out macromolecular shape is very similar to the presented *ab-initio* model for SC sample (in aqueous emulsion form) (Farrell Jr, Brown, & Malin, 2013). It was observed that, lipid addition caused an increase in particle size and globular-like formations in both SC and 80H samples. However, pressurization caused more globular forms and decrease in size for SC samples, while in 80H samples, it cannot be observed any significant change in particle size and structure shift to rod-like structure with respect to unpressurized 80H samples (Sevdin, Çınar Bam, et al., 2017).

CHAPTER 4

CONCLUSION

The effect of HHP treatment on lipid crystallization process was monitored at 100 and 500 MPa at 10, 20 and 40 °C for 15 minutes with two different emulsion samples. DSC, particle size analysis, NMR relaxation and self-diffusion coefficient measurements were conducted at 1^{st}, 8^{th}, 14^{th} and 28^{th} days of storage period at 4°C. Also, SAXS analysis were conducted for selected emulsion samples for the inspection of changes in structural conformation due to HHP process within in the 1^{st} week of storage. The statistical analysis revealed that the results can be generalized as follows;

- HHP has no significant effect on the melting temperature of polymorphs; but pressure and storage time have significant effect on crystal polymorphs' content in emulsions.
- HHP did not affect droplet size of SC emulsions so it is seen that mean particle size was affected by the types of emulsifiers and storage time.
- Sodium caseinate has a capability of producing smaller particles than 80H_XG emulsion.
- HHP treatment has the capacity of controlling lipid crystallization process and altering the crystal structure in emulsions. The investigation of DSC

curves and relative areas of these curves provided α and β contents. HHP induced formation of more stable β lipid crystals.

- Changes in α and β contents with respect to pressure and storage time were detected by T_2 and SDC measurements. An increasing trend for T_2 was observed with respect to increase in both pressure and storage time. Formation of β crystals was discernible with the increase in T_2. These findings suggested that the beginning of destabilization of emulsions can be detected by NMR measurements.
- The obtained pair distance distributions in SAXS measurements were indicating uniform dispersed nano-globules with cylindrical and spherical shapes.
- The pressure effect may be easily seen in the *ab-initio* structural model with SAXS measurements. The pressure application caused a structural change from spherical form to cylindrical form while SC solution and SC emulsion droplets reach more compact spherical like aggregations.

This study demonstrated that HHP produced stable lipid crystal forms, presence and type of emulsifier affected the crystal structures and NMR relaxometry was an alternative method to track the polymorphic changes of lipid crystals under pressure treatment and storage. In near future, thermodynamic effects and different aqueous concentrations may be also investigated and in addition to the size, shape and distribution controls, the optical transparent properties may be also characterized by SAXS technique for the potential usage of the newly defined nano-emulsions in technological application. Future researches make capital out of this study to increase the use of HHP technology in encapsulation processes.

REFERENCES

Aertsen, A., Meersman, F., Hendrickx, M. E. G., Vogel, R. F., & Michiels, C. W. (2009). Biotechnology under high pressure: applications and implications. *Trends in Biotechnology*, *27*(7), 434–441. https://doi.org/10.1016/j.tibtech.2009.04.001

Balci, A. T., & Wilbey, R. A. (1999). High pressure processing of milk-the first 100 years in the development of a new technology. *International Journal of Dairy Technology*, *52*(4), 149–155. https://doi.org/10.1111/j.1471-0307.1999.tb02858.x

Barba, F. J., Esteve, M. J., & Frígola, A. (2012). High Pressure Treatment Effect on Physicochemical and Nutritional Properties of Fluid Foods During Storage: A Review. *Comprehensive Reviews in Food Science and Food Safety*, *11*(3), 307–322. https://doi.org/10.1111/j.1541-4337.2012.00185.x

Barrabino, A., Keleşoğlu, S., Sørland, G. H., Simon, S., & Sjöblom, J. (2014). Phase inversion in emulsions studied by low field NMR. *Colloids and Surfaces A: Physicochemical and Engineering Aspects*, *443*, 368–376. https://doi.org/10.1016/j.colsurfa.2013.11.016

Bigikocin, E., Mert, B., & Alpas, H. (2011). Effect of high hydrostatic pressure and high dynamic pressure on stability and rheological properties of model oil-in-water emulsions. *High Pressure Research*, *31*(October), 462–474. https://doi.org/10.1080/08957959.2011.589842

Blümer, C., & Mäder, K. (2005). Isostatic ultra-high-pressure effects on supercooled melts in colloidal triglyceride dispersions. *Pharmaceutical Research*, *22*(10), 1708–1715. https://doi.org/10.1007/s11095-005-6949-x

Boldon, L., Laliberte, F., & Liu, L. (2015). Review of the fundamental theories behind small angle X-ray scattering, molecular dynamics simulations, and relevant integrated application. *Nano Reviews*, *6*(1), 25661. https://doi.org/10.3402/nano.v6.25661

Bouteille, R., Perez, J., Khifer, F., Jouan-Rimbaud-Bouveresse, D., Lecanu, B., & This, H. (2013). Influence of the Colloidal Structure of Dairy Gels on Milk Fat Fusion Behavior: Quantification of the Liquid Fat Content by In Situ Quantitative Proton Nuclear Magnetic Resonance Spectroscopy (isq 1H NMR). *Journal of Food Science*, *78*(4), 535–541. https://doi.org/10.1111/1750-3841.12072

Bridgman, P. W. (1914). The Coagulation of Albumin by Pressure. *Journal of Biological Chemistry*, *19*, 511–512. Retrieved from http://www.jbc.org/content/19/4/511.citation

Coupland, J. N. (2002). Crystallization in emulsions. *Current Opinion in Colloid and Interface Science*, *7*(5–6), 445–450. https://doi.org/10.1016/S1359-0294(02)00080-8

Darling, D. F., & Birkett, R. J. (1987). Food Colloids in Practice. In E. Dickinson (Ed.), *Food Emulsions and Foams* (pp. 1–29). London: The Royal Society of Chemistry.

Dickinson, E. (1999). Caseins in emulsions: interfacial properties and interactions. *International Dairy Journal*, *9*(3), 305–312. https://doi.org/10.1016/S0958-6946(99)00079-5

Dickinson, E., & Golding, M. (1997). Rheology of Sodium Caseinate Stabilized Oil-in-Water Emulsions. *Journal of Colloid and Interface Science*, *191*(1), 166–176.

Farrell Jr, H. M., Brown, E. M., & Malin, E. L. (2013). Higher Order Structures of the Caseins: A Paradox? In P. L. H. McSweeney & P. F. Fox (Eds.), *Advanced Dairy Chemistry: Volume 1A: Proteins: Basic Aspects* (4th ed., pp. 161–184). New York: Springer Science+Business Media. https://doi.org/10.1007/978-1-464-4714-6_5

Fellows, P. (2000). *Food Processing Technology: Principles and Practice* (2nd ed.). Cambrigde: Woodhead Publishing Limited & CRC Press LLC.

Ferstl, P., Eder, C., Ruß, W., & Wierschem, A. (2011). Pressure-induced crystallization of triacylglycerides. *High Pressure Research*, *31*(2), 339–349. https://doi.org/10.1080/08957959.2011.582870

Franke, D., & Svergun, D. I. (2009). DAMMIF, a program for rapid ab-initio shape determination in small-angle scattering. *Journal of Applied Crystallography*, *42*, 342–346. https://doi.org/10.1107/S0021889809000338

Freitas, C., & Müller, R. H. (1999). Correlation between long-term stability of solid lipid nanoparticles (SLN™) and crystallinity of the lipid phase. *European Journal of Pharmaceutics and Biopharmaceutics*, *47*(2), 125–132. https://doi.org/10.1016/S0939-6411(98)00074-5

Gould, G. W. (2012). The Evolution of High Pressure Processing of Foods. In M. E. G. Hendrickx & D. Knorr (Eds.), *Ultra High Pressure Treatment of Foods* (pp. 1–23). New York: Springer Science & Business Media.

Greiff, K., Fuentes, A., Aursand, I. G., Erikson, U., Masot, R., Alcańiz, M., & Barat, J. M. (2014). Innovative nondestructive measurements of water activity and the content of salts in low-salt hake minces. *Journal of Agricultural and Food Chemistry*, *62*(12), 2496–2505. https://doi.org/10.1021/jf405527t

Grishaev, A. (2012). Sample preparation, data collection, and preliminary data analysis in biomolecular solution X-ray scattering. *Current Protocols in Protein Science*, *70*, 17.14.1-17.14.18. https://doi.org/10.1002/0471140864.ps1714s70

Han, L., Li, L., Li, B., Zhao, L., Liu, G., Liu, X., & Wang, X. (2014). Effect of High Pressure Microfluidization on the Crystallization Behavior of Palm Stearin — Palm Olein Blends. *Molecules*, *19*(4), 5348–5359. https://doi.org/10.3390/molecules19045348

Hasenhuettl, G. L., & Hartel, R. W. (2008). *Food Emulsifiers and Their Applications* (2nd ed.). New York: Springer.

Hite, B. H. (1899). The Effect of Pressure in the Preservation of Milk. *Bulletin West Virginia University Agricultural Experiment Station*, *58*, 15–35. Retrieved from https://archive.org/details/effectofpressure58hite

Horiba Scientific. (n.d.). *A Guidebook to Particle Size Analysis*. Retrieved from https://www.horiba.com/fileadmin/uploads/Scientific/eMag/PSA/Guidebook/pdf/PSA_Guidebook.pdf

Jacques, D. A., & Trewhella, J. (2010). Small-angle scattering for structural biology--Expanding the frontier while avoiding the pitfalls. *Protein Science*, *19*(4), 642–657. https://doi.org/10.1002/pro.351

Jores, K., Mehnert, W., Drechsler, M., Bunjes, H., Johann, C., & Mäder, K. (2004). Investigations on the structure of solid lipid nanoparticles (SLN) and oil-loaded solid lipid nanoparticles by photon correlation spectroscopy, field-flow fractionation and transmission electron microscopy. *Journal of Controlled Release : Official Journal of the Controlled Release Society*, *95*(2), 217–27. https://doi.org/10.1016/j.jconrel.2003.11.012

Jores, K., Mehnert, W., & Mäder, K. (2003). Physicochemical Investigations on Solid Lipid Nanoparticles and on Oil-Loaded Solid Lipid Nanoparticles: A Nuclear Magnetic Resonance and Electron Spin Resonance Study. *Pharmaceutical Research*, *20*(8), 1274–1283. https://doi.org/10.1023/A:1025065418309

Kaneko, N., Horie, T., Ueno, S., Yano, J., Katsuragi, T., & Sato, K. (1999). Impurity effects on crystallization rates of n-hexadecane in oil-in-water emulsions. *Journal of Crystal Growth*, *197*(1–2), 263–270. https://doi.org/10.1016/S0022-0248(98)00933-6

Kellens, M., Gibon, V., Hendrix, M., & De Greyt, W. (2007). Palm oil fractionation. *European Journal of Lipid Science and Technology*, *109*(4), 336–349. https://doi.org/10.1002/ejlt.200600309

Khan, N. M., Mu, T. H., Zhang, M., & Arogundade, L. a. (2014). The effects of pH and high hydrostatic pressure on the physicochemical properties of a sweet potato protein emulsion. *Food Hydrocolloids*, *35*, 209–216. https://doi.org/10.1016/j.foodhyd.2013.05.011

Kikhney, A. (2012). SAXS data reduction and processing. Retrieved June 1, 2017, from https://www.embl-hamburg.de/biosaxs/courses/embo2012/slides/data-reduction-processing-kikhney.pdf

Kikhney, A. G., & Svergun, D. I. (2015). A practical guide to small angle X-ray scattering (SAXS) of flexible and intrinsically disordered proteins. *FEBS Letters*, *589*(19), 2570–2577. https://doi.org/10.1016/j.febslet.2015.08.027

Kirtil, E., & Oztop, M. H. (2016). 1H Nuclear Magnetic Resonance Relaxometry and Magnetic Resonance Imaging and Applications in Food Science and Processing. *Food Engineering Reviews*, *8*(1), 1–22. https://doi.org/10.1007/s12393-015-9118-y

Kline, S. R. (2006). Reduction and analysis of SANS and USANS data using IGOR Pro. *Journal of Applied Crystallography*, *39*, 895–900. https://doi.org/10.1107/S0021889806035059

Macfarlane, J. J. (1973). Pre-Rigor Pressurization of Muscle: Effects on pH, Shear Value and Taste Panel Assessment. *Journal of Food Science*, *38*, 294–298. https://doi.org/10.1111/j.1365-2621.1973.tb01409.x

Mandal, P. K., & Jayanthi, M. (2011). Palm Oil: nutrition, uses and impacts. In M. L. Palmetti (Ed.), *Palm Oil: nutrition, uses and impacts* (pp. 1–46). New York: Nova Science Publishers, Inc.

Mazzanti, G., Mudge, E. M., & Anom, E. Y. (2008). In situ rheo-NMR measurements of solid fat content. *Journal of the American Oil Chemists' Society*, *85*(5), 405–412. https://doi.org/10.1007/s11746-008-1227-9

McClements, D. J. (2005). *Food Emulsions Principles, Practices, and Techniques*. *Food Emulsions Principles, Practices, and Techniques*. https://doi.org/10.1093/acprof:oso/9780195383607.003.0002

Misra, N. N., Koubaa, M., Roohinejad, S., Juliano, P., Alpas, H., Inácio, R. S., … Barba, F. J. (2017). Landmarks in the historical development of twenty first century food processing technologies. *Food Research International*, *In press*(February), Corrected Proof. https://doi.org/10.1016/j.foodres.2017.05.001

Mylonas, E., & Svergun, D. I. (2007). Accuracy of molecular mass determination of proteins in solution by small-angle X-ray scattering. *J. Appl. Cryst*, *40*, 245–249. Retrieved from http://journals.iucr.org/j/issues/2007/s1/00/sm6016/sm6016.pdf

Nadakatti, S. M. (1999). Modified data handling for rapid low-field nuclear magnetic resonance characterization of lyotropic liquid crystal composites. *Journal of Surfactants and Detergents*, *2*(4), 515–521. https://doi.org/10.1007/s11743-999-0100-9

Nosho, Y., Ueshima, K., Ikehara, T., Hashimoto, S., & Kato, M. (1999). Process for producing fat composition. Retrieved from http://www.google.com/patents/US6495189

Oh, J. H., & Swanson, B. G. (2006). Polymorphic transitions of cocoa butter affected by high hydrostatic pressure and sucrose polyesters. *Journal of the American Oil Chemists' Society*, *83*(12), 1007–1014. https://doi.org/10.1007/s11746-006-5155-2

Palm oil production. (2016). Retrieved June 3, 2017, from https://www.palmoilandfood.eu/en/palm-oil-production

Pérez, B., Li, J., & Guo, Z. (2008). Chemistry and Properties of Lipids and Phospholipids. In C. C. Akoh & D. B. Min (Eds.), *Food lipids : Chemistry, Nutrition, and Biotechnology* (4th ed., pp. 37–72). Boca Raton: CRC Press/Taylor & Francis Group.

PerkinElmer Inc. (n.d.). *Differential Scanning Calorimetry (DSC): A Beginner's Guide*. Retrieved from https://www.perkinelmer.com/CMSResources/Images/44-74542GDE_DSCBeginnersGuide.pdf

Peyronel, M. F., & Marangoni, A. G. (2014). *Differential Scanning Calorimetry*. https://doi.org/10.21748/lipidlibrary.40884

Rahman, S. M. (2007). Food preservation methods. In *Handbook of Food Preservation* (pp. 8–10).

Ritzoulis, C. (2013). *Introduction to the physical chemistry of foods*. Boca Raton: Taylor & Francis.

Rostocki, A. J., Siegoczyński, ; R M, Kiełczyński, ; P, Szalewski, ; M, Balcerzak, ; A, Zduniak, ; M, … Zduniak, M. (2011). Employment of a novel ultrasonic method to investigate high pressure phase transitions in oleic acid. *High Pressure Research*, *31*(2), 334–338. https://doi.org/10.1080/08957959.2011.552907

Rostocki, A. J., Tarakowski, R., Kiełczyński, P., Szalewski, M., Balcerzak, A., & Ptasznik, S. (2013). The ultrasonic investigation of phase transition in olive oil up to 0.7 GPa. *Journal of the American Oil Chemists' Society*, *90*(6), 813–818. https://doi.org/10.1007/s11746-013-2223-2

Roth, K. (2010). Chocolate - The Noblest Polymorphism II. *ChemViews*. https://doi.org/10.1002/chemv.201000030

Salami, S., Rondeau-Mouro, C., van Duynhoven, J., & Mariette, F. (2013). PFG-NMR self-diffusion in casein dispersions: Effects of probe size and protein aggregate size. *Food Hydrocolloids*, *31*(2), 248–255. https://doi.org/10.1016/j.foodhyd.2012.10.020

Salgarkar, R. (2015). Latest report on the HPP products market that is expected to reach $12 billion by 2018 scrutinized in new research - WhaTech. Retrieved June 12, 2017, from https://www.whatech.com/market-research/industrial/95428-latest-report-on-the-hpp-products-market-that-is-expected-to-reach-12-billion-by-2018-scrutinized-in-new-research

Salminen, H., Helgason, T., Aulbach, S., Kristinsson, B., Kristbergsson, K., & Weiss, J. (2014). Influence of co-surfactants on crystallization and stability of solid lipid nanoparticles. *Journal of Colloid and Interface Science*, *426*, 256–263. https://doi.org/10.1016/j.jcis.2014.04.009

Sato, K., Bayés-García, L., Calvet, T., Cuevas-Diarte, M. À., & Ueno, S. (2013). External factors affecting polymorphic crystallization of lipids. *European Journal of Lipid Science and Technology*, *115*(11), 1224–1238. https://doi.org/10.1002/ejlt.201300049

Saupe, A., & Rades, T. (2006). Solid Lipid Nanoparticles. In M. R. Mozafari (Ed.), *Nanocarrier Technologies: Frontiers of Nanotherapy* (pp. 41–50). Dordrecht: Springer.

Schawe, J., Riese, R., Widmann, J., Schubnell, M., & Jörimann, U. (2000). *Interpreting DSC curves Part 1: Dynamic measurements*. Schwerzenbach. Retrieved from http://www.masontechnology.ie/x/Usercom_11.pdf

Semenyuk, A. V., & Svergun, D. I. (1991). GNOM. A program package for small-angle scattering data processing. *Journal of Applied Crystallography*, *24*, 537–540. https://doi.org/10.1107/S002188989100081X

Sevdin, S., Çınar Bam, B., Alpas, H., Öztop, M. H., & İde, S. (2017). Nano scale analysis on water emulsions of Palm Stearin: The effect of hydrostatic pressure and the stabilizers (sodium caseinate and lecithin). *Colloids and Surfaces A: Physicochemical and Engineering Aspects*, (under revision).

Sevdin, S., Özel, B., Yücel, U., Öztop, M. H., & Alpas, H. (2017). Monitoring the High Hydrostatic Pressure (HHP) Induced Changes in the Crystal Structures of Palm Stearin Emulsions Emulsified with Sodium Caseinate by Differential Scanning Calorimetry (DSC) and Nuclear Magnetic Resonance (NMR) Relaxometry. *Journal of Food Engineering*, (under revision).

Sevdin, S., Yücel, U., & Alpas, H. (2017). Effect of High Hydrostatic Pressure (HHP) on Crystal Structure of Palm Stearin Emulsions. *Innovative Food Science and Emerging Technologies*. https://doi.org/https://doi.org/10.1016/j.ifset.2017.05.005

Sonoda, T., Takata, Y., Ueno, S., & Sato, K. (2004). DSC and synchrotron-radiation X-ray diffraction studies on crystallization and polymorphic behavior of palm stearin in bulk and oil-in-water emulsion states. *Journal of the American Oil Chemists' Society*, *81*(4), 365–373. https://doi.org/10.1007/s11746-004-0908-5

Sugimoto, T., Mori, T., Mano, J. I., Mutoh, T.-A., Shiinoki, Y., & Matsumura, Y. (2001). Effects of fat crystallization on the behavior of proteins and lipids at oil droplet surfaces. *Journal of the American Oil Chemists' Society*, *78*(2), 183–188. https://doi.org/10.1007/s11746-001-0241-z

Tadros, T. F. (2009). Emulsion Science and Technology: A General Introduction. In *Emulsion Science and Technology* (pp. 1–56). Weinheim: Wiley-VCH Verlag GmbH & Co. KGaA.

Tan, T. B., Yussof, N. S., Abas, F., Mirhosseini, H., Nehdi, I. A., & Tan, C. P. (2016). Comparing the formation of lutein nanodispersion prepared by using solvent displacement method and high-pressure valve homogenization: Effects of formulation parameters. *Journal of Food Engineering*, *177*, 65–71. https://doi.org/10.1016/j.jfoodeng.2015.12.020

Tanaka, S. (1992). Theory of power-compensated DSC. *Thermochimica Acta*, *210*, 67–76. https://doi.org/10.1016/0040-6031(92)80277-4

Trujillo-Cayado, L. A., Santos, J., Alfaro, M. C., Calero, N., & Muñoz, J. (2016). A Further Step in the Development of Oil-in-Water Emulsions Formulated with a Mixture of Green Solvents. *Industrial & Engineering Chemistry Research*, *55*(27), 7259–7266. https://doi.org/10.1021/acs.iecr.6b01320

Ultrasonic Homogenizing And Blending. (n.d.). Retrieved June 12, 2017, from https://www.hielscher.com/homogenize_01.htm

Van Duynhoven, J., Dubourg, I., Goudappel, G. J., & Roijers, E. (2002). Determination of MG and TG phase composition by time-domain NMR. *Journal of the American Oil Chemists' Society*, *79*(4), 383–388. https://doi.org/10.1007/s11746-002-0493-7

Vanapalli, S. A., Palanuwech, J., & Coupland, J. N. (2002). Stability of emulsions to dispersed phase crystallization: effect of oil type, dispersed phase volume fraction, and cooling rate. *Colloids and Surfaces A: Physicochemical and Engineering Aspects*, *204*, 227–237.

Wright, A. J., & Marangoni, A. G. (2006). Formation, structure, and rheological properties of ricinelaidic acid-vegetable oil organogels. *Journal of the American Oil Chemists' Society*, *83*(6), 497–503. https://doi.org/10.1007/s11746-006-1232-9

Yucel, U., Elias, R. J., & Coupland, J. N. (2013). Localization and reactivity of a hydrophobic solute in lecithin and caseinate stabilized solid lipid nanoparticles and nanoemulsions. *Journal of Colloid and Interface Science*, *394*, 20–25. https://doi.org/10.1016/j.jcis.2012.12.042

Zhang, R., Huo, J., Peng, Z., Feng, Q., Wang, J., & Zhang, J. (2016). Research on Oil-Based Drilling Fluids Emulsion Droplet by Low-Field NMR. *Applied Magnetic Resonance*, *47*(12), 1339–1352. https://doi.org/10.1007/s00723-016-0845-x

Zulkurnain, M., Maleky, F., & Balasubramaniam, V. M. (2016). High Pressure Processing Effects on Lipids Thermophysical Properties and Crystallization Kinetics. *Food Engineering Reviews*, *8*(4), 1–21. https://doi.org/10.1007/s12393-016-9144-4

APPENDIX A

ANOVA Results of General Full Factorial Regressions

General Factorial Regression: α Melting T versus Emulsifier; Pressure; Temperature; Storage

Factor Information

Factor	Levels	Values
Emulsifier	2	SC; 80H_XG
Pressure	3	0; 100; 500
Temperature	3	10; 20; 40
Storage	4	1; 8; 14; 28

Analysis of Variance

Source	DF	Adj SS	Adj MS	F-Value	P-Value
Model	8	21,1742	2,64678	27,61	0,000
Linear	8	21,1742	2,64678	27,61	0,000
Emulsifier	1	0,0084	0,00844	0,09	0,767
Pressure	2	10,3494	5,17472	53,99	0,000
Temperature	2	1,0319	0,51595	5,38	0,005
Storage	3	9,7845	3,26149	34,03	0,000
Error	207	19,8418	0,09585		
Lack-of-Fit	63	7,8837	0,12514	1,51	0,023
Pure Error	144	11,9581	0,08304		
Total	215	41,0160			

Model Summary

S	R-sq	R-sq(adj)	R-sq(pred)
0,309603	51,62%	49,75%	47,33%

General Factorial Regression: α Content versus Emulsifier; Pressure; Temperature; Storage

Factor Information

Factor	Levels	Values
Emulsifier	2	SC; 80H_XG
Pressure	3	0; 100; 500
Temperature	3	10; 20; 40
Storage	4	1; 8; 14; 28

Analysis of Variance

Source	DF	Adj SS	Adj MS	F-Value	P-Value
Model	8	23509,9	2938,73	54,87	0,000
Linear	8	23509,9	2938,73	54,87	0,000
Emulsifier	1	2348,2	2348,20	43,85	0,000
Pressure	2	5481,5	2740,77	51,18	0,000
Temperature	2	243,2	121,61	2,27	0,106
Storage	3	15436,9	5145,63	96,08	0,000
Error	207	11085,6	53,55		
Lack-of-Fit	63	10630,1	168,73	53,34	0,000
Pure Error	144	455,5	3,16		
Total	215	34595,5			

Model Summary

S	R-sq	R-sq(adj)	R-sq(pred)
7,31803	67,96%	66,72%	65,11%

General Factorial Regression: β Melting T versus Emulsifier; Pressure; Temperature; Storage

Factor Information

Factor	Levels	Values
Emulsifier	2	SC; 80H_XG
Pressure	3	0; 100; 500
Temperature	3	10; 20; 40
Storage	4	1; 8; 14; 28

Analysis of Variance

Source	DF	Adj SS	Adj MS	F-Value	P-Value
Model	8	9,2046	1,15058	17,64	0,000
Linear	8	9,2046	1,15058	17,64	0,000
Emulsifier	1	7,4185	7,41852	113,74	0,000
Pressure	2	1,5130	0,75651	11,60	0,000
Temperature	2	0,1489	0,07445	1,14	0,321
Storage	3	0,1242	0,04138	0,63	0,594
Error	207	13,5008	0,06522		
Lack-of-Fit	63	3,3964	0,05391	0,77	0,881
Pure Error	144	10,1045	0,07017		
Total	215	22,7054			

Model Summary

S	R-sq	R-sq(adj)	R-sq(pred)
0,255385	40,54%	38,24%	35,26%

General Factorial Regression: β Content versus Emulsifier; Pressure; Temperature; Storage

Factor Information

Factor	Levels	Values
Emulsifier	2	SC; 80H_XG
Pressure	3	0; 100; 500
Temperature	3	10; 20; 40
Storage	4	1; 8; 14; 28

Analysis of Variance

Source	DF	Adj SS	Adj MS	F-Value	P-Value
Model	8	21710,6	2713,82	51,39	0,000
Linear	8	21710,6	2713,82	51,39	0,000
Emulsifier	1	248,2	248,25	4,70	0,031
Pressure	2	6139,0	3069,49	58,13	0,000
Temperature	2	238,8	119,40	2,26	0,107
Storage	3	15084,6	5028,19	95,22	0,000
Error	207	10931,3	52,81		
Lack-of-Fit	63	10516,3	166,92	57,92	0,000
Pure Error	144	415,0	2,88		
Total	215	32641,9			

Model Summary

S	R-sq	R-sq(adj)	R-sq(pred)
7,26692	66,51%	65,22%	63,54%

General Factorial Regression: 3rd Peak Content versus Emulsifier; Pressure; Temperature; Storage

Factor Information

Factor	Levels	Values
Emulsifier	2	SC; 80H_XG
Pressure	3	0; 100; 500
Temperature	3	10; 20; 40
Storage	4	1; 8; 14; 28

Analysis of Variance

Source	DF	Adj SS	Adj MS	F-Value	P-Value
Model	8	4264,32	533,04	586,29	0,000
Linear	8	4264,32	533,04	586,29	0,000
Emulsifier	1	4193,65	4193,65	4612,58	0,000
Pressure	2	31,26	15,63	17,19	0,000
Temperature	2	1,02	0,51	0,56	0,572
Storage	3	38,40	12,80	14,08	0,000
Error	207	188,20	0,91		
Lack-of-Fit	63	122,26	1,94	4,24	0,000
Pure Error	144	65,94	0,46		
Total	215	4452,52			

Model Summary

S	R-sq	R-sq(adj)	R-sq(pred)
0,953508	95,77%	95,61%	95,40%

General Factorial Regression: D[3,2] versus Emulsifier; Pressure; Temperature; Storage

```
Factor Information

Factor        Levels  Values
Emulsifier         2  SC; 80H_XG
Pressure           3  0; 100; 500
Temperature        3  10; 20; 40
Storage            4  1; 8; 14; 28


Analysis of Variance

Source            DF   Adj SS   Adj MS  F-Value  P-Value
Model              8  4693,70   586,71   113,43    0,000
  Linear           8  4693,70   586,71   113,43    0,000
    Emulsifier     1  3940,20  3940,20   761,74    0,000
    Pressure       2   264,33   132,17    25,55    0,000
    Temperature    2    29,57    14,79     2,86    0,060
    Storage        3   459,59   153,20    29,62    0,000
Error            207  1070,73     5,17
  Lack-of-Fit     63  1039,28    16,50    75,54    0,000
  Pure Error     144    31,45     0,22
Total            215  5764,43


Model Summary

      S    R-sq  R-sq(adj)  R-sq(pred)
2,27434  81,43%     80,71%      79,77%
```

General Factorial Regression: D[4,3] versus Emulsifier; Pressure; Temperature; Storage

Factor Information

Factor	Levels	Values
Emulsifier	2	SC; 80H_XG
Pressure	3	0; 100; 500
Temperature	3	10; 20; 40
Storage	4	1; 8; 14; 28

Analysis of Variance

Source	DF	Adj SS	Adj MS	F-Value	P-Value
Model	8	60330,0	7541,3	116,92	0,000
Linear	8	60330,0	7541,3	116,92	0,000
Emulsifier	1	54567,3	54567,3	845,98	0,000
Pressure	2	258,9	129,4	2,01	0,137
Temperature	2	360,9	180,5	2,80	0,063
Storage	3	5142,9	1714,3	26,58	0,000
Error	207	13351,8	64,5		
Lack-of-Fit	63	12602,1	200,0	38,42	0,000
Pure Error	144	749,7	5,2		
Total	215	73681,8			

Model Summary

S	R-sq	R-sq(adj)	R-sq(pred)
8,03129	81,88%	81,18%	80,27%

General Factorial Regression: Span versus Emulsifier; Pressure; Temperature; Storage

Factor Information

Factor	Levels	Values
Emulsifier	2	SC; 80H_XG
Pressure	3	0; 100; 500
Temperature	3	10; 20; 40
Storage	4	1; 8; 14; 28

Analysis of Variance

Source	DF	Adj SS	Adj MS	F-Value	P-Value
Model	8	39,949	4,9936	51,66	0,000
Linear	8	39,949	4,9936	51,66	0,000
Emulsifier	1	11,812	11,8121	122,19	0,000
Pressure	2	1,341	0,6704	6,93	0,001
Temperature	2	1,737	0,8687	8,99	0,000
Storage	3	25,058	8,3527	86,41	0,000
Error	207	20,010	0,0967		
Lack-of-Fit	63	16,823	0,2670	12,06	0,000
Pure Error	144	3,187	0,0221		
Total	215	59,959			

Model Summary

S	R-sq	R-sq(adj)	R-sq(pred)
0,310914	66,63%	65,34%	63,66%

General Factorial Regression: T2 versus Emulsifier; Pressure; Temperature; Storage

Factor Information

Factor	Levels	Values
Emulsifier	2	SC; 80H_XG
Pressure	3	0; 100; 500
Temperature	3	10; 20; 40
Storage	4	1; 8; 14; 28

Analysis of Variance

Source	DF	Adj SS	Adj MS	F-Value	P-Value
Model	8	4811508	601438	69,02	0,000
Linear	8	4811508	601438	69,02	0,000
Emulsifier	1	4317610	4317610	495,49	0,000
Pressure	2	24236	12118	1,39	0,251
Temperature	2	11587	5793	0,66	0,515
Storage	3	458076	152692	17,52	0,000
Error	207	1803752	8714		
Lack-of-Fit	63	1146323	18196	3,99	0,000
Pure Error	144	657429	4565		
Total	215	6615260			

Model Summary

S	R-sq	R-sq(adj)	R-sq(pred)
93,3476	72,73%	71,68%	70,31%

General Factorial Regression: SDC*10^9 versus Emulsifier; Pressure; Temperature; Storage

Factor Information

Factor	Levels	Values
Emulsifier	2	SC; 80H_XG
Pressure	3	0; 100; 500
Temperature	3	10; 20; 40
Storage	4	1; 8; 14; 28

Analysis of Variance

Source	DF	Adj SS	Adj MS	F-Value	P-Value
Model	8	33,3520	4,1690	206,27	0,000
Linear	8	33,3520	4,1690	206,27	0,000
Emulsifier	1	32,0346	32,0346	1585,00	0,000
Pressure	2	0,8310	0,4155	20,56	0,000
Temperature	2	0,0414	0,0207	1,03	0,361
Storage	3	0,4450	0,1483	7,34	0,000
Error	207	4,1837	0,0202		
Lack-of-Fit	63	1,9787	0,0314	2,05	0,000
Pure Error	144	2,2050	0,0153		
Total	215	37,5357			

Model Summary

S	R-sq	R-sq(adj)	R-sq(pred)
0,142166	88,85%	88,42%	87,86%

APPENDIX B

Comparison of 80H_XG Emulsion Samples at 1st Day of Storage and Grouping Information

General Linear Model: α Melting T versus Sample Name

Method

Factor coding (-1; 0; +1)

Factor Information

```
Factor       Type   Levels  Values
Sample Name  Fixed       7  PS_80H_XG_100_10_15_0week;
PS_80H_XG_100_20_15_0week;
                            PS_80H_XG_100_40_15_0week;
PS_80H_XG_500_10_15_0week;
                            PS_80H_XG_500_20_15_0week;
PS_80H_XG_500_40_15_0week;
                            PS_80H_XG_unpressurized_0week
```

Analysis of Variance

Source	DF	Adj SS	Adj MS	F-Value	P-Value
Sample Name	6	1,036	0,1727	0,69	0,663
Error	14	3,519	0,2514		
Total	20	4,555			

Model Summary

S	R-sq	R-sq(adj)	R-sq(pred)
0,501351	22,75%	0,00%	0,00%

General Linear Model: α Content versus Sample Name

Method

Factor coding (-1; 0; +1)

Factor Information

Factor	Type	Levels	Values
Sample Name	Fixed	7	PS_80H_XG_100_10_15_0week; PS_80H_XG_100_20_15_0week; PS_80H_XG_100_40_15_0week; PS_80H_XG_500_10_15_0week; PS_80H_XG_500_20_15_0week; PS_80H_XG_500_40_15_0week; PS_80H_XG_unpressurized_0week

Analysis of Variance

Source	DF	Adj SS	Adj MS	F-Value	P-Value
Sample Name	6	3142,3	523,72	47,59	0,000
Error	14	154,1	11,00		
Total	20	3296,4			

Model Summary

S	R-sq	R-sq(adj)	R-sq(pred)
3,31728	95,33%	93,32%	89,48%

General Linear Model: β Melting T versus Sample Name

Method

Factor coding (-1; 0; +1)

Factor Information

```
Factor       Type   Levels  Values
Sample Name  Fixed       7  PS_80H_XG_100_10_15_0week;
PS_80H_XG_100_20_15_0week;
                            PS_80H_XG_100_40_15_0week;
PS_80H_XG_500_10_15_0week;
                            PS_80H_XG_500_20_15_0week;
PS_80H_XG_500_40_15_0week;
                            PS_80H_XG_unpressurized_0week
```

Analysis of Variance

Source	DF	Adj SS	Adj MS	F-Value	P-Value
Sample Name	6	0,1227	0,02045	0,56	0,757
Error	14	0,5139	0,03670		
Total	20	0,6366			

Model Summary

S	R-sq	R-sq(adj)	R-sq(pred)
0,191585	19,28%	0,00%	0,00%

General Linear Model: β Content versus Sample Name

Method

Factor coding (-1; 0; +1)

Factor Information

Factor	Type	Levels	Values
Sample Name	Fixed	7	PS_80H_XG_100_10_15_0week; PS_80H_XG_100_20_15_0week; PS_80H_XG_100_40_15_0week; PS_80H_XG_500_10_15_0week; PS_80H_XG_500_20_15_0week; PS_80H_XG_500_40_15_0week; PS_80H_XG_unpressurized_0week

Analysis of Variance

Source	DF	Adj SS	Adj MS	F-Value	P-Value
Sample Name	6	3228,02	538,003	151,15	0,000
Error	14	49,83	3,559		
Total	20	3277,85			

Model Summary

S	R-sq	R-sq(adj)	R-sq(pred)
1,88662	98,48%	97,83%	96,58%

General Linear Model: 3rd Peak Melting T versus Sample Name

```
Method

Factor coding  (-1; 0; +1)


Factor Information

Factor       Type   Levels  Values
Sample Name  Fixed       7  PS_80H_XG_100_10_15_0week;
PS_80H_XG_100_20_15_0week;
                            PS_80H_XG_100_40_15_0week;
PS_80H_XG_500_10_15_0week;
                            PS_80H_XG_500_20_15_0week;
PS_80H_XG_500_40_15_0week;
                            PS_80H_XG_unpressurized_0week


Analysis of Variance

Source          DF   Adj SS    Adj MS  F-Value  P-Value
  Sample Name    6  0,05751  0,009586     0,78    0,600
Error           14  0,17220  0,012300
Total           20  0,22971


Model Summary

       S    R-sq  R-sq(adj)  R-sq(pred)
0,110905  25,04%      0,00%       0,00%
```

General Linear Model: 3rd Peak Content versus Sample Name

Method

Factor coding (-1; 0; +1)

Factor Information

Factor	Type	Levels	Values
Sample Name	Fixed	7	PS_80H_XG_100_10_15_0week; PS_80H_XG_100_20_15_0week; PS_80H_XG_100_40_15_0week; PS_80H_XG_500_10_15_0week; PS_80H_XG_500_20_15_0week; PS_80H_XG_500_40_15_0week; PS_80H_XG_unpressurized_0week

Analysis of Variance

Source	DF	Adj SS	Adj MS	F-Value	P-Value
Sample Name	6	5,511	0,9184	0,71	0,647
Error	14	18,101	1,2930		
Total	20	23,612			

Model Summary

S	R-sq	R-sq(adj)	R-sq(pred)
1,13708	23,34%	0,00%	0,00%

General Linear Model: D[3,2] versus Sample Name

```
Method

Factor coding  (-1; 0; +1)


Factor Information

Factor       Type   Levels  Values
Sample Name  Fixed       7  PS_80H_XG_100_10_15_0week;
PS_80H_XG_100_20_15_0week;
                            PS_80H_XG_100_40_15_0week;
PS_80H_XG_500_10_15_0week;
                            PS_80H_XG_500_20_15_0week;
PS_80H_XG_500_40_15_0week;
                            PS_80H_XG_unpressurized_0week


Analysis of Variance

Source         DF  Adj SS  Adj MS  F-Value  P-Value
  Sample Name   6  25,106  4,1844    30,76    0,000
Error          14   1,905  0,1360
Total          20  27,011


Model Summary

       S    R-sq  R-sq(adj)  R-sq(pred)
0,368832  92,95%     89,93%      84,14%
```

General Linear Model: D[4,3] versus Sample Name

Method

Factor coding (-1; 0; +1)

Factor Information

Factor	Type	Levels	Values
Sample Name	Fixed	7	PS_80H_XG_100_10_15_0week; PS_80H_XG_100_20_15_0week; PS_80H_XG_100_40_15_0week; PS_80H_XG_500_10_15_0week; PS_80H_XG_500_20_15_0week; PS_80H_XG_500_40_15_0week; PS_80H_XG_unpressurized_0week

Analysis of Variance

Source	DF	Adj SS	Adj MS	F-Value	P-Value
Sample Name	6	57,62	9,604	2,24	0,100
Error	14	60,03	4,288		
Total	20	117,65			

Model Summary

S	R-sq	R-sq(adj)	R-sq(pred)
2,07071	48,98%	27,11%	0,00%

General Linear Model: Span versus Sample Name

Method

Factor coding (-1; 0; +1)

Factor Information

Factor	Type	Levels	Values
Sample Name	Fixed	7	PS_80H_XG_100_10_15_0week; PS_80H_XG_100_20_15_0week; PS_80H_XG_100_40_15_0week; PS_80H_XG_500_10_15_0week; PS_80H_XG_500_20_15_0week; PS_80H_XG_500_40_15_0week; PS_80H_XG_unpressurized_0week

Analysis of Variance

Source	DF	Adj SS	Adj MS	F-Value	P-Value
Sample Name	6	1,7938	0,29896	11,42	0,000
Error	14	0,3665	0,02618		
Total	20	2,1602			

Model Summary

S	R-sq	R-sq(adj)	R-sq(pred)
0,161789	83,04%	75,77%	61,83%

General Linear Model: T2 versus Sample Name

Method

Factor coding (-1; 0; +1)

Factor Information

```
Factor       Type   Levels  Values
Sample Name  Fixed       7  PS_80H_XG_100_10_15_0week;
PS_80H_XG_100_20_15_0week;
                            PS_80H_XG_100_40_15_0week;
PS_80H_XG_500_10_15_0week;
                            PS_80H_XG_500_20_15_0week;
PS_80H_XG_500_40_15_0week;
                            PS_80H_XG_unpressurized_0week
```

Analysis of Variance

Source	DF	Adj SS	Adj MS	F-Value	P-Value
Sample Name	6	14800	2467	0,29	0,934
Error	14	120841	8631		
Total	20	135641			

Model Summary

S	R-sq	R-sq(adj)	R-sq(pred)
92,9058	10,91%	0,00%	0,00%

General Linear Model: SDC*10^9 versus Sample Name

Method

Factor coding (-1; 0; +1)

Factor Information

Factor	Type	Levels	Values
Sample Name	Fixed	7	PS_80H_XG_100_10_15_0week; PS_80H_XG_100_20_15_0week; PS_80H_XG_100_40_15_0week; PS_80H_XG_500_10_15_0week; PS_80H_XG_500_20_15_0week; PS_80H_XG_500_40_15_0week; PS_80H_XG_unpressurized_0week

Analysis of Variance

Source	DF	Adj SS	Adj MS	F-Value	P-Value
Sample Name	6	0,1083	0,01805	1,02	0,451
Error	14	0,2474	0,01767		
Total	20	0,3557			

Model Summary

S	R-sq	R-sq(adj)	R-sq(pred)
0,132924	30,46%	0,65%	0,00%

Comparisons for α Content

Tukey Pairwise Comparisons: Response = α Content, Term = Sample Name

Grouping Information Using the Tukey Method and 95% Confidence

Sample Name	N	Mean	Grouping	
PS_80H_XG_unpressurized_0week	3	48,4533	A	
PS_80H_XG_100_10_15_0week	3	17,2492		B
PS_80H_XG_100_20_15_0week	3	15,9204		B
PS_80H_XG_100_40_15_0week	3	15,0686		B
PS_80H_XG_500_10_15_0week	3	14,8579		B
PS_80H_XG_500_40_15_0week	3	11,6265		B
PS_80H_XG_500_20_15_0week	3	10,0330		B

Means that do not share a letter are significantly different.

Comparisons for β Content

Tukey Pairwise Comparisons: Response = β Content, Term = Sample Name

Grouping Information Using the Tukey Method and 95% Confidence

Sample Name	N	Mean	Grouping		
PS_80H_XG_500_20_15_0week	3	81,5786	A		
PS_80H_XG_500_40_15_0week	3	79,8637	A	B	
PS_80H_XG_100_40_15_0week	3	77,8463	A	B	
PS_80H_XG_500_10_15_0week	3	76,6528	A	B	
PS_80H_XG_100_20_15_0week	3	76,2850		B	
PS_80H_XG_100_10_15_0week	3	74,8560		B	
PS_80H_XG_unpressurized_0week	3	42,9271			C

Means that do not share a letter are significantly different.

Comparisons for D[3,2]

Tukey Pairwise Comparisons: Response = D[3,2], Term = Sample Name

Grouping Information Using the Tukey Method and 95% Confidence

Sample Name	N	Mean	Grouping			
PS_80H_XG_100_10_15_0week	3	6,48933	A			
PS_80H_XG_unpressurized_0week	3	5,17667		B		
PS_80H_XG_500_20_15_0week	3	4,75333		B		
PS_80H_XG_500_10_15_0week	3	4,44467		B	C	
PS_80H_XG_100_40_15_0week	3	3,53333			C	D
PS_80H_XG_100_20_15_0week	3	3,35800				D
PS_80H_XG_500_40_15_0week	3	3,20000				D

Means that do not share a letter are significantly different.

Comparisons for Span

Tukey Pairwise Comparisons: Response = Span, Term = Sample Name

Grouping Information Using the Tukey Method and 95% Confidence

Sample Name	N	Mean	Grouping	
PS_80H_XG_100_20_15_0week	3	2,77867	A	
PS_80H_XG_100_10_15_0week	3	2,27467		B
PS_80H_XG_500_10_15_0week	3	2,08200		B
PS_80H_XG_100_40_15_0week	3	2,06533		B
PS_80H_XG_500_40_15_0week	3	2,05233		B
PS_80H_XG_unpressurized_0week	3	1,87467		B
PS_80H_XG_500_20_15_0week	3	1,84867		B

Means that do not share a letter are significantly different.

100

APPENDIX C

Comparison of 80H_XG Emulsion Samples at 8th Day of Storage and Grouping Information

General Linear Model: α Melting T versus Sample Name

```
Method

Factor coding  (-1; 0; +1)


Factor Information

Factor       Type   Levels  Values
Sample Name  Fixed       7  PS_80H_XG_100_10_15_1week;
PS_80H_XG_100_20_15_1week;
                            PS_80H_XG_100_40_15_1week;
PS_80H_XG_500_10_15_1week;
                            PS_80H_XG_500_20_15_1week;
PS_80H_XG_500_40_15_1week;
                            PS_80H_XG_unpressurized_1week


Analysis of Variance

Source          DF  Adj SS   Adj MS  F-Value  P-Value
  Sample Name    6   2,398  0,39967     4,43    0,010
Error           14   1,263  0,09020
Total           20   3,661


Model Summary

       S    R-sq  R-sq(adj)  R-sq(pred)
0,300341  65,50%     50,72%      22,38%
```

General Linear Model: α Content versus Sample Name

```
Method

Factor coding  (-1; 0; +1)


Factor Information

Factor       Type   Levels  Values
Sample Name  Fixed       7  PS_80H_XG_100_10_15_1week;
PS_80H_XG_100_20_15_1week;
                            PS_80H_XG_100_40_15_1week;
PS_80H_XG_500_10_15_1week;
                            PS_80H_XG_500_20_15_1week;
PS_80H_XG_500_40_15_1week;
                            PS_80H_XG_unpressurized_1week


Analysis of Variance

Source         DF   Adj SS   Adj MS  F-Value  P-Value
  Sample Name   6  133,560  22,2601    38,59    0,000
Error          14    8,076   0,5769
Total          20  141,637


Model Summary

       S    R-sq  R-sq(adj)  R-sq(pred)
0,759517  94,30%     91,85%      87,17%
```

General Linear Model: β Melting T versus Sample Name

Method

Factor coding (-1; 0; +1)

Factor Information

Factor	Type	Levels	Values
Sample Name	Fixed	7	PS_80H_XG_100_10_15_1week; PS_80H_XG_100_20_15_1week; PS_80H_XG_100_40_15_1week; PS_80H_XG_500_10_15_1week; PS_80H_XG_500_20_15_1week; PS_80H_XG_500_40_15_1week; PS_80H_XG_unpressurized_1week

Analysis of Variance

Source	DF	Adj SS	Adj MS	F-Value	P-Value
Sample Name	6	0,5979	0,09964	0,52	0,781
Error	14	2,6651	0,19037		
Total	20	3,2630			

Model Summary

S	R-sq	R-sq(adj)	R-sq(pred)
0,436310	18,32%	0,00%	0,00%

General Linear Model: β Content versus Sample Name

```
Method

Factor coding  (-1; 0; +1)


Factor Information

Factor       Type   Levels  Values
Sample Name  Fixed       7  PS_80H_XG_100_10_15_1week;
PS_80H_XG_100_20_15_1week;
                            PS_80H_XG_100_40_15_1week;
PS_80H_XG_500_10_15_1week;
                            PS_80H_XG_500_20_15_1week;
PS_80H_XG_500_40_15_1week;
                            PS_80H_XG_unpressurized_1week


Analysis of Variance

Source         DF  Adj SS  Adj MS  F-Value  P-Value
  Sample Name   6  137,24  22,873    12,27    0,000
Error          14   26,10   1,864
Total          20  163,34


Model Summary

      S    R-sq  R-sq(adj)  R-sq(pred)
1,36546  84,02%     77,17%      64,04%
```

General Linear Model: 3rd Peak Melting T versus Sample Name

Method

Factor coding (-1; 0; +1)

Factor Information

Factor	Type	Levels	Values
Sample Name	Fixed	7	PS_80H_XG_100_10_15_1week; PS_80H_XG_100_20_15_1week; PS_80H_XG_100_40_15_1week; PS_80H_XG_500_10_15_1week; PS_80H_XG_500_20_15_1week; PS_80H_XG_500_40_15_1week; PS_80H_XG_unpressurized_1week

Analysis of Variance

Source	DF	Adj SS	Adj MS	F-Value	P-Value
Sample Name	6	0,02678	0,004463	0,31	0,919
Error	14	0,19860	0,014186		
Total	20	0,22538			

Model Summary

S	R-sq	R-sq(adj)	R-sq(pred)
0,119104	11,88%	0,00%	0,00%

General Linear Model: 3rd Peak Content versus Sample Name

Method

Factor coding (-1; 0; +1)

Factor Information

Factor	Type	Levels	Values
Sample Name	Fixed	7	PS_80H_XG_100_10_15_1week; PS_80H_XG_100_20_15_1week; PS_80H_XG_100_40_15_1week; PS_80H_XG_500_10_15_1week; PS_80H_XG_500_20_15_1week; PS_80H_XG_500_40_15_1week; PS_80H_XG_unpressurized_1week

Analysis of Variance

Source	DF	Adj SS	Adj MS	F-Value	P-Value
Sample Name	6	13,93	2,3214	2,58	0,067
Error	14	12,59	0,8989		
Total	20	26,51			

Model Summary

S	R-sq	R-sq(adj)	R-sq(pred)
0,948120	52,53%	32,19%	0,00%

General Linear Model: D[3,2] versus Sample Name

Method

Factor coding (-1; 0; +1)

Factor Information

Factor	Type	Levels	Values
Sample Name	Fixed	7	PS_80H_XG_100_10_15_1week; PS_80H_XG_100_20_15_1week; PS_80H_XG_100_40_15_1week; PS_80H_XG_500_10_15_1week; PS_80H_XG_500_20_15_1week; PS_80H_XG_500_40_15_1week; PS_80H_XG_unpressurized_1week

Analysis of Variance

Source	DF	Adj SS	Adj MS	F-Value	P-Value
Sample Name	6	59,704	9,9507	31,77	0,000
Error	14	4,385	0,3132		
Total	20	64,090			

Model Summary

S	R-sq	R-sq(adj)	R-sq(pred)
0,559681	93,16%	90,22%	84,60%

General Linear Model: D[4,3] versus Sample Name

Method

Factor coding (-1; 0; +1)

Factor Information

```
Factor       Type   Levels  Values
Sample Name  Fixed       7  PS_80H_XG_100_10_15_1week;
PS_80H_XG_100_20_15_1week;
                            PS_80H_XG_100_40_15_1week;
PS_80H_XG_500_10_15_1week;
                            PS_80H_XG_500_20_15_1week;
PS_80H_XG_500_40_15_1week;
                            PS_80H_XG_unpressurized_1week
```

Analysis of Variance

Source	DF	Adj SS	Adj MS	F-Value	P-Value
Sample Name	6	73,72	12,286	1,95	0,142
Error	14	88,17	6,298		
Total	20	161,89			

Model Summary

S	R-sq	R-sq(adj)	R-sq(pred)
2,50960	45,53%	22,19%	0,00%

General Linear Model: Span versus Sample Name

```
Method

Factor coding  (-1; 0; +1)


Factor Information

Factor       Type   Levels  Values
Sample Name  Fixed       7  PS_80H_XG_100_10_15_1week;
PS_80H_XG_100_20_15_1week;
                            PS_80H_XG_100_40_15_1week;
PS_80H_XG_500_10_15_1week;
                            PS_80H_XG_500_20_15_1week;
PS_80H_XG_500_40_15_1week;
                            PS_80H_XG_unpressurized_1week


Analysis of Variance

Source         DF  Adj SS   Adj MS  F-Value  P-Value
  Sample Name   6  0,4884  0,08141     1,88    0,154
Error          14  0,6050  0,04321
Total          20  1,0934


Model Summary

       S    R-sq  R-sq(adj)  R-sq(pred)
0,207872  44,67%     20,96%       0,00%
```

General Linear Model: T2 versus Sample Name

Method

Factor coding (-1; 0; +1)

Factor Information

Factor	Type	Levels	Values
Sample Name	Fixed	7	PS_80H_XG_100_10_15_1week; PS_80H_XG_100_20_15_1week; PS_80H_XG_100_40_15_1week; PS_80H_XG_500_10_15_1week; PS_80H_XG_500_20_15_1week; PS_80H_XG_500_40_15_1week; PS_80H_XG_unpressurized_1week

Analysis of Variance

Source	DF	Adj SS	Adj MS	F-Value	P-Value
Sample Name	6	91578	15263	2,65	0,062
Error	14	80499	5750		
Total	20	172078			

Model Summary

S	R-sq	R-sq(adj)	R-sq(pred)
75,8285	53,22%	33,17%	0,00%

General Linear Model: SDC*10^9 versus Sample Name

Method

Factor coding (-1; 0; +1)

Factor Information

```
Factor       Type   Levels  Values
Sample Name  Fixed       7  PS_80H_XG_100_10_15_1week;
PS_80H_XG_100_20_15_1week;
                            PS_80H_XG_100_40_15_1week;
PS_80H_XG_500_10_15_1week;
                            PS_80H_XG_500_20_15_1week;
PS_80H_XG_500_40_15_1week;
                            PS_80H_XG_unpressurized_1week
```

Analysis of Variance

Source	DF	Adj SS	Adj MS	F-Value	P-Value
Sample Name	6	0,1430	0,02383	1,57	0,228
Error	14	0,2126	0,01518		
Total	20	0,3556			

Model Summary

S	R-sq	R-sq(adj)	R-sq(pred)
0,123221	40,22%	14,60%	0,00%

Comparisons for α Melting T

Tukey Pairwise Comparisons: Response = α Melting T, Term = Sample Name

Grouping Information Using the Tukey Method and 95% Confidence

Sample Name	N	Mean	Grouping	
PS_80H_XG_unpressurized_1week	3	44,8800	A	
PS_80H_XG_100_40_15_1week	3	44,5700	A	B
PS_80H_XG_100_20_15_1week	3	44,3133	A	B
PS_80H_XG_500_40_15_1week	3	44,1600	A	B
PS_80H_XG_100_10_15_1week	3	44,1433	A	B
PS_80H_XG_500_20_15_1week	3	43,9867		B
PS_80H_XG_500_10_15_1week	3	43,7933		B

Means that do not share a letter are significantly different.

Comparisons for α Content

Tukey Pairwise Comparisons: Response = α Content, Term = Sample Name

```
Grouping Information Using the Tukey Method and 95% Confidence

Sample Name                    N     Mean  Grouping
PS_80H_XG_100_40_15_1week      3  11,2900  A
PS_80H_XG_unpressurized_1week  3   9,4404  A
PS_80H_XG_100_20_15_1week      3   5,8967      B
PS_80H_XG_500_40_15_1week      3   5,4834      B  C
PS_80H_XG_500_20_15_1week      3   5,3041      B  C
PS_80H_XG_100_10_15_1week      3   5,0481      B  C
PS_80H_XG_500_10_15_1week      3   3,6627         C

Means that do not share a letter are significantly different.
```

Comparisons for β Content

Tukey Pairwise Comparisons: Response = β Content, Term = Sample Name

```
Grouping Information Using the Tukey Method and 95% Confidence

Sample Name                    N     Mean  Grouping
PS_80H_XG_500_10_15_1week      3  88,1310  A
PS_80H_XG_500_20_15_1week      3  87,8102  A
PS_80H_XG_100_10_15_1week      3  87,0704  A
PS_80H_XG_500_40_15_1week      3  86,4215  A
PS_80H_XG_100_20_15_1week      3  85,6180  A   B
PS_80H_XG_100_40_15_1week      3  81,8883      B  C
PS_80H_XG_unpressurized_1week  3  81,3624         C

Means that do not share a letter are significantly different.
```

Comparisons for D[3,2]

Tukey Pairwise Comparisons: Response = D[3,2], Term = Sample Name

Grouping Information Using the Tukey Method and 95% Confidence

Sample Name	N	Mean	Grouping			
PS_80H_XG_unpressurized_1week	3	10,7633	A			
PS_80H_XG_500_20_15_1week	3	7,6100		B		
PS_80H_XG_100_40_15_1week	3	7,2300		B	C	
PS_80H_XG_500_10_15_1week	3	7,0400		B	C	
PS_80H_XG_100_20_15_1week	3	6,3200		B	C	D
PS_80H_XG_100_10_15_1week	3	6,0333			C	D
PS_80H_XG_500_40_15_1week	3	4,9867				D

Means that do not share a letter are significantly different.

APPENDIX D

Comparison of 80H_XG Emulsion Samples at 14th Day of Storage and Grouping Information

General Linear Model: α Melting T versus Sample Name

```
Method

Factor coding  (-1; 0; +1)


Factor Information

Factor       Type   Levels  Values
Sample Name  Fixed       7  PS_80H_XG_100_10_15_2week;
PS_80H_XG_100_20_15_2week;
                            PS_80H_XG_100_40_15_2week;
PS_80H_XG_500_10_15_2week;
                            PS_80H_XG_500_20_15_2week;
PS_80H_XG_500_40_15_2week;
                            PS_80H_XG_unpressurized_2week


Analysis of Variance

Source         DF  Adj SS   Adj MS  F-Value  P-Value
  Sample Name   6  4,0232  0,67053     9,54    0,000
Error          14  0,9843  0,07031
Total          20  5,0075


Model Summary

       S    R-sq  R-sq(adj)  R-sq(pred)
0,265159  80,34%     71,92%      55,77%
```

General Linear Model: α Content versus Sample Name

Method

Factor coding (-1; 0; +1)

Factor Information

```
Factor       Type   Levels  Values
Sample Name  Fixed       7  PS_80H_XG_100_10_15_2week;
PS_80H_XG_100_20_15_2week;
                            PS_80H_XG_100_40_15_2week;
PS_80H_XG_500_10_15_2week;
                            PS_80H_XG_500_20_15_2week;
PS_80H_XG_500_40_15_2week;
                            PS_80H_XG_unpressurized_2week
```

Analysis of Variance

Source	DF	Adj SS	Adj MS	F-Value	P-Value
Sample Name	6	74,984	12,4974	71,05	0,000
Error	14	2,463	0,1759		
Total	20	77,447			

Model Summary

S	R-sq	R-sq(adj)	R-sq(pred)
0,419405	96,82%	95,46%	92,85%

General Linear Model: β Melting T versus Sample Name

```
Method

Factor coding  (-1; 0; +1)


Factor Information

Factor       Type   Levels  Values
Sample Name  Fixed       7  PS_80H_XG_100_10_15_2week;
PS_80H_XG_100_20_15_2week;
                            PS_80H_XG_100_40_15_2week;
PS_80H_XG_500_10_15_2week;
                            PS_80H_XG_500_20_15_2week;
PS_80H_XG_500_40_15_2week;
                            PS_80H_XG_unpressurized_2week


Analysis of Variance

Source         DF  Adj SS  Adj MS  F-Value  P-Value
  Sample Name   6   1,177  0,1961     0,70    0,658
Error          14   3,950  0,2822
Total          20   5,127


Model Summary

       S    R-sq  R-sq(adj)  R-sq(pred)
0,531185  22,95%      0,00%       0,00%
```

General Linear Model: β Content versus Sample Name

```
Method

Factor coding  (-1; 0; +1)


Factor Information

Factor       Type   Levels  Values
Sample Name  Fixed       7  PS_80H_XG_100_10_15_2week;
PS_80H_XG_100_20_15_2week;
                            PS_80H_XG_100_40_15_2week;
PS_80H_XG_500_10_15_2week;
                            PS_80H_XG_500_20_15_2week;
PS_80H_XG_500_40_15_2week;
                            PS_80H_XG_unpressurized_2week


Analysis of Variance

Source          DF  Adj SS  Adj MS  F-Value  P-Value
  Sample Name    6  182,64  30,440    24,32    0,000
Error           14   17,52   1,251
Total           20  200,16


Model Summary

      S    R-sq  R-sq(adj)  R-sq(pred)
1,11869  91,25%     87,50%      80,31%
```

General Linear Model: 3rd Peak Melting T versus Sample Name

Method

Factor coding (-1; 0; +1)

Factor Information

```
Factor       Type   Levels  Values
Sample Name  Fixed       7  PS_80H_XG_100_10_15_2week;
PS_80H_XG_100_20_15_2week;
                            PS_80H_XG_100_40_15_2week;
PS_80H_XG_500_10_15_2week;
                            PS_80H_XG_500_20_15_2week;
PS_80H_XG_500_40_15_2week;
                            PS_80H_XG_unpressurized_2week
```

Analysis of Variance

Source	DF	Adj SS	Adj MS	F-Value	P-Value
Sample Name	6	0,2378	0,03963	1,03	0,448
Error	14	0,5401	0,03858		
Total	20	0,7779			

Model Summary

S	R-sq	R-sq(adj)	R-sq(pred)
0,196420	30,57%	0,81%	0,00%

General Linear Model: 3rd Peak Content versus Sample Name

Method

Factor coding (-1; 0; +1)

Factor Information

Factor	Type	Levels	Values
Sample Name	Fixed	7	PS_80H_XG_100_10_15_2week; PS_80H_XG_100_20_15_2week; PS_80H_XG_100_40_15_2week; PS_80H_XG_500_10_15_2week; PS_80H_XG_500_20_15_2week; PS_80H_XG_500_40_15_2week; PS_80H_XG_unpressurized_2week

Analysis of Variance

Source	DF	Adj SS	Adj MS	F-Value	P-Value
Sample Name	6	42,790	7,1317	11,36	0,000
Error	14	8,792	0,6280		
Total	20	51,583			

Model Summary

S	R-sq	R-sq(adj)	R-sq(pred)
0,792475	82,96%	75,65%	61,65%

General Linear Model: D[3,2] versus Sample Name

Method

Factor coding (-1; 0; +1)

Factor Information

Factor	Type	Levels	Values
Sample Name	Fixed	7	PS_80H_XG_100_10_15_2week; PS_80H_XG_100_20_15_2week; PS_80H_XG_100_40_15_2week; PS_80H_XG_500_10_15_2week; PS_80H_XG_500_20_15_2week; PS_80H_XG_500_40_15_2week; PS_80H_XG_unpressurized_2week

Analysis of Variance

Source	DF	Adj SS	Adj MS	F-Value	P-Value
Sample Name	6	229,242	38,2070	71,10	0,000
Error	14	7,523	0,5374		
Total	20	236,766			

Model Summary

S	R-sq	R-sq(adj)	R-sq(pred)
0,733069	96,82%	95,46%	92,85%

General Linear Model: D[4,3] versus Sample Name

Method

Factor coding (-1; 0; +1)

Factor Information

```
Factor       Type   Levels  Values
Sample Name  Fixed       7  PS_80H_XG_100_10_15_2week;
PS_80H_XG_100_20_15_2week;
                            PS_80H_XG_100_40_15_2week;
PS_80H_XG_500_10_15_2week;
                            PS_80H_XG_500_20_15_2week;
PS_80H_XG_500_40_15_2week;
                            PS_80H_XG_unpressurized_2week
```

Analysis of Variance

Source	DF	Adj SS	Adj MS	F-Value	P-Value
Sample Name	6	6898,9	1149,82	40,23	0,000
Error	14	400,1	28,58		
Total	20	7299,0			

Model Summary

S	R-sq	R-sq(adj)	R-sq(pred)
5,34607	94,52%	92,17%	87,67%

General Linear Model: Span versus Sample Name

Method

Factor coding (-1; 0; +1)

Factor Information

Factor	Type	Levels	Values
Sample Name	Fixed	7	PS_80H_XG_100_10_15_2week; PS_80H_XG_100_20_15_2week; PS_80H_XG_100_40_15_2week; PS_80H_XG_500_10_15_2week; PS_80H_XG_500_20_15_2week; PS_80H_XG_500_40_15_2week; PS_80H_XG_unpressurized_2week

Analysis of Variance

Source	DF	Adj SS	Adj MS	F-Value	P-Value
Sample Name	6	12,7367	2,12278	44,08	0,000
Error	14	0,6742	0,04816		
Total	20	13,4109			

Model Summary

S	R-sq	R-sq(adj)	R-sq(pred)
0,219446	94,97%	92,82%	88,69%

General Linear Model: T2 versus Sample Name

Method

Factor coding (-1; 0; +1)

Factor Information

Factor	Type	Levels	Values
Sample Name	Fixed	7	PS_80H_XG_100_10_15_2week; PS_80H_XG_100_20_15_2week; PS_80H_XG_100_40_15_2week; PS_80H_XG_500_10_15_2week; PS_80H_XG_500_20_15_2week; PS_80H_XG_500_40_15_2week; PS_80H_XG_unpressurized_2week

Analysis of Variance

Source	DF	Adj SS	Adj MS	F-Value	P-Value
Sample Name	6	170014	28336	2,76	0,055
Error	14	143511	10251		
Total	20	313524			

Model Summary

S	R-sq	R-sq(adj)	R-sq(pred)
101,246	54,23%	34,61%	0,00%

General Linear Model: SDC*10^9 versus Sample Name

Method

Factor coding (-1; 0; +1)

Factor Information

Factor	Type	Levels	Values
Sample Name	Fixed	7	PS_80H_XG_100_10_15_2week; PS_80H_XG_100_20_15_2week; PS_80H_XG_100_40_15_2week; PS_80H_XG_500_10_15_2week; PS_80H_XG_500_20_15_2week; PS_80H_XG_500_40_15_2week; PS_80H_XG_unpressurized_2week

Analysis of Variance

Source	DF	Adj SS	Adj MS	F-Value	P-Value
Sample Name	6	0,3154	0,05256	4,89	0,007
Error	14	0,1506	0,01076		
Total	20	0,4659			

Model Summary

S	R-sq	R-sq(adj)	R-sq(pred)
0,103707	67,68%	53,83%	27,29%

Comparisons for α Melting T

Tukey Pairwise Comparisons: Response = α Melting T, Term = Sample Name

Grouping Information Using the Tukey Method and 95% Confidence

Sample Name	N	Mean	Grouping		
PS_80H_XG_unpressurized_2week	3	44,8233	A		
PS_80H_XG_100_40_15_2week	3	44,5667	A	B	
PS_80H_XG_100_10_15_2week	3	43,9000		B	C
PS_80H_XG_500_40_15_2week	3	43,8033			C
PS_80H_XG_500_20_15_2week	3	43,7600			C
PS_80H_XG_100_20_15_2week	3	43,7267			C
PS_80H_XG_500_10_15_2week	3	43,5933			C

Means that do not share a letter are significantly different.

Comparisons for α Content

Tukey Pairwise Comparisons: Response = α Content, Term = Sample Name

Grouping Information Using the Tukey Method and 95% Confidence

Sample Name	N	Mean	Grouping		
PS_80H_XG_100_40_15_2week	3	7,67270	A		
PS_80H_XG_unpressurized_2week	3	7,02725	A		
PS_80H_XG_500_40_15_2week	3	3,97732		B	
PS_80H_XG_100_10_15_2week	3	3,47478		B	C
PS_80H_XG_500_20_15_2week	3	3,18159		B	C
PS_80H_XG_100_20_15_2week	3	3,02723		B	C
PS_80H_XG_500_10_15_2week	3	2,67205			C

Means that do not share a letter are significantly different.

Comparisons for β Content

Tukey Pairwise Comparisons: Response = β Content, Term = Sample Name

Grouping Information Using the Tukey Method and 95% Confidence

Sample Name	N	Mean	Grouping	
PS_80H_XG_100_10_15_2week	3	90,2982	A	
PS_80H_XG_100_20_15_2week	3	90,2866	A	
PS_80H_XG_500_20_15_2week	3	89,8413	A	
PS_80H_XG_500_40_15_2week	3	88,7809	A	
PS_80H_XG_500_10_15_2week	3	88,2747	A	
PS_80H_XG_100_40_15_2week	3	84,0941		B
PS_80H_XG_unpressurized_2week	3	82,3752		B

Means that do not share a letter are significantly different.

Comparisons for 3rd Peak Content

Tukey Pairwise Comparisons: Response = 3rd Peak Content, Term = Sample Name

Grouping Information Using the Tukey Method and 95% Confidence

Sample Name	N	Mean	Grouping		
PS_80H_XG_unpressurized_2week	3	10,5975	A		
PS_80H_XG_500_10_15_2week	3	9,0533	A	B	
PS_80H_XG_100_40_15_2week	3	8,2332		B	C
PS_80H_XG_500_40_15_2week	3	7,2418		B	C
PS_80H_XG_500_20_15_2week	3	6,9771		B	C
PS_80H_XG_100_20_15_2week	3	6,6862			C
PS_80H_XG_100_10_15_2week	3	6,2270			C

Means that do not share a letter are significantly different.

Comparisons for D[3,2]

Tukey Pairwise Comparisons: Response = D[3,2], Term = Sample Name

Grouping Information Using the Tukey Method and 95% Confidence

Sample Name	N	Mean	Grouping				
PS_80H_XG_unpressurized_2week	3	17,8433	A				
PS_80H_XG_500_10_15_2week	3	12,6533		B			
PS_80H_XG_100_20_15_2week	3	12,1067		B			
PS_80H_XG_500_20_15_2week	3	10,6667		B	C		
PS_80H_XG_100_10_15_2week	3	9,6467			C	D	
PS_80H_XG_500_40_15_2week	3	8,1733				D	E
PS_80H_XG_100_40_15_2week	3	7,0167					E

Means that do not share a letter are significantly different.

Comparisons for D[4,3]

Tukey Pairwise Comparisons: Response = D[4,3], Term = Sample Name

Grouping Information Using the Tukey Method and 95% Confidence

Sample Name	N	Mean	Grouping	
PS_80H_XG_500_10_15_2week	3	84,9333	A	
PS_80H_XG_100_20_15_2week	3	70,4667	A	
PS_80H_XG_100_10_15_2week	3	45,3667	B	
PS_80H_XG_500_20_15_2week	3	44,2333	B	C
PS_80H_XG_500_40_15_2week	3	43,4667	B	C
PS_80H_XG_unpressurized_2week	3	37,2667	B	C
PS_80H_XG_100_40_15_2week	3	29,8667		C

Means that do not share a letter are significantly different.

Comparisons for Span

Tukey Pairwise Comparisons: Response = Span, Term = Sample Name

Grouping Information Using the Tukey Method and 95% Confidence

Sample Name	N	Mean	Grouping			
PS_80H_XG_500_10_15_2week	3	4,83633	A			
PS_80H_XG_100_20_15_2week	3	3,26400		B		
PS_80H_XG_100_10_15_2week	3	2,97200		B	C	
PS_80H_XG_500_40_15_2week	3	2,82433		B	C	D
PS_80H_XG_500_20_15_2week	3	2,75500		B	C	D
PS_80H_XG_unpressurized_2week	3	2,63467			C	D
PS_80H_XG_100_40_15_2week	3	2,21600				D

Means that do not share a letter are significantly different.

Comparisons for SDC*10^9

Tukey Pairwise Comparisons: Response = SDC*10^9, Term = Sample Name

Grouping Information Using the Tukey Method and 95% Confidence

Sample Name	N	Mean	Grouping	
PS_80H_XG_unpressurized_2week	3	1,59980	A	
PS_80H_XG_100_10_15_2week	3	1,59927	A	
PS_80H_XG_100_20_15_2week	3	1,43743	A	B
PS_80H_XG_500_20_15_2week	3	1,38530	A	B
PS_80H_XG_500_40_15_2week	3	1,34323	A	B
PS_80H_XG_100_40_15_2week	3	1,32900	A	B
PS_80H_XG_500_10_15_2week	3	1,26187		B

Means that do not share a letter are significantly different.

APPENDIX E

Comparison of 80H_XG Emulsion Samples at 28th Day of Storage and Grouping Information

General Linear Model: α Melting T versus Sample Name

```
Method

Factor coding  (-1; 0; +1)


Factor Information

Factor       Type   Levels  Values
Sample Name  Fixed       7  PS_80H_XG_100_10_15_4week;
PS_80H_XG_100_20_15_4week;
                            PS_80H_XG_100_40_15_4week;
PS_80H_XG_500_10_15_4week;
                            PS_80H_XG_500_20_15_4week;
PS_80H_XG_500_40_15_4week;
                            PS_80H_XG_unpressurized_4week


Analysis of Variance

Source         DF  Adj SS  Adj MS  F-Value  P-Value
  Sample Name   6   1,488  0,2480     1,98    0,137
Error          14   1,756  0,1254
Total          20   3,244


Model Summary

       S    R-sq  R-sq(adj)  R-sq(pred)
0,354112  45,88%     22,68%       0,00%
```

General Linear Model: α Content versus Sample Name

```
Method

Factor coding  (-1; 0; +1)


Factor Information

Factor       Type   Levels  Values
Sample Name  Fixed       7  PS_80H_XG_100_10_15_4week;
PS_80H_XG_100_20_15_4week;
                            PS_80H_XG_100_40_15_4week;
PS_80H_XG_500_10_15_4week;
                            PS_80H_XG_500_20_15_4week;
PS_80H_XG_500_40_15_4week;
                            PS_80H_XG_unpressurized_4week


Analysis of Variance

Source         DF   Adj SS   Adj MS  F-Value  P-Value
  Sample Name   6  161,325  26,8874    47,23    0,000
Error          14    7,970   0,5693
Total          20  169,294


Model Summary

       S    R-sq  R-sq(adj)  R-sq(pred)
0,754501  95,29%     93,27%      89,41%
```

General Linear Model: β Melting T versus Sample Name

```
Method

Factor coding  (-1; 0; +1)


Factor Information

Factor       Type   Levels  Values
Sample Name  Fixed       7  PS_80H_XG_100_10_15_4week;
PS_80H_XG_100_20_15_4week;
                            PS_80H_XG_100_40_15_4week;
PS_80H_XG_500_10_15_4week;
                            PS_80H_XG_500_20_15_4week;
PS_80H_XG_500_40_15_4week;
                            PS_80H_XG_unpressurized_4week


Analysis of Variance

Source          DF  Adj SS   Adj MS  F-Value  P-Value
  Sample Name    6  0,5478  0,09130     0,96    0,486
Error           14  1,3312  0,09509
Total           20  1,8790


Model Summary

       S    R-sq  R-sq(adj)  R-sq(pred)
0,308360  29,15%      0,00%       0,00%
```

General Linear Model: β Content versus Sample Name

```
Method

Factor coding  (-1; 0; +1)


Factor Information

Factor       Type   Levels  Values
Sample Name  Fixed       7  PS_80H_XG_100_10_15_4week;
PS_80H_XG_100_20_15_4week;
                            PS_80H_XG_100_40_15_4week;
PS_80H_XG_500_10_15_4week;
                            PS_80H_XG_500_20_15_4week;
PS_80H_XG_500_40_15_4week;
                            PS_80H_XG_unpressurized_4week


Analysis of Variance

Source          DF  Adj SS  Adj MS  F-Value  P-Value
  Sample Name    6  133,33  22,221    13,00    0,000
Error           14   23,94   1,710
Total           20  157,26


Model Summary

      S    R-sq  R-sq(adj)  R-sq(pred)
1,30760  84,78%     78,26%      65,75%
```

General Linear Model: 3rd Peak Melting T versus Sample Name

Method

Factor coding (-1; 0; +1)

Factor Information

```
Factor       Type   Levels  Values
Sample Name  Fixed       7  PS_80H_XG_100_10_15_4week;
PS_80H_XG_100_20_15_4week;
                            PS_80H_XG_100_40_15_4week;
PS_80H_XG_500_10_15_4week;
                            PS_80H_XG_500_20_15_4week;
PS_80H_XG_500_40_15_4week;
                            PS_80H_XG_unpressurized_4week
```

Analysis of Variance

Source	DF	Adj SS	Adj MS	F-Value	P-Value
Sample Name	6	0,003914	0,000652	0,10	0,995
Error	14	0,092867	0,006633		
Total	20	0,096781			

Model Summary

S	R-sq	R-sq(adj)	R-sq(pred)
0,0814453	4,04%	0,00%	0,00%

General Linear Model: 3rd Peak Content versus Sample Name

```
Method

Factor coding  (-1; 0; +1)


Factor Information

Factor       Type   Levels  Values
Sample Name  Fixed       7  PS_80H_XG_100_10_15_4week;
PS_80H_XG_100_20_15_4week;
                            PS_80H_XG_100_40_15_4week;
PS_80H_XG_500_10_15_4week;
                            PS_80H_XG_500_20_15_4week;
PS_80H_XG_500_40_15_4week;
                            PS_80H_XG_unpressurized_4week


Analysis of Variance

Source         DF  Adj SS  Adj MS  F-Value  P-Value
  Sample Name   6   6,558  1,0929     1,15    0,384
Error          14  13,268  0,9477
Total          20  19,825


Model Summary

       S    R-sq  R-sq(adj)  R-sq(pred)
0,973494  33,08%      4,40%       0,00%
```

General Linear Model: D[3,2] versus Sample Name

```
Method

Factor coding  (-1; 0; +1)


Factor Information

Factor       Type   Levels  Values
Sample Name  Fixed       7  PS_80H_XG_100_10_15_4week;
PS_80H_XG_100_20_15_4week;
                            PS_80H_XG_100_40_15_4week;
PS_80H_XG_500_10_15_4week;
                            PS_80H_XG_500_20_15_4week;
PS_80H_XG_500_40_15_4week;
                            PS_80H_XG_unpressurized_4week


Analysis of Variance

Source          DF   Adj SS   Adj MS  F-Value  P-Value
  Sample Name    6  168,694  28,1157    44,49    0,000
Error           14    8,847   0,6319
Total           20  177,541


Model Summary

       S    R-sq  R-sq(adj)  R-sq(pred)
0,794942  95,02%     92,88%      88,79%
```

General Linear Model: D[4,3] versus Sample Name

```
Method

Factor coding  (-1; 0; +1)


Factor Information

Factor       Type   Levels  Values
Sample Name  Fixed       7  PS_80H_XG_100_10_15_4week;
PS_80H_XG_100_20_15_4week;
                            PS_80H_XG_100_40_15_4week;
PS_80H_XG_500_10_15_4week;
                            PS_80H_XG_500_20_15_4week;
PS_80H_XG_500_40_15_4week;
                            PS_80H_XG_unpressurized_4week


Analysis of Variance

Source         DF  Adj SS  Adj MS  F-Value  P-Value
  Sample Name   6  321,41  53,568     9,90    0,000
Error          14   75,74   5,410
Total          20  397,15


Model Summary

      S    R-sq  R-sq(adj)  R-sq(pred)
2,32594  80,93%     72,76%      57,09%
```

General Linear Model: Span versus Sample Name

```
Method

Factor coding  (-1; 0; +1)


Factor Information

Factor       Type   Levels  Values
Sample Name  Fixed       7  PS_80H_XG_100_10_15_4week;
PS_80H_XG_100_20_15_4week;
                            PS_80H_XG_100_40_15_4week;
PS_80H_XG_500_10_15_4week;
                            PS_80H_XG_500_20_15_4week;
PS_80H_XG_500_40_15_4week;
                            PS_80H_XG_unpressurized_4week


Analysis of Variance

Source         DF  Adj SS   Adj MS  F-Value  P-Value
  Sample Name   6  1,7992  0,29987     7,33    0,001
Error          14  0,5725  0,04090
Total          20  2,3718


Model Summary

       S    R-sq  R-sq(adj)  R-sq(pred)
0,202228  75,86%     65,51%      45,68%
```

General Linear Model: T2 versus Sample Name

Method

Factor coding (-1; 0; +1)

Factor Information

Factor	Type	Levels	Values
Sample Name	Fixed	7	PS_80H_XG_100_10_15_4week; PS_80H_XG_100_20_15_4week; PS_80H_XG_100_40_15_4week; PS_80H_XG_500_10_15_4week; PS_80H_XG_500_20_15_4week; PS_80H_XG_500_40_15_4week; PS_80H_XG_unpressurized_4week

Analysis of Variance

Source	DF	Adj SS	Adj MS	F-Value	P-Value
Sample Name	6	26813	4469	1,25	0,342
Error	14	50246	3589		
Total	20	77059			

Model Summary

S	R-sq	R-sq(adj)	R-sq(pred)
59,9085	34,79%	6,85%	0,00%

General Linear Model: SDC*10^9 versus Sample Name

Method

Factor coding (-1; 0; +1)

Factor Information

Factor	Type	Levels	Values
Sample Name	Fixed	7	PS_80H_XG_100_10_15_4week; PS_80H_XG_100_20_15_4week; PS_80H_XG_100_40_15_4week; PS_80H_XG_500_10_15_4week; PS_80H_XG_500_20_15_4week; PS_80H_XG_500_40_15_4week; PS_80H_XG_unpressurized_4week

Analysis of Variance

Source	DF	Adj SS	Adj MS	F-Value	P-Value
Sample Name	6	0,82761	0,137935	20,61	0,000
Error	14	0,09370	0,006693		
Total	20	0,92131			

Model Summary

S	R-sq	R-sq(adj)	R-sq(pred)
0,0818091	89,83%	85,47%	77,12%

Comparisons for α Content

Tukey Pairwise Comparisons: Response = α Content, Term = Sample Name

Grouping Information Using the Tukey Method and 95% Confidence

Sample Name	N	Mean	Grouping	
PS_80H_XG_100_40_15_4week	3	14,6743	A	
PS_80H_XG_100_20_15_4week	3	8,3636	B	
PS_80H_XG_500_20_15_4week	3	8,1301	B	
PS_80H_XG_unpressurized_4week	3	7,5454	B	
PS_80H_XG_100_10_15_4week	3	7,0618	B	C
PS_80H_XG_500_40_15_4week	3	6,9815	B	C
PS_80H_XG_500_10_15_4week	3	5,2553		C

Means that do not share a letter are significantly different.

Comparisons for β Content

Tukey Pairwise Comparisons: Response = β Content, Term = Sample Name

Grouping Information Using the Tukey Method and 95% Confidence

Sample Name	N	Mean	Grouping	
PS_80H_XG_500_10_15_4week	3	84,8344	A	
PS_80H_XG_500_40_15_4week	3	83,4557	A	
PS_80H_XG_100_10_15_4week	3	82,7166	A	
PS_80H_XG_500_20_15_4week	3	81,6022	A	
PS_80H_XG_100_20_15_4week	3	81,5242	A	
PS_80H_XG_unpressurized_4week	3	81,3969	A	
PS_80H_XG_100_40_15_4week	3	76,1888		B

Means that do not share a letter are significantly different.

Comparisons for D[3,2]

Tukey Pairwise Comparisons: Response = D[3,2], Term = Sample Name

Grouping Information Using the Tukey Method and 95% Confidence

Sample Name	N	Mean	Grouping				
PS_80H_XG_unpressurized_4week	3	13,6333	A				
PS_80H_XG_100_10_15_4week	3	10,1667		B			
PS_80H_XG_500_10_15_4week	3	9,9233		B			
PS_80H_XG_100_20_15_4week	3	8,8333		B	C		
PS_80H_XG_500_40_15_4week	3	6,9667			C	D	
PS_80H_XG_500_20_15_4week	3	6,5733				D	
PS_80H_XG_100_40_15_4week	3	4,1433					E

Means that do not share a letter are significantly different.

Comparisons for D[4,3]

Tukey Pairwise Comparisons: Response = D[4,3], Term = Sample Name

Grouping Information Using the Tukey Method and 95% Confidence

Sample Name	N	Mean	Grouping		
PS_80H_XG_500_10_15_4week	3	34,1000	A		
PS_80H_XG_100_10_15_4week	3	33,8000	A		
PS_80H_XG_unpressurized_4week	3	33,3667	A	B	
PS_80H_XG_100_20_15_4week	3	32,4333	A	B	
PS_80H_XG_500_40_15_4week	3	31,6000	A	B	
PS_80H_XG_500_20_15_4week	3	27,0000		B	C
PS_80H_XG_100_40_15_4week	3	22,8667			C

Means that do not share a letter are significantly different.

Comparisons for Span

Tukey Pairwise Comparisons: Response = Span, Term = Sample Name

Grouping Information Using the Tukey Method and 95% Confidence

Sample Name	N	Mean	Grouping		
PS_80H_XG_100_10_15_4week	3	2,82900	A		
PS_80H_XG_500_10_15_4week	3	2,46367	A	B	
PS_80H_XG_500_40_15_4week	3	2,33533	A	B	C
PS_80H_XG_unpressurized_4week	3	2,24067		B	C
PS_80H_XG_100_20_15_4week	3	2,22967		B	C
PS_80H_XG_500_20_15_4week	3	2,01933		B	C
PS_80H_XG_100_40_15_4week	3	1,84467			C

Means that do not share a letter are significantly different.

Comparisons for SDC*10^9

Tukey Pairwise Comparisons: Response = SDC*10^9, Term = Sample Name

Grouping Information Using the Tukey Method and 95% Confidence

Sample Name	N	Mean	Grouping			
PS_80H_XG_100_10_15_4week	3	1,73800	A			
PS_80H_XG_unpressurized_4week	3	1,50520		B		
PS_80H_XG_500_20_15_4week	3	1,46000		B		
PS_80H_XG_500_40_15_4week	3	1,37170		B	C	
PS_80H_XG_500_10_15_4week	3	1,21380			C	D
PS_80H_XG_100_40_15_4week	3	1,21143			C	D
PS_80H_XG_100_20_15_4week	3	1,11580				D

Means that do not share a letter are significantly different.

APPENDIX F

Comparison of SC Emulsion Samples at 1st Day of Storage and Grouping Information

General Linear Model: α Melting T versus Sample Name

Method

Factor coding (-1; 0; +1)

Factor Information

Factor	Type	Levels	Values
Sample Name	Fixed	7	PS_SC_100_10_15_0week; PS_SC_100_20_15_0week; PS_SC_100_40_15_0week; PS_SC_500_10_15_0week; PS_SC_500_20_15_0week; PS_SC_500_40_15_0week; PS_SC_unpressurized_0week

Analysis of Variance

Source	DF	Adj SS	Adj MS	F-Value	P-Value
Sample Name	6	1,3588	0,22647	5,21	0,005
Error	14	0,6091	0,04350		
Total	20	1,9679			

Model Summary

S	R-sq	R-sq(adj)	R-sq(pred)
0,208578	69,05%	55,78%	30,36%

General Linear Model: α Content versus Sample Name

Method

Factor coding (-1; 0; +1)

Factor Information

Factor	Type	Levels	Values
Sample Name	Fixed	7	PS_SC_100_10_15_0week; PS_SC_100_20_15_0week; PS_SC_100_40_15_0week; PS_SC_500_10_15_0week; PS_SC_500_20_15_0week; PS_SC_500_40_15_0week; PS_SC_unpressurized_0week

Analysis of Variance

Source	DF	Adj SS	Adj MS	F-Value	P-Value
Sample Name	6	4481,82	746,970	149,80	0,000
Error	14	69,81	4,986		
Total	20	4551,63			

Model Summary

S	R-sq	R-sq(adj)	R-sq(pred)
2,23301	98,47%	97,81%	96,55%

General Linear Model: β Melting T versus Sample Name

Method

Factor coding (-1; 0; +1)

Factor Information

Factor	Type	Levels	Values
Sample Name	Fixed	7	PS_SC_100_10_15_0week; PS_SC_100_20_15_0week; PS_SC_100_40_15_0week; PS_SC_500_10_15_0week; PS_SC_500_20_15_0week; PS_SC_500_40_15_0week; PS_SC_unpressurized_0week

Analysis of Variance

Source	DF	Adj SS	Adj MS	F-Value	P-Value
Sample Name	6	0,02452	0,004087	1,08	0,420
Error	14	0,05300	0,003786		
Total	20	0,07752			

Model Summary

S	R-sq	R-sq(adj)	R-sq(pred)
0,0615282	31,63%	2,33%	0,00%

General Linear Model: β Content versus Sample Name

Method

Factor coding (-1; 0; +1)

Factor Information

Factor	Type	Levels	Values
Sample Name	Fixed	7	PS_SC_100_10_15_0week; PS_SC_100_20_15_0week; PS_SC_100_40_15_0week; PS_SC_500_10_15_0week; PS_SC_500_20_15_0week; PS_SC_500_40_15_0week; PS_SC_unpressurized_0week

Analysis of Variance

Source	DF	Adj SS	Adj MS	F-Value	P-Value
Sample Name	6	4483,10	747,184	110,61	0,000
Error	14	94,57	6,755		
Total	20	4577,67			

Model Summary

S	R-sq	R-sq(adj)	R-sq(pred)
2,59901	97,93%	97,05%	95,35%

General Linear Model: D[3,2] versus Sample Name

Method

Factor coding (-1; 0; +1)

Factor Information

Factor	Type	Levels	Values
Sample Name	Fixed	7	PS_SC_100_10_15_0week; PS_SC_100_20_15_0week; PS_SC_100_40_15_0week; PS_SC_500_10_15_0week; PS_SC_500_20_15_0week; PS_SC_500_40_15_0week; PS_SC_unpressurized_0week

Analysis of Variance

Source	DF	Adj SS	Adj MS	F-Value	P-Value
Sample Name	6	0,000093	0,000016	1,23	0,349
Error	14	0,000177	0,000013		
Total	20	0,000270			

Model Summary

S	R-sq	R-sq(adj)	R-sq(pred)
0,0035523	34,52%	6,46%	0,00%

General Linear Model: D[4,3] versus Sample Name

Method

Factor coding (-1; 0; +1)

Factor Information

Factor	Type	Levels	Values
Sample Name	Fixed	7	PS_SC_100_10_15_0week; PS_SC_100_20_15_0week; PS_SC_100_40_15_0week; PS_SC_500_10_15_0week; PS_SC_500_20_15_0week; PS_SC_500_40_15_0week; PS_SC_unpressurized_0week

Analysis of Variance

Source	DF	Adj SS	Adj MS	F-Value	P-Value
Sample Name	6	0,000555	0,000093	1,76	0,180
Error	14	0,000737	0,000053		
Total	20	0,001293			

Model Summary

S	R-sq	R-sq(adj)	R-sq(pred)
0,0072572	42,96%	18,51%	0,00%

General Linear Model: Span versus Sample Name

Method

Factor coding (-1; 0; +1)

Factor Information

Factor	Type	Levels	Values
Sample Name	Fixed	7	PS_SC_100_10_15_0week; PS_SC_100_20_15_0week; PS_SC_100_40_15_0week; PS_SC_500_10_15_0week; PS_SC_500_20_15_0week; PS_SC_500_40_15_0week; PS_SC_unpressurized_0week

Analysis of Variance

Source	DF	Adj SS	Adj MS	F-Value	P-Value
Sample Name	6	0,004213	0,000702	0,73	0,631
Error	14	0,013413	0,000958		
Total	20	0,017625			

Model Summary

S	R-sq	R-sq(adj)	R-sq(pred)
0,0309523	23,90%	0,00%	0,00%

General Linear Model: T2 versus Sample Name

Method

Factor coding (-1; 0; +1)

Factor Information

Factor	Type	Levels	Values
Sample Name	Fixed	7	PS_SC_100_10_15_0week; PS_SC_100_20_15_0week; PS_SC_100_40_15_0week; PS_SC_500_10_15_0week; PS_SC_500_20_15_0week; PS_SC_500_40_15_0week; PS_SC_unpressurized_0week

Analysis of Variance

Source	DF	Adj SS	Adj MS	F-Value	P-Value
Sample Name	6	10716	1786	1,21	0,359
Error	14	20708	1479		
Total	20	31424			

Model Summary

S	R-sq	R-sq(adj)	R-sq(pred)
38,4595	34,10%	5,86%	0,00%

General Linear Model: SDC*10^9 versus Sample Name

Method

Factor coding (-1; 0; +1)

Factor Information

Factor	Type	Levels	Values
Sample Name	Fixed	7	PS_SC_100_10_15_0week; PS_SC_100_20_15_0week; PS_SC_100_40_15_0week; PS_SC_500_10_15_0week; PS_SC_500_20_15_0week; PS_SC_500_40_15_0week; PS_SC_unpressurized_0week

Analysis of Variance

Source	DF	Adj SS	Adj MS	F-Value	P-Value
Sample Name	6	0,1175	0,01958	0,88	0,536
Error	14	0,3126	0,02233		
Total	20	0,4300			

Model Summary

S	R-sq	R-sq(adj)	R-sq(pred)
0,149418	27,31%	0,00%	0,00%

Comparisons for α Melting T

Tukey Pairwise Comparisons: Response = α Melting T, Term = Sample Name

Grouping Information Using the Tukey Method and 95% Confidence

Sample Name	N	Mean	Grouping	
PS_SC_unpressurized_0week	3	45,1033	A	
PS_SC_100_40_15_0week	3	44,8733	A	B
PS_SC_100_20_15_0week	3	44,7900	A	B
PS_SC_500_40_15_0week	3	44,7367	A	B
PS_SC_100_10_15_0week	3	44,4900		B
PS_SC_500_20_15_0week	3	44,4167		B
PS_SC_500_10_15_0week	3	44,3400		B

Means that do not share a letter are significantly different.

Comparisons for α Content

Tukey Pairwise Comparisons: Response = α Content, Term = Sample Name

Grouping Information Using the Tukey Method and 95% Confidence

Sample Name	N	Mean	Grouping			
PS_SC_unpressurized_0week	3	54,2121	A			
PS_SC_100_40_15_0week	3	38,3800		B		
PS_SC_100_20_15_0week	3	32,0337			C	
PS_SC_500_40_15_0week	3	26,4267			C	
PS_SC_100_10_15_0week	3	15,3700				D
PS_SC_500_20_15_0week	3	13,8600				D
PS_SC_500_10_15_0week	3	9,9538				D

Means that do not share a letter are significantly different.

Comparisons for β Content

Tukey Pairwise Comparisons: Response = β Content, Term = Sample Name

Grouping Information Using the Tukey Method and 95% Confidence

Sample Name	N	Mean	Grouping			
PS_SC_500_10_15_0week	3	90,0462	A			
PS_SC_500_20_15_0week	3	86,1400	A			
PS_SC_100_10_15_0week	3	84,6300	A			
PS_SC_500_40_15_0week	3	71,5734		B		
PS_SC_100_20_15_0week	3	67,9663		B	C	
PS_SC_100_40_15_0week	3	61,6200			C	
PS_SC_unpressurized_0week	3	45,7879				D

Means that do not share a letter are significantly different.

APPENDIX G

Comparison of SC Emulsion Samples at 8th Day of Storage and Grouping Information

General Linear Model: α Melting T versus Sample Name

```
Method

Factor coding  (-1; 0; +1)


Factor Information

Factor       Type   Levels  Values
Sample Name  Fixed       7  PS_SC_100_10_15_1week; PS_SC_100_20_15_1week;
                            PS_SC_100_40_15_1week; PS_SC_500_10_15_1week;
                            PS_SC_500_20_15_1week; PS_SC_500_40_15_1week;
                            PS_SC_unpressurized_1week


Analysis of Variance

Source          DF  Adj SS   Adj MS  F-Value  P-Value
  Sample Name    6  0,7066  0,11777     2,19    0,107
Error           14  0,7537  0,05383
Total           20  1,4603


Model Summary

       S    R-sq  R-sq(adj)  R-sq(pred)
0,232020  48,39%     26,27%       0,00%
```

General Linear Model: α Content versus Sample Name

Method

Factor coding (-1; 0; +1)

Factor Information

Factor	Type	Levels	Values
Sample Name	Fixed	7	PS_SC_100_10_15_1week; PS_SC_100_20_15_1week; PS_SC_100_40_15_1week; PS_SC_500_10_15_1week; PS_SC_500_20_15_1week; PS_SC_500_40_15_1week; PS_SC_unpressurized_1week

Analysis of Variance

Source	DF	Adj SS	Adj MS	F-Value	P-Value
Sample Name	6	268,66	44,777	35,31	0,000
Error	14	17,75	1,268		
Total	20	286,42			

Model Summary

S	R-sq	R-sq(adj)	R-sq(pred)
1,12615	93,80%	91,14%	86,05%

General Linear Model: β Melting T versus Sample Name

Method

Factor coding (-1; 0; +1)

Factor Information

Factor	Type	Levels	Values
Sample Name	Fixed	7	PS_SC_100_10_15_1week; PS_SC_100_20_15_1week; PS_SC_100_40_15_1week; PS_SC_500_10_15_1week; PS_SC_500_20_15_1week; PS_SC_500_40_15_1week; PS_SC_unpressurized_1week

Analysis of Variance

Source	DF	Adj SS	Adj MS	F-Value	P-Value
Sample Name	6	0,09556	0,015927	1,99	0,135
Error	14	0,11187	0,007990		
Total	20	0,20743			

Model Summary

S	R-sq	R-sq(adj)	R-sq(pred)
0,0893895	46,07%	22,96%	0,00%

General Linear Model: β Content versus Sample Name

Method

Factor coding (-1; 0; +1)

Factor Information

Factor	Type	Levels	Values
Sample Name	Fixed	7	PS_SC_100_10_15_1week; PS_SC_100_20_15_1week; PS_SC_100_40_15_1week; PS_SC_500_10_15_1week; PS_SC_500_20_15_1week; PS_SC_500_40_15_1week; PS_SC_unpressurized_1week

Analysis of Variance

Source	DF	Adj SS	Adj MS	F-Value	P-Value
Sample Name	6	268,66	44,777	35,31	0,000
Error	14	17,75	1,268		
Total	20	286,42			

Model Summary

S	R-sq	R-sq(adj)	R-sq(pred)
1,12615	93,80%	91,14%	86,05%

General Linear Model: D[3,2] versus Sample Name

Method

Factor coding (-1; 0; +1)

Factor Information

Factor	Type	Levels	Values
Sample Name	Fixed	7	PS_SC_100_10_15_1week; PS_SC_100_20_15_1week; PS_SC_100_40_15_1week; PS_SC_500_10_15_1week; PS_SC_500_20_15_1week; PS_SC_500_40_15_1week; PS_SC_unpressurized_1week

Analysis of Variance

Source	DF	Adj SS	Adj MS	F-Value	P-Value
Sample Name	6	0,000007	0,000001	0,60	0,724
Error	14	0,000028	0,000002		
Total	20	0,000035			

Model Summary

S	R-sq	R-sq(adj)	R-sq(pred)
0,0014142	20,54%	0,00%	0,00%

General Linear Model: D[4,3] versus Sample Name

Method

Factor coding (-1; 0; +1)

Factor Information

Factor	Type	Levels	Values
Sample Name	Fixed	7	PS_SC_100_10_15_1week; PS_SC_100_20_15_1week; PS_SC_100_40_15_1week; PS_SC_500_10_15_1week; PS_SC_500_20_15_1week; PS_SC_500_40_15_1week; PS_SC_unpressurized_1week

Analysis of Variance

Source	DF	Adj SS	Adj MS	F-Value	P-Value
Sample Name	6	0,000494	0,000082	2,81	0,052
Error	14	0,000409	0,000029		
Total	20	0,000903			

Model Summary

S	R-sq	R-sq(adj)	R-sq(pred)
0,0054072	54,68%	35,25%	0,00%

General Linear Model: Span versus Sample Name

Method

Factor coding (-1; 0; +1)

Factor Information

Factor	Type	Levels	Values
Sample Name	Fixed	7	PS_SC_100_10_15_1week; PS_SC_100_20_15_1week; PS_SC_100_40_15_1week; PS_SC_500_10_15_1week; PS_SC_500_20_15_1week; PS_SC_500_40_15_1week; PS_SC_unpressurized_1week

Analysis of Variance

Source	DF	Adj SS	Adj MS	F-Value	P-Value
Sample Name	6	0,06966	0,011609	4,81	0,007
Error	14	0,03378	0,002413		
Total	20	0,10344			

Model Summary

S	R-sq	R-sq(adj)	R-sq(pred)
0,0491242	67,34%	53,34%	26,51%

General Linear Model: T2 versus Sample Name

Method

Factor coding (-1; 0; +1)

Factor Information

Factor	Type	Levels	Values
Sample Name	Fixed	7	PS_SC_100_10_15_1week; PS_SC_100_20_15_1week; PS_SC_100_40_15_1week; PS_SC_500_10_15_1week; PS_SC_500_20_15_1week; PS_SC_500_40_15_1week; PS_SC_unpressurized_1week

Analysis of Variance

Source	DF	Adj SS	Adj MS	F-Value	P-Value
Sample Name	6	16463	2744	1,19	0,368
Error	14	32404	2315		
Total	20	48867			

Model Summary

S	R-sq	R-sq(adj)	R-sq(pred)
48,1097	33,69%	5,27%	0,00%

General Linear Model: SDC*10^9 versus Sample Name

Method

Factor coding (-1; 0; +1)

Factor Information

Factor	Type	Levels	Values
Sample Name	Fixed	7	PS_SC_100_10_15_1week; PS_SC_100_20_15_1week; PS_SC_100_40_15_1week; PS_SC_500_10_15_1week; PS_SC_500_20_15_1week; PS_SC_500_40_15_1week; PS_SC_unpressurized_1week

Analysis of Variance

Source	DF	Adj SS	Adj MS	F-Value	P-Value
Sample Name	6	0,1361	0,02268	1,46	0,260
Error	14	0,2170	0,01550		
Total	20	0,3531			

Model Summary

S	R-sq	R-sq(adj)	R-sq(pred)
0,124494	38,54%	12,21%	0,00%

Comparisons for α Content

Tukey Pairwise Comparisons: Response = α Content, Term = Sample Name

Grouping Information Using the Tukey Method and 95% Confidence

Sample Name	N	Mean	Grouping	
PS_SC_unpressurized_1week	3	17,4381	A	
PS_SC_100_20_15_1week	3	15,8767	A	
PS_SC_100_40_15_1week	3	15,1700	A	
PS_SC_100_10_15_1week	3	14,5167	A	
PS_SC_500_40_15_1week	3	10,5594		B
PS_SC_500_10_15_1week	3	8,7100		B
PS_SC_500_20_15_1week	3	7,4833		B

Means that do not share a letter are significantly different.

Comparisons for β Content

Tukey Pairwise Comparisons: Response = β Content, Term = Sample Name

```
Grouping Information Using the Tukey Method and 95% Confidence

Sample Name                N     Mean  Grouping
PS_SC_500_20_15_1week      3  92,5167  A
PS_SC_500_10_15_1week      3  91,2900  A
PS_SC_500_40_15_1week      3  89,4406  A
PS_SC_100_10_15_1week      3  85,4833         B
PS_SC_100_40_15_1week      3  84,8300         B
PS_SC_100_20_15_1week      3  84,1233         B
PS_SC_unpressurized_1week  3  82,5619         B

Means that do not share a letter are significantly different.
```

Comparisons for Span

Tukey Pairwise Comparisons: Response = Span, Term = Sample Name

```
Grouping Information Using the Tukey Method and 95% Confidence

Sample Name                N     Mean  Grouping
PS_SC_500_40_15_1week      3  1,81267  A
PS_SC_100_20_15_1week      3  1,69200  A      B
PS_SC_unpressurized_1week  3  1,66267         B
PS_SC_500_10_15_1week      3  1,65800         B
PS_SC_100_10_15_1week      3  1,65567         B
PS_SC_100_40_15_1week      3  1,64300         B
PS_SC_500_20_15_1week      3  1,62767         B

Means that do not share a letter are significantly different.
```

APPENDIX H

Comparison of SC Emulsion Samples at 14th Day of Storage and Grouping Information

General Linear Model: α Melting T versus Sample Name

```
Method

Factor coding  (-1; 0; +1)


Factor Information

Factor       Type   Levels  Values
Sample Name  Fixed       7  PS_SC_100_10_15_2week; PS_SC_100_20_15_2week;
                            PS_SC_100_40_15_2week; PS_SC_500_10_15_2week;
                            PS_SC_500_20_15_2week; PS_SC_500_40_15_2week;
                            PS_SC_unpressurized_2week


Analysis of Variance

Source         DF   Adj SS   Adj MS  F-Value  P-Value
  Sample Name   6  0,08631  0,01439     0,43    0,850
Error          14  0,47267  0,03376
Total          20  0,55898


Model Summary

       S    R-sq  R-sq(adj)  R-sq(pred)
0,183744  15,44%      0,00%       0,00%
```

General Linear Model: α Content versus Sample Name

Method

Factor coding (-1; 0; +1)

Factor Information

Factor	Type	Levels	Values
Sample Name	Fixed	7	PS_SC_100_10_15_2week; PS_SC_100_20_15_2week; PS_SC_100_40_15_2week; PS_SC_500_10_15_2week; PS_SC_500_20_15_2week; PS_SC_500_40_15_2week; PS_SC_unpressurized_2week

Analysis of Variance

Source	DF	Adj SS	Adj MS	F-Value	P-Value
Sample Name	6	150,23	25,039	12,01	0,000
Error	14	29,19	2,085		
Total	20	179,42			

Model Summary

S	R-sq	R-sq(adj)	R-sq(pred)
1,44400	83,73%	76,76%	63,39%

General Linear Model: β Melting T versus Sample Name

Method

Factor coding (-1; 0; +1)

Factor Information

Factor	Type	Levels	Values
Sample Name	Fixed	7	PS_SC_100_10_15_2week; PS_SC_100_20_15_2week; PS_SC_100_40_15_2week; PS_SC_500_10_15_2week; PS_SC_500_20_15_2week; PS_SC_500_40_15_2week; PS_SC_unpressurized_2week

Analysis of Variance

Source	DF	Adj SS	Adj MS	F-Value	P-Value
Sample Name	6	0,01407	0,002344	0,39	0,871
Error	14	0,08333	0,005952		
Total	20	0,09740			

Model Summary

S	R-sq	R-sq(adj)	R-sq(pred)
0,0771517	14,44%	0,00%	0,00%

General Linear Model: β Content versus Sample Name

Method

Factor coding (-1; 0; +1)

Factor Information

Factor	Type	Levels	Values
Sample Name	Fixed	7	PS_SC_100_10_15_2week; PS_SC_100_20_15_2week; PS_SC_100_40_15_2week; PS_SC_500_10_15_2week; PS_SC_500_20_15_2week; PS_SC_500_40_15_2week; PS_SC_unpressurized_2week

Analysis of Variance

Source	DF	Adj SS	Adj MS	F-Value	P-Value
Sample Name	6	150,23	25,039	12,01	0,000
Error	14	29,19	2,085		
Total	20	179,42			

Model Summary

S	R-sq	R-sq(adj)	R-sq(pred)
1,44400	83,73%	76,76%	63,39%

General Linear Model: D[3,2] versus Sample Name

Method

Factor coding (-1; 0; +1)

Factor Information

Factor	Type	Levels	Values
Sample Name	Fixed	7	PS_SC_100_10_15_2week; PS_SC_100_20_15_2week; PS_SC_100_40_15_2week; PS_SC_500_10_15_2week; PS_SC_500_20_15_2week; PS_SC_500_40_15_2week; PS_SC_unpressurized_2week

Analysis of Variance

Source	DF	Adj SS	Adj MS	F-Value	P-Value
Sample Name	6	0,000583	0,000097	1,89	0,153
Error	14	0,000721	0,000051		
Total	20	0,001304			

Model Summary

S	R-sq	R-sq(adj)	R-sq(pred)
0,0071747	44,73%	21,04%	0,00%

General Linear Model: D[4,3] versus Sample Name

Method

Factor coding (-1; 0; +1)

Factor Information

Factor	Type	Levels	Values
Sample Name	Fixed	7	PS_SC_100_10_15_2week; PS_SC_100_20_15_2week; PS_SC_100_40_15_2week; PS_SC_500_10_15_2week; PS_SC_500_20_15_2week; PS_SC_500_40_15_2week; PS_SC_unpressurized_2week

Analysis of Variance

Source	DF	Adj SS	Adj MS	F-Value	P-Value
Sample Name	6	0,20749	0,034581	28,67	0,000
Error	14	0,01689	0,001206		
Total	20	0,22437			

Model Summary

S	R-sq	R-sq(adj)	R-sq(pred)
0,0347296	92,47%	89,25%	83,07%

General Linear Model: Span versus Sample Name

Method

Factor coding (-1; 0; +1)

Factor Information

Factor	Type	Levels	Values
Sample Name	Fixed	7	PS_SC_100_10_15_2week; PS_SC_100_20_15_2week; PS_SC_100_40_15_2week; PS_SC_500_10_15_2week; PS_SC_500_20_15_2week; PS_SC_500_40_15_2week; PS_SC_unpressurized_2week

Analysis of Variance

Source	DF	Adj SS	Adj MS	F-Value	P-Value
Sample Name	6	1,1715	0,19525	10,29	0,000
Error	14	0,2656	0,01897		
Total	20	1,4371			

Model Summary

S	R-sq	R-sq(adj)	R-sq(pred)
0,137737	81,52%	73,60%	58,42%

General Linear Model: T2 versus Sample Name

Method

Factor coding (-1; 0; +1)

Factor Information

Factor	Type	Levels	Values
Sample Name	Fixed	7	PS_SC_100_10_15_2week; PS_SC_100_20_15_2week; PS_SC_100_40_15_2week; PS_SC_500_10_15_2week; PS_SC_500_20_15_2week; PS_SC_500_40_15_2week; PS_SC_unpressurized_2week

Analysis of Variance

Source	DF	Adj SS	Adj MS	F-Value	P-Value
Sample Name	6	13570	2262	0,78	0,598
Error	14	40539	2896		
Total	20	54109			

Model Summary

S	R-sq	R-sq(adj)	R-sq(pred)
53,8109	25,08%	0,00%	0,00%

General Linear Model: SDC*10^9 versus Sample Name

```
Method

Factor coding  (-1; 0; +1)


Factor Information

Factor       Type   Levels  Values
Sample Name  Fixed       7  PS_SC_100_10_15_2week; PS_SC_100_20_15_2week;
                            PS_SC_100_40_15_2week; PS_SC_500_10_15_2week;
                            PS_SC_500_20_15_2week; PS_SC_500_40_15_2week;
                            PS_SC_unpressurized_2week


Analysis of Variance

Source         DF  Adj SS   Adj MS  F-Value  P-Value
  Sample Name   6  0,1069  0,01782     1,41    0,278
Error          14  0,1768  0,01263
Total          20  0,2837


Model Summary

       S    R-sq  R-sq(adj)  R-sq(pred)
0,112382  37,68%     10,98%       0,00%
```

Comparisons for α Content

Tukey Pairwise Comparisons: Response = α Content, Term = Sample Name

```
Grouping Information Using the Tukey Method and 95% Confidence

Sample Name                N     Mean  Grouping
PS_SC_100_40_15_2week      3  18,0361  A
PS_SC_500_10_15_2week      3  13,4233     B
PS_SC_unpressurized_2week  3  13,1205     B  C
PS_SC_500_20_15_2week      3  12,4367     B  C
PS_SC_100_10_15_2week      3  11,8033     B  C
PS_SC_100_20_15_2week      3   9,9367     B  C
PS_SC_500_40_15_2week      3   9,1600        C
```

Means that do not share a letter are significantly different.

Comparisons for β Content

Tukey Pairwise Comparisons: Response = β Content, Term = Sample Name

Grouping Information Using the Tukey Method and 95% Confidence

Sample Name	N	Mean	Grouping		
PS_SC_500_40_15_2week	3	90,8400	A		
PS_SC_100_20_15_2week	3	90,0633	A	B	
PS_SC_100_10_15_2week	3	88,1967	A	B	
PS_SC_500_20_15_2week	3	87,5633	A	B	
PS_SC_unpressurized_2week	3	86,8795	A	B	
PS_SC_500_10_15_2week	3	86,5767		B	
PS_SC_100_40_15_2week	3	81,9639			C

Means that do not share a letter are significantly different.

Comparisons for D[4,3]

Tukey Pairwise Comparisons: Response = D[4,3], Term = Sample Name

Grouping Information Using the Tukey Method and 95% Confidence

Sample Name	N	Mean	Grouping		
PS_SC_100_10_15_2week	3	0,732000	A		
PS_SC_unpressurized_2week	3	0,539333		B	
PS_SC_500_20_15_2week	3	0,514667		B	
PS_SC_500_10_15_2week	3	0,500333		B	
PS_SC_500_40_15_2week	3	0,465667		B	C
PS_SC_100_40_15_2week	3	0,464667		B	C
PS_SC_100_20_15_2week	3	0,387333			C

Means that do not share a letter are significantly different.

Comparisons for Span

Tukey Pairwise Comparisons: Response = Span, Term = Sample Name

Grouping Information Using the Tukey Method and 95% Confidence

Sample Name	N	Mean	Grouping			
PS_SC_500_20_15_2week	3	2,7770	A			
PS_SC_500_10_15_2week	3	2,7400	A	B		
PS_SC_100_10_15_2week	3	2,5875	A	B	C	
PS_SC_unpressurized_2week	3	2,4125	A	B	C	D
PS_SC_500_40_15_2week	3	2,3675		B	C	D
PS_SC_100_40_15_2week	3	2,2210			C	D
PS_SC_100_20_15_2week	3	2,1030				D

Means that do not share a letter are significantly different.

APPENDIX I

Comparison of SC Emulsion Samples at 28th Day of Storage and Grouping Information

General Linear Model: α Melting T versus Sample Name

```
Method

Factor coding  (-1; 0; +1)


Factor Information

Factor       Type   Levels  Values
Sample Name  Fixed       7  PS_SC_100_10_15_4week; PS_SC_100_20_15_4week;
                            PS_SC_100_40_15_4week; PS_SC_500_10_15_4week;
                            PS_SC_500_20_15_4week; PS_SC_500_40_15_4week;
                            PS_SC_unpressurized_4week


Analysis of Variance

Source         DF  Adj SS   Adj MS  F-Value  P-Value
  Sample Name   6  0,3118  0,05196     2,82    0,051
Error          14  0,2578  0,01841
Total          20  0,5696


Model Summary

       S    R-sq  R-sq(adj)  R-sq(pred)
0,135699  54,74%     35,34%       0,00%
```

General Linear Model: α Content versus Sample Name

Method

Factor coding (-1; 0; +1)

Factor Information

Factor	Type	Levels	Values
Sample Name	Fixed	7	PS_SC_100_10_15_4week; PS_SC_100_20_15_4week; PS_SC_100_40_15_4week; PS_SC_500_10_15_4week; PS_SC_500_20_15_4week; PS_SC_500_40_15_4week; PS_SC_unpressurized_4week

Analysis of Variance

Source	DF	Adj SS	Adj MS	F-Value	P-Value
Sample Name	6	217,09	36,182	25,26	0,000
Error	14	20,05	1,432		
Total	20	237,14			

Model Summary

S	R-sq	R-sq(adj)	R-sq(pred)
1,19679	91,54%	87,92%	80,97%

General Linear Model: β Melting T versus Sample Name

Method

Factor coding (-1; 0; +1)

Factor Information

Factor	Type	Levels	Values
Sample Name	Fixed	7	PS_SC_100_10_15_4week; PS_SC_100_20_15_4week; PS_SC_100_40_15_4week; PS_SC_500_10_15_4week; PS_SC_500_20_15_4week; PS_SC_500_40_15_4week; PS_SC_unpressurized_4week

Analysis of Variance

Source	DF	Adj SS	Adj MS	F-Value	P-Value
Sample Name	6	0,04076	0,006794	1,56	0,231
Error	14	0,06107	0,004362		
Total	20	0,10183			

Model Summary

S	R-sq	R-sq(adj)	R-sq(pred)
0,0660447	40,03%	14,33%	0,00%

General Linear Model: β Content versus Sample Name

Method

Factor coding (-1; 0; +1)

Factor Information

Factor	Type	Levels	Values
Sample Name	Fixed	7	PS_SC_100_10_15_4week; PS_SC_100_20_15_4week; PS_SC_100_40_15_4week; PS_SC_500_10_15_4week; PS_SC_500_20_15_4week; PS_SC_500_40_15_4week; PS_SC_unpressurized_4week

Analysis of Variance

Source	DF	Adj SS	Adj MS	F-Value	P-Value
Sample Name	6	217,09	36,182	25,26	0,000
Error	14	20,05	1,432		
Total	20	237,14			

Model Summary

S	R-sq	R-sq(adj)	R-sq(pred)
1,19679	91,54%	87,92%	80,97%

General Linear Model: D[3,2] versus Sample Name

Method

Factor coding (-1; 0; +1)

Factor Information

Factor	Type	Levels	Values
Sample Name	Fixed	7	PS_SC_100_10_15_4week; PS_SC_100_20_15_4week; PS_SC_100_40_15_4week; PS_SC_500_10_15_4week; PS_SC_500_20_15_4week; PS_SC_500_40_15_4week; PS_SC_unpressurized_4week

Analysis of Variance

Source	DF	Adj SS	Adj MS	F-Value	P-Value
Sample Name	6	0,000049	0,000008	0,88	0,533
Error	14	0,000130	0,000009		
Total	20	0,000179			

Model Summary

S	R-sq	R-sq(adj)	R-sq(pred)
0,0030472	27,43%	0,00%	0,00%

General Linear Model: D[4,3] versus Sample Name

Method

Factor coding (-1; 0; +1)

Factor Information

Factor	Type	Levels	Values
Sample Name	Fixed	7	PS_SC_100_10_15_4week; PS_SC_100_20_15_4week; PS_SC_100_40_15_4week; PS_SC_500_10_15_4week; PS_SC_500_20_15_4week; PS_SC_500_40_15_4week; PS_SC_unpressurized_4week

Analysis of Variance

Source	DF	Adj SS	Adj MS	F-Value	P-Value
Sample Name	6	0,005641	0,000940	5,59	0,004
Error	14	0,002355	0,000168		
Total	20	0,007996			

Model Summary

S	R-sq	R-sq(adj)	R-sq(pred)
0,0129688	70,55%	57,93%	33,74%

General Linear Model: Span versus Sample Name

Method

Factor coding (-1; 0; +1)

Factor Information

Factor	Type	Levels	Values
Sample Name	Fixed	7	PS_SC_100_10_15_4week; PS_SC_100_20_15_4week; PS_SC_100_40_15_4week; PS_SC_500_10_15_4week; PS_SC_500_20_15_4week; PS_SC_500_40_15_4week; PS_SC_unpressurized_4week

Analysis of Variance

Source	DF	Adj SS	Adj MS	F-Value	P-Value
Sample Name	6	0,003479	0,000580	2,90	0,047
Error	14	0,002799	0,000200		
Total	20	0,006278			

Model Summary

S	R-sq	R-sq(adj)	R-sq(pred)
0,0141396	55,41%	36,30%	0,00%

General Linear Model: T2 versus Sample Name

Method

Factor coding (-1; 0; +1)

Factor Information

Factor	Type	Levels	Values
Sample Name	Fixed	7	PS_SC_100_10_15_4week; PS_SC_100_20_15_4week; PS_SC_100_40_15_4week; PS_SC_500_10_15_4week; PS_SC_500_20_15_4week; PS_SC_500_40_15_4week; PS_SC_unpressurized_4week

Analysis of Variance

Source	DF	Adj SS	Adj MS	F-Value	P-Value
Sample Name	6	9799	1633	1,48	0,255
Error	14	15442	1103		
Total	20	25242			

Model Summary

S	R-sq	R-sq(adj)	R-sq(pred)
33,2119	38,82%	12,60%	0,00%

General Linear Model: SDC*10^9 versus Sample Name

Method

Factor coding (-1; 0; +1)

Factor Information

Factor	Type	Levels	Values
Sample Name	Fixed	7	PS_SC_100_10_15_4week; PS_SC_100_20_15_4week; PS_SC_100_40_15_4week; PS_SC_500_10_15_4week; PS_SC_500_20_15_4week; PS_SC_500_40_15_4week; PS_SC_unpressurized_4week

Analysis of Variance

Source	DF	Adj SS	Adj MS	F-Value	P-Value
Sample Name	6	0,2080	0,03466	2,22	0,103
Error	14	0,2187	0,01562		
Total	20	0,4267			

Model Summary

S	R-sq	R-sq(adj)	R-sq(pred)
0,124991	48,74%	26,77%	0,00%

Comparisons for α Content

Tukey Pairwise Comparisons: Response = α Content, Term = Sample Name

Grouping Information Using the Tukey Method and 95% Confidence

Sample Name	N	Mean	Grouping	
PS_SC_100_10_15_4week	3	16,8767	A	
PS_SC_100_40_15_4week	3	15,0233	A	
PS_SC_100_20_15_4week	3	14,0626	A	
PS_SC_unpressurized_4week	3	13,7100	A	
PS_SC_500_40_15_4week	3	9,1647		B
PS_SC_500_10_15_4week	3	8,8351		B
PS_SC_500_20_15_4week	3	8,1672		B

Means that do not share a letter are significantly different.

Comparisons for β Content

Tukey Pairwise Comparisons: Response = β Content, Term = Sample Name

Grouping Information Using the Tukey Method and 95% Confidence

Sample Name	N	Mean	Grouping	
PS_SC_500_20_15_4week	3	91,8328	A	
PS_SC_500_10_15_4week	3	91,1649	A	
PS_SC_500_40_15_4week	3	90,8353	A	
PS_SC_unpressurized_4week	3	86,2900		B
PS_SC_100_20_15_4week	3	85,9374		B
PS_SC_100_40_15_4week	3	84,9767		B
PS_SC_100_10_15_4week	3	83,1233		B

Means that do not share a letter are significantly different.

Comparisons for D[4,3]

Tukey Pairwise Comparisons: Response = D[4,3], Term = Sample Name

Grouping Information Using the Tukey Method and 95% Confidence

Sample Name	N	Mean	Grouping	
PS_SC_100_20_15_4week	3	0,326000	A	
PS_SC_100_40_15_4week	3	0,286667		B
PS_SC_500_40_15_4week	3	0,284000		B
PS_SC_100_10_15_4week	3	0,283000		B
PS_SC_500_20_15_4week	3	0,281667		B
PS_SC_unpressurized_4week	3	0,275667		B
PS_SC_500_10_15_4week	3	0,273667		B

Means that do not share a letter are significantly different.

Comparisons for Span

Tukey Pairwise Comparisons: Response = Span, Term = Sample Name

Grouping Information Using the Tukey Method and 95% Confidence

Sample Name	N	Mean	Grouping	
PS_SC_100_20_15_4week	3	1,7465	A	
PS_SC_500_40_15_4week	3	1,7310	A	B
PS_SC_500_20_15_4week	3	1,7300	A	B
PS_SC_100_40_15_4week	3	1,7290	A	B
PS_SC_500_10_15_4week	3	1,7265	A	B
PS_SC_100_10_15_4week	3	1,7180	A	B
PS_SC_unpressurized_4week	3	1,7010		B

Means that do not share a letter are significantly different.

VITA

PERSONAL INFORMATION

Name, Surname: Sezen Sevdin

E-mail: dsezen@metu.edu.tr

Mobile: +90542 821 4070

Address: Zühtüpaşa Mahallesi, Cumhur Sokak Güler Apartmanı Daire:1 Kadıköy-İstanbul

Nationality: Turkish

Date of Birth: 21.01.1986

Gender /Marital Status: Female / Married

EDUCATIONAL INFORMATION

2012-Present: PhD. Food Engineering Department, Middle East Technical University GPA: 3.43 / 4.00

Thesis Title: Effect of High Hydrostatic Pressure on Lipid Crystalline Structures in Palm Stearin Emulsions

2009-2012: MSc. Food Engineering Department, Middle East Technical University GPA: 3.38 / 4.00

Thesis Title: Chemical and Rheological Properties of Yoghurt Produced by Lactic Acid Cultures Isolated from Traditional Turkish Yoghurt

2004-2009 : BSc. Food Engineering Department, Middle East Technical University
GPA: 2.87 / 4.00

ACADEMICAL EXPERIENCES

2010-Present: Research Assistant, Food Engineering Department, Middle East Technical University.

PUBLICATIONS

a. Full Research Publications in International Journals (SCI Expanded)

Sevdin, S., Yücel, U, Alpas, Hami (2017). Effect of High Hydrostatic Pressure (HHP) on Crystal Structure of Palm Stearin Emulsions. *Innovative Food Science and Emerging Technologies.* https://doi.org/10.1016/j.ifset.2017.05.005

Sevdin, S., Özel, B., Yücel, U., Öztop, M.H., Alpas, H.. Monitoring the High Hydrostatic Pressure (HHP) Induced Changes in the Crystal Structures of Palm Stearin Emulsions Emulsified with Sodium Caseinate by Differential Scanning Calorimetry (DSC) and Nuclear Magnetic Resonance (NMR) Relaxometry. (Under Review in *Journal of Food Engineering* since February, 2017)

Sevdin, S., Çınar Bam, B., Alpas, H., Öztop, M.H., İde, S. Nano scale analysis on water emulsions of Palm Stearin: The effect of hydrostatic pressure and the stabilizers (sodium caseinate and lecithin). (Under Review in *Colloids and Surfaces A: Physicochemical and Engineering Aspects* since June, 2017)

b. Oral Presentations

Sevdin, S., Özel, B., Öztop, M.H., Alpas, H. (2017). High Hydrostatic Pressure (HHP) Treated Palm Stearin Emulsions: Characterization of Lipid Crystals. 6^{th} International Conference on Nutrition and Food Sciences, May, 10-12, 2017, Budapest, Hungary.

c. Poster Presentations

Sevdin, S., Yücel, U., Öztop, M. H., Alpas, H. (2016). Crystal Structure of Lipid in Palm Stearin Emulsions Treated with High Hydrostatic Pressure. 2. Congress on Food Structure Design. 26-28th October 2016, Antalya, Turkey.

Sevdin, S., Yücel, U., Alpas, H. (2016). Yüksek Hidrostatik Basıncın (YHB) Su içinde Yağ Emülsiyonlarının Kristallenme Özellikleri Üzerine Etkisi. Turkey 12. Food Congress. October 5-7, 2016, Edirne, Turkey.